Momentum diffusion from a two-dimensional jet. September 1966.

Author:
Choi, Yu-Leuk; Wood, I. R.

Publication details:
Report No. UNSW Water Research Laboratory Report No. 90

Publication Date:
1966

DOI:
https://doi.org/10.4225/53/5796e95b6312b

THE UNIVERSITY OF NEW SOUTH WALES

water research laboratory

Manly Vale, N.S.W., Australia

Report No. 90

MOMENTUM DIFFUSION FROM A TWO-DIMENSIONAL JET

by

Yu-Leuk Choi and I. R. Wood

September, 1966

MOMENTUM DIFFUSION FROM A TWO-DIMENSIONAL JET DIRECTED INTO A DEFLECTING UNIFORM STREAM.

by

Yu-Leuk Choi

and

I. R. Wood

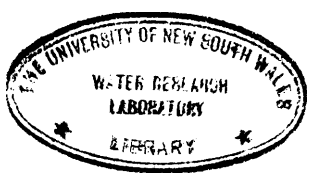

Report No. 90

September, 1966.

https://doi.org/10.4225/53/5796e95b6312b

PREFACE

The work reported in this document was carried out as part fulfilment of the requirements for a degree of Master of Engineering. It forms an integral part of the programme of basic research in fluid mechanics in the Water Research Laboratory at the present time.

R. T. Hattersley,
Assoc. Professor of Civil Engineering,
Officer in Charge,
Water Research Laboratory.

September, 1967.

Summary

The equations of mean motion for a two-dimensional jet deflected by an ambient stream are studied. On condition that the initial velocities of the jet and the ambient stream differ not too much in direction and not too little in magnitude, the equations holding in certain regions of the deflected jet flow field are shown to be similar to those for a jet in a coflowing stream. A preliminary study of self-preservation is also attempted. Experimental measurements are made to confirm the similarity of the mean velocity fields of the two kinds of jet flows. Self-preservation of the excess dynamic pressure is confirmed for the deflected two-dimensional jet. The jet axial location is found to be independent of the jet-to-ambient velocity ratio if all lengths are divided by the square of that ratio.

The initial report is concerned with jet deflection angles of 25^{o}, 17^{o} and 9^{o}. In Appendix 3 mention is made of some additional experiments at 45^{o} deflection at which angle some of the conclusions of the initial report are found to be no longer valid.

Table of Contents

Notations

b	length scale
D	initial thickness of a two-dimensional jet
K	curvature of a dynamic pressure contour
l, L	length scale
n	coordinate perpendicular to jet axis
p, P	static pressure
q	dynamic pressure
R	initial jet-to-ambient velocity ratio
s	coordinate parallel to jet axis
U, u	velocity in s- or x-direction
U_1	velocity of ambient stream
U_j	velocity of jet
V, v	velocity in n- or y- direction
x, y	cartesian coordinates through the centre of jet nozzle exit
α	angle between s- and x-axes
β	inclination of excess dynamic pressure contour to s-axis
ρ	radius of curvature of jet axis

Suffixes:

o	in general refers to the values at nozzle exit
s, n	components in s- and n-directions respectively
A	values in the ambient stream
C	values at the jet axis.

Illustrative Figures.

Fig. T1 - Development of a Plane Jet

Fig. T2 - Coordinate System

Fig. T3 - General View of the Experimental Arrangement

Fig. T4 - Jet Deflector
- (a) General view
- (b) Cross-section

Fig. T5 - Instruments for Velocity Head Measurement
- (a) General view
- (b) Close-up View of Velocity Probe
- (c) Cross-section of Probing Stem

1. Introduction

The jet flow is a fluid flow phenomenon when there is a discontinuity of some parameters such as velocity in some part of the flow field. The fluids separated by the discontinuity need not have the same thermodynamic properties. The flow may be bounded or unbounded, laminar or turbulent.

The flow of a turbulent jet into an unbounded region of fluid with the same properties is a relatively simple type of shear flow. It is of both basic and applied interest. For practical applications, it serves as a model for problems such as the dilution of sewage from a submarine outfall. From the theoretical standpoint, the importance of this kind of flow lies in the fact that it possesses certain simplifying properties, which enables a more detailed study of the observed properties of the flow field and the use of the results to interpret observations of more common types of turbulent shear flows. Consequently, the diffusion phenomena of this free turbulent shear flow have been examined both theoretically and experimentally by many investigators over the past four decades.

All free turbulent shear flows are simplified by the absence of solid boundaries. Hence there is no restriction on the lateral spread of turbulence into the surrounding fluid, and the flow exhibits inhomogeneity in the direction of the mean motion. Transverse to this direction, the velocity and the length scale (characterized by the lateral spread of jet) are both small. Thus a simplification is possible in a manner similar to the boundary layer approximation. A consequence of this on the equations of motion is that, provided the Reynolds number is high enough, the mean static pressure must have a small yet significant decrease relative to that in the surrounding fluid. Another simplification is valid for fully-developed flows of free turbulence. At sufficiently high Reynolds numbers, these flows are usually found to exhibit geometrical similarity. Hence the mean flow is effectively independent of the viscosity. These two simplifications reduce the governing equations to a set analogous to those for a laminar boundary layer. But the analogy is incomplete, for the apparent shear stress cannot be related to the mean velocity gradient in any simple way [24]. *

---

* Numbers in brackets refer to Bibliography.

Earlier works on jets have dealt fairly extensively with unidirectional flows, i.e. a plane jet or an axi-symmetric jet discharging into a quiescent or uniform co-flowing (viz. flowing in the same direction as the jet) medium, and the mixing of two semi-infinite uniform streams. An important property usually found is self-preservation, i.e., the transverse distributions of some mean quantities for various positions in the downstream direction retain the same functional forms, merely changing in scale. Mathematically this simply means that (in the case of two independent variables) a solution in terms of those mean quantities can be found by separation of variables after an appropriate change of the independent variables. Physically this implies a state of moving equilibrium uninfluenced by the upstream history [25].

Experimental measurements on a two-dimensional jet and on an axi-symmetric jet discharging into a stationary medium have indicated the existence of self-preservation of the mean flow velocity and the Reynolds stresses. Theoretical analysis has also shown that this can be consistent with the equations of motion. However, when the ambient fluid is a uniform coflowing stream, the situation is more complex. Although experiments have also indicated the self-preservation of the excess velocity (i.e., velocity relative to the ambient stream) profiles, analysis has ruled out the possibility of its exactness and shown that at best it can only be approximately true provided the maximum velocity excess in a transverse section is of an order larger or smaller than the velocity of the ambient fluid.

Another type of self-preservation has been observed, in which the excess dynamic pressure is substituted for the excess velocity. When the ambient fluid is at rest, these two types of self-preservation are exactly equivalent. But, this is not so when the ambient fluid is moving. Intensive measurements [16] made on compound jets have indicated this second type. Correlation theory, using a hypothesis which is in effect the self-preservation of excess dynamic pressure, was found quite successful in problems of round jets and of two-dimensional jets [see 26] in both moving and stationary ambient fluid. These lend much weight to the preference for the self-preservation of excess dynamic pressure to that of excess velocity.

Only in recent years has the problem of jets issuing into a deflecting (i.e. non-coflowing) ambient stream been considered. Most of these works have been concerned principally with the location of the jet axis [1]. An experimental investigation was recently made on the upstream region of the zone of established flow from a round

jet in a cross-wind [27]. It claimed to have obtained a similarity of the difference in magnitude of the velocities in the jet and in the ambient stream when the profiles normal to the jet axis were considered. However, this similarity is not satisfactory, since it is not logically sound to form the difference in magnitude of two differently-directed vectors. No similar work has appeared for the two-dimensional problem.

In view of the meanings of self-preservation, we would expect it to be found in some more general type of jet flow governed by similar equations. One such flow is a two-dimensional jet emitted at a small angle to a uniform ambient stream. The present investigation attempts to provide some information on the momentum diffusion in such a flow. Following some simple analytical considerations, measurements of dynamic pressure were carried out for three different initial jet directions and several jet-to-ambient velocity ratios. Unfortunately, no instruments were available in the laboratory to enable measurements on turbulence, although its importance in jet mixing has always been well understood. Nevertheless, an important conclusion can be drawn, confirming the self-preservation of excess dynamic pressure. Some remarks are also made on the location of the jet axis.

2. Critical Review of Literature

2.1 Preliminary

The study of jets dates back to the last century when Helmholtz first solved the problem of the Borda mouthpiece by using the free streamline theory [4]. Since then, many other models have been constructed. These are all based on the inviscid theory and the hodograph transformation. Most such solutions involve cases where the diagram in the hodograph plane is a circular sector or a rectangular polygon. Even in these comparatively simple cases, the mathematical solutions are highly complex. This theory has been found in reasonable agreement with experiments in the cases of liquid jets issuing into air or some other low-density medium. However, discrepancies arise in the general case of jets and wakes.

The failure of free streamline theory applied to jets and wakes in a homogeneous fluid pertains to the important roles played by viscosity, vorticity, and turbulence. The effect of viscosity reduces the number of degrees of freedom of the fluid in laminar motion by

damping the motion of small eddies [19] thus drawing the well-known distinction between laminar and turbulent flows. The laminar flow of all Newtonian fluids can be described by the Navier-Stokes equations with suitable boundary conditions. However, the non-linearity of the equations has made it very difficult to solve this boundary value problem. In particular, no special analytic solutions are known which describe wakes and jets [5]. Besides, although it is known theoretically that solutions do exist, it has never been proved that the solution is unique. Hence we do not even know whether the problem is mathematically well-set. Nevertheless, the Navier-Stokes equations have been used universally, even in the study of turbulent flows. Leaving aside the question of uniqueness, much work has been done in attempting to solve these equations for various problems. Apart from a few exact solutions, many known solutions generally follow either of two types of approximations. One is the linearization by means of perturbation methods, such as Stokes approximation and Oseen approximation. The other type is the boundary layer approximation. Besides, numerical methods have also been used to find approximate solutions, but these have been criticised [5] regarding the justification of the methods used and some usual assumptions adopted in the calculation.

At very low Reynolds numbers (creeping flow) some solutions have been obtained for steady jet flows, using the two types of approximations. In these solutions, similarity has been found (involving the kinematic viscosity). Among these, the analytic solution of Yatseev and Squire [5] deserves particular attention. Schlichting's model was used and an exact solution to the Navier-Stokes equations in spherical coordinates was obtained for the creeping jet flow from a tube of infinitesimal diameter, under the self-similarity hypothesis. This is in agreement with the experimental fact, at least qualitatively, that only in the case of outflow from a tube does one observe radial streamlines. Although there is still some lack of rigour in part of the mathematical argument, this has the important indication that exact self-similarity only exists in an appropriate coordinate system which is inherent in the nature of the problem.

At intermediate Reynolds numbers, homogeneous jets often exhibit periodic behaviour just like wakes. For instance, in a plane jet vorticity has been observed to be shed alternately on both of the jet boundaries. However, the theory of periodic jets is still only very rudimentary [5]. At higher Reynolds numbers,

the periodicity breaks down and the jet becomes turbulent, and the flow becomes time-dependent even though the mean flow may still remain steady.

In the analysis of turbulent fluid motion, the Navier-Stokes equations have been assumed to be satisfied by the instantaneous values of the flow parameters. Each instantaneous value is again assumed separable into a mean and fluctuating component. Taking mean values of the resulting equations yields the well-known Reynolds equations. But the appearance of the eddy stresses renders the problem indeterminate since the governing equations do not furnish a sufficient number of conditions. To find a complete solution of the problem, two lines of approach have been used, viz. the semi-empirical approach and the statistical approach. Since turbulent fluctuations are random in nature, the methods of statistical mechanics are applied in the latter approach. The essential features of this theory [12, 19] are to study the correlation function, the spectral function, the probability distribution and the joint probability distribution of the random functions at different time and different position in space. Although this is generally believed to be the final approach to the study of turbulence, the present status of the statistical theory is still far from being complete and satisfactory [19]. In particular, our knowledge of non-isotropic turbulence is meagre. Besides, in the absence of an ergodic theorem which asserts the equality of time average and ensemble average, it is doubtful whether we can compare the deductions of the theory with the experimental data which are nearly invariably temporal mean values.

In the semi-empirical theories, the additional relations required for a full description of the turbulent flow are generally provided by two kinds of hypotheses, viz. the self-similarity or self-preservation of some flow parameters, and some physical assumption such as the mixing-length theory. Based on these hypotheses, solutions to many simpler free turbulence problems have been worked out [1, 18]. Although on the macroscopic scale most of these solutions give predictions in satisfactory agreement with observations, the measured value (or calculated value based on measurements) of some quantities on whose property the physical assumption is based do not in general support the assumption (and indeed sometimes even prove the contrary) [24]. For example, the criticisms on the various forms of mixing length theory are quite well known. On the other hand, the property of self-preservation seems to be exhibited by a wide class of free turbulent shear flows [25].

In the following, we shall review some essential features of the previous works which are most relevant to the mean flow of a turbulent jet.

2. 2 Some Properties of Turbulent Jets

In all actual cases, a jet is emitted from a nozzle of finite dimensions. At the nozzle exit the velocity distribution in the jet is usually very nearly uniform except in the wall boundary layers. As soon as the jet enters into the ambient fluid, a discontinuity of fluid velocity is created. But stability consideration does not permit the vortex sheets to persist. In addition, viscosity will diffuse the vorticity. Consequently, the uniform velocity profile is gradually reduced in width and eventually disappears at a certain distance from the nozzle exit plane. This part of the flow field is termed the initial region or the zone of establishment. It is characterized by the existence of a constant velocity core (or potential core). The velocity distribution in this region is the same as a plane mixing region (except perhaps in the vicinity of the tip of the potential core) [1]. The flow field downstream of the end of the initial region is sometimes called the zone of established flow.

Sufficiently far downstream, the jet appears to behave as if it were emitted from a source of infinitely small width (i. e. a line source in the two-dimensional case or a point source in the axisymmetric case). This region (which extends in the downstream direction) is called the main region. Certainly the location of the beginning section of this region is only tentative and depends entirely on the accuracy of measurements. The flow field between the initial and the main regions is called the transition region.

A characteristic feature of the turbulent jet is the smallness of the transverse velocity component compared with the longitudinal velocity component in any section normal to the direction of mainstream flow. Thus the total velocity head is used to determine the longitudinal velocity component in nearly all experimental investigations on a symmetrically spread jet. Evidently this is false outside or near the jet 'edge' except with a sufficiently fast coflowing ambient stream. In addition, the effect of turbulence in the total head has almost always been neglected. However, this would only cause a small error since the turbulence intensity is always very small compared with the mean velocity.

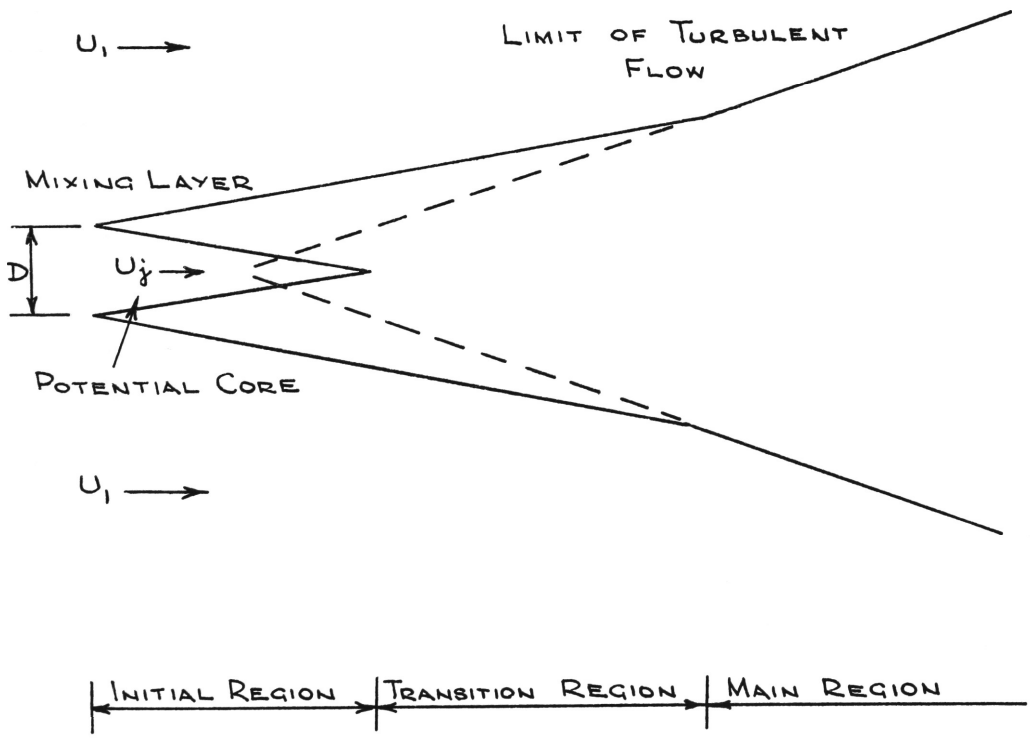

FIG. T 1. DEVELOPMENT OF A PLANE JET.

Experimental data have shown that in the main region the velocity distribution at every transverse section is bell-shaped, with the maximum velocity (at the jet axis) decreasing with the distance from the nozzle and the effective width of the profile increasing. The most important fact is revealed by plotting the velocity profiles in dimensionless form by dividing the velocity in a transverse section by the maximum (axial) velocity in that section and dividing the distance from the axis of symmetry by a transverse length scale characteristic of that section which is generally taken as the distance from the axis to the point where the velocity has fallen to a certain fraction of the axial velocity. This has revealed that for a jet discharging into a still medium, all such profiles are nearly identical [1], i.e. such dimensionless profiles are independent of the downstream distance from the nozzle. This affirms the self-preservation of the mean velocity of a submerged jet.

The experimental data for a jet in a coflowing stream have been analysed in the same way [1]. Here the velocity relative to the external stream is substituted for the absolute velocity in the submerged case. At first sight it would seem that such a simple transformation* would reduce the problem to the submerged case. Yet this is not so, for the point where the jet starts to diffuse (the nozzle exit) is stationary. However, it is surprising that universality of such profiles seems to exist [1]. But closer examination reveals a tendency for the dimensionless excess velocity profile to vary (though slightly) with the jet-to-ambient velocity ratio, although such a universal profile seems to exist for each velocity ratio. The dimensionless profiles of temperature and admixture concentration for jet flows at various velocity ratios are further evidences of this dependence on the velocity ratio [see e.g. 1].

Experimental data also shows that the transverse length scale of a jet as determined by the velocity profiles is approximately proportional to the distance from a certain point (the virtual origin) on the axis and the axial velocity varies approximately inversely with the square root of that distance, the effect of the velocity in the ambient fluid appearing to prolong the axial length scale only. These are in fact necessary conditions for the self-preservation of the velocity. But by using the conservation of momentum it can be shown that these two simple relations cannot be true simultaneously when there is an ambient stream. This is also reflected by the non-coincidence of the

* This is in fact the basic idea underlying the transformation described in [15].

virtual origins determined from the graphs of transverse length scale and the reciprocal of the axial velocity versus axial distance respectively. Hence it may be concluded that the self-preservation of velocity for a jet in a coflowing stream is not a particularly good approximation. Nevertheless, it is a convenient and useful one.

It seems that the position of the virtual origin for the above self-preservation is independent of the velocity ratio [11]. However, this position must obviously be related to the dimension of the nozzle exit and the initial velocity distribution in the jet. But no single relation applies to the results of all investigations. Therefore it seems tempting to suggest that this position also depends on the range of axial distance considered.

Measurements of the Reynolds stresses (turbulence) have been made for two-dimensional and axi-symmetric jets. It seems conclusive that beyond an axial distance of about 30 nozzle widths, similarity is attained [10, 15, 28], although some earlier work [e.g. 13] contradicts this.

When the jet axis is curved, symmetry of diffusion no longer exists. This can occur when the external stream is not uniform, or at an angle to the jet, or when free spreading is prohibited on one side as in a ground-effect-machine. The first case seems yet not attacked. A particular problem of the second case, viz. a round jet in a cross-wind, was examined for a small range of downstream distance [27]. Two results may be of some significance. First, the jet centre-line has small curvature, and its location is the same for all velocity ratios if the co-ordinates are divided by the square of the jet-to-ambient velocity ratio and if the direction of the jet at the end of the potential core is the same. Secondly, self-preservation has been indicated for the difference in magnitude of the velocity in a plane perpendicular to the jet centre-line and the velocity of the cross-wind. However, this second formulation of similarity is unsatisfactory, for the difference in magnitude is formed from two differently-directed vectors. In [29], a 'free' curved two-dimensional jet bent outwards due to the cavity on one side was studied. One of the conclusions suggested is the similarity of the velocity profiles, but the range of observation was necessarily small (only up to an axial distance of 10 times initial jet width). Thus similarity has not really been defined and verified for 'curved' jet flows. In fact, even the method of determining the jet axis from experimental measurements of the velocity seems not yet clear.

A characteristic feature of jets, laminar or turbulent, is that during spreading it induces a small transverse velocity in the surrounding fluid. This induced inflow velocity of course decreases with downstream distance. According to [16], the ratio of the influx per unit length (of the jet boundary in a transverse plane) to the 'top-hat' mean velocity excess (for a round jet in a coflowing stream) falls from the constant value of 0.07, appropriate to a jet in a still fluid, to zero at large distance downstream of the orifice, characteristic of a wake. The entrainment is made up of a combination of the lateral inflow (jet-like) and the encroachment of the jet boundary on the ambient flow, as in a wake. The entrainment coefficient, E, in any transverse plane may be defined as the axial rate of change of the excess discharge per unit length of the jet boundary divided by the mean velocity excess in that plane. Measurements in [16] were made over a fairly large range of the dimensionless distance downstream (up to 80 times momentum thickness) covering down to a rather small axial velocity excess (about 16 pc. of the ambient velocity). These have shown that E is not even approximately constant, as reported or implied by others. E increases between the initial region where the ratio of the axial velocity excess to ambient flow velocity is much greater than one and the region far downstream where that ratio is much smaller than one. This is quite reasonable, for far downstream the flow will behave more like a wake which is known to have a greater entrainment coefficient [25].

When the jet is in a deflecting stream, the lateral inflow may be defined as that due to the velocity component in the ambient fluid perpendicular to the jet axis. Because of the presence of a component of the original ambient flow in the same direction, the lateral inflow can be expected to be greater than for the coflowing case. This should partly account for the fairly high inflow rate reported in [27]. An entrainment coefficient, however, is difficult to define. In [27], it is defined as the ratio of the inflow velocity to the difference in magnitude of the velocity at the axis and in the ambient. Evidently this is very imprecise. Hence it seems better in this case to consider the inflow rate alone.

2.3 Equations of Motion

The theoretical basis of the Navier-Stokes equations rests on the asymptotic expansion of the Boltzmann equation and on the assumption of thermodynamic quasi-equilibrium. Although these are not of unquestionable validity, available experimental evidence provides a strong justification of the applicability of the equations, and they are

taken as axiomatic in the study of laminar flows [30]. However, their applicability in turbulent motion is not indusputable. A very attractive criticism is that since turbulence is random in nature, the instantaneous velocity field can hardly be regarded as differentiable [4, 19]. But a guess based on the statistical theory of turbulence is that the velocities have up to the fifth derivatives [4]. The best justifications of the use of the Navier-Stokes equations perhaps lie in the consistency of its consequences with experiments. The most detailed verification is provided by Stewart's experimental verification of Howarth-Karman equation in homogeneous isotropic turbulence [12, 25]. Thus it is considered [25] that only when either the velocities involved greatly exceed the molecular velocities or the pressure is so low that the mean free path is comparable with the dimensions of the whole flow, will the scale of the molecular motion approach that of the turbulent motion, and the Navier-Stokes equations become inapplicable.

The Navier-Stokes equations for a viscous incompressible fluid of unit density can be written

$$\frac{\partial(u_i + U_i)}{\partial t} + (u_\ell + U_\ell)\frac{\partial(u_i + U_i)}{\partial x_\ell} = -\frac{\partial(P+p)}{\partial x_i} + \nu\frac{\partial^2(u_i+U_i)}{\partial x_\ell^2} \qquad (1)$$

in cartesian coordinates, where $(P + p)$, $(u_i + U_i)$ are respectively the instantaneous values of pressure and the i component of velocity, capitals and small letters denoting respectively mean and fluctuating parts. The equation of continuity is

$$\frac{\partial(u_i + U_i)}{\partial x_i} = 0 \qquad (2)$$

Taking mean values, we obtain

$$U_\ell\frac{\partial U_i}{\partial x_\ell} + \frac{\partial\overline{u_i u_\ell}}{\partial x_\ell} = -\frac{\partial P}{\partial x_i} + \nu\frac{\partial^2 U_i}{\partial x_\ell^2} \qquad (3)$$

$$\frac{\partial U_i}{\partial x_i} = 0 \qquad (4)$$

for the mean motion, where $\overline{u_i u_\ell}$ are the well-known Reynolds stresses.

For two-dimensional* flows parallel to the xy plane, these equations reduce to

* The axi-symmetric flows in cylindrical coordinates are similar to the two-dimensional flows.

$$U\frac{\partial U}{\partial x} + V\frac{\partial U}{\partial y} + \frac{\partial \overline{u^2}}{\partial x} + \frac{\partial \overline{uv}}{\partial y} = -\frac{\partial P}{\partial x} + \nu\left(\frac{\partial^2 U}{\partial x^2} + \frac{\partial^2 U}{\partial y^2}\right) \tag{5}$$

$$U\frac{\partial V}{\partial x} + V\frac{\partial V}{\partial y} + \frac{\partial \overline{uv}}{\partial x} + \frac{\partial \overline{v^2}}{\partial y} = -\frac{\partial P}{\partial y} + \nu\left(\frac{\partial^2 V}{\partial x^2} + \frac{\partial^2 V}{\partial y^2}\right) \tag{6}$$

$$\frac{\partial U}{\partial x} + \frac{\partial V}{\partial y} = 0 \tag{7}$$

For unidirectional free turbulent flows in the x-direction, there exists a reference plane $y = y_o$ along which $V = 0$. Hence equation (7) can be integrated to give

$$V = -\int_{y_o}^{y} \frac{\partial U(y')}{\partial x} dy' \tag{8}$$

The longitudinal length scale of variation, L, in the x-direction is of an order greater than, 1, that in the y-direction. If in each section

$$U_s = U_{max.} - U_{min.}$$

then from (8) V can at most be of order $U_s \ell/L$. Using the empirical fact that $\overline{u^2}$, $\overline{uv}$, $\overline{v^2}$ are of order $\left(\frac{\ell}{L}\right)^{\delta} U_s^2$, and U of order $U_s\left(\frac{\ell}{L}\right)^{\delta-1}$ where $\delta = 0$ for wakes and $\delta = 1$ for jets, a comparison of order of magnitude for the different terms reduces equation (6) to

$$\frac{\partial \overline{v^2}}{\partial y} = -\frac{\partial P}{\partial y} + \nu\frac{\partial^2 V}{\partial y^2}$$

At sufficiently high Reynolds number, the last term is negligible compared with the first term. Then the equation can be integrated to give

$$P + \overline{v^2} = P_o(x) \tag{9}$$

In ordinary free turbulence, P_o is a constant.

Substitution of (9) in (5) gives, to the same approximation,

$$U\frac{\partial U}{\partial x} + V\frac{\partial U}{\partial y} + \frac{\partial(\overline{u^2} - \overline{v^2})}{\partial x} + \frac{\partial \overline{uv}}{\partial y} = \nu\frac{\partial^2 U}{\partial y^2} \tag{10}$$[1]

If $U^2 \gg (\overline{u^2} - \overline{v^2})^*$, we have, neglecting the viscous term,

$$U \frac{\partial U}{\partial x} + V \frac{\partial U}{\partial y} = - \frac{\partial \overline{uv}}{\partial y} \tag{10}$$

Integrating (10), we have

$$\int_{-\infty}^{\infty} U (U - U_1) \, dy = F \text{ (a const.)} \tag{11}$$

where U_1 is the velocity outside the flow. Equation (11) simply expresses the conservation of momentum, but it is only approximate due to the growth of turbulence. As is well-known [18], equations(7) and (10) make it clear that the two-dimensional turbulent jet flow is governed by the same equations as the boundary layer over a flat plate (provided we neglect $\overline{u^2} - \overline{v^2}$). These equations reduce to one in U of parabolic type, thus bell-shaped velocity profiles are to be expected [5], as is indeed typical for jets and wakes.

2. 4 Reynolds Number Similarity and Self-preservation

Two fundamental hypotheses about the general nature of fully developed turbulent motion are made in nearly all theories. The first is the similarity of the flow structure at all high Reynolds numbers. This Reynolds number similarity is attained when the Reynolds stresses greatly exceed the mean viscous stresses, and the mean motion and the motion of the energy-containing components of the turbulence are determined by the boundary conditions of the flow alone. This similarity implies that geometrically similar flows are similar at all sufficiently high Reynolds numbers, and that the mean kinematic quantities and the turbulent structure are completely determined by a velocity scale and a length scale. Such a property has been established experimentally [see e.g. 25] for most problems of free turbulence, except for flows such as an axi-symmetric wake where the Reynolds number has been shown to decrease in the downstream direction and the flow will thus eventually become laminar. Therefore, the viscous term in the equation of motion (10) will be neglected for jet flows.

The second hypothesis is the self-preservation of some mean flow parameters. This postulates the invariance of the functional form of the transverse distribution of these parameters for different positions in the downstream direction (x-direction), merely with modifications in scale which depends only on the x distance. Expressed mathematically, this states that for the mean quantity f (x, y), we have [25]

$$f(x, y) = f_0(x) \, g\left(\frac{y}{L_0(x)}\right)$$

---

* $\frac{\overline{u^2} - \overline{v^2}}{U^2}$ is at most of order $\left(\frac{\ell}{L}\right)^{2-\delta}$

where $f_o(x)$ is a suitable scale for f, $l_o(x)$ is a suitable length scale in y-direction, and g is the universal transverse distribution function for f. If the turbulent motion and the mean velocity profile are to be self-preserving

$$U = U_1 + U_o f\left(\frac{y}{l_o}\right)$$
$$\overline{uv} = U_o^2 g_{12}\left(\frac{y}{l_o}\right) \qquad (12)$$
$$\overline{u^2} = U_o^2 g_1\left(\frac{y}{l_o}\right) \quad , \quad \overline{v^2} = U_o^2 g_2\left(\frac{y}{l_o}\right)$$

where U_1 is the constant velocity of translation of the flow,

U_o is a suitable velocity scale, usually chosen as the maximum velocity difference in a section of a jet or wake.

Substitution of equation (12) into equations (7) and (10) gives a relation between the universal functions. Universality of these functions imposes conditions on the coefficients of that resulting equation, which lead to two possible cases of exact self-preservation:

(a) For general U_1, necessary conditions are

$$U_o = \text{constant}, \quad \frac{dl_o}{dx} = \text{constant} \qquad (13)$$

which represents the plane mixing region.

(b) $U_1 = 0$, necessary conditions are

$$\frac{l_o}{U_o}\frac{dU_o}{dx} = \text{constant}, \quad \frac{dl_o}{dx} = \text{constant} \qquad (14)$$

which refers to a two-dimensional jet in a still fluid. The momentum integral equation (11) further requires (14) to become

$$l_o \propto (x - x_o) \quad , \quad U_o \propto (x - x_o)^{-\frac{1}{2}} \qquad (15)$$

where x_o is an integration constant representing the position of the virtual origin.

Besides these two exact self-preserving flows, two approximate forms of self-preservation are possible.

(c) $U_o / U_1 \gg f$, the conditions are

$$l_o \propto (x - x_o) \quad , \quad U_o \propto (x - x_o)^{-\frac{1}{2}}$$

which is typical of the upstream of a jet.

(d) $U_o / U_1 \ll f$, the conditions are

$$l_o \propto (x - x_o)^{\frac{1}{2}} \quad , \quad U_o \propto (x - x_o)^{-\frac{1}{2}}$$

representing the plane wake or the far downstream of a plane jet.

The necessary departure from self-preservation for type (d) is a well-established fact for a wake [25]. By using the momentum integral and the energy integral, it can be shown that this departure is represented quite clearly by the continuous shift of the virtual origin towards negative values with increase of downstream distance x. Besides, the virtual origins for the velocity and length scales should strictly be different.

2.5 Free Turbulence Theories and Their Application to Two-dimensional Jets

The application of the hypotheses of similarity and self-preservation to the approximated equation of motion (10) gives rise to a relation between the universal functions for mean velocity and the apparent shear stress $\overline{uv}$, with one indeterminate constant which, e.g. can be chosen to represent the rate of spread of the jet. Some further physical assumptions or experimental measurements must be introduced to determine these functions completely.

The best known of such attempts are the mixing length theories originated by Prandtl. In analogy with the kinetic theory of gases, a mixing length l' is introduced such that a property q of the fluid preserves its mean value $\bar{q}$ during the turbulent mixing process over the path l' [19]. If l' is small, we have for the fluctuation of q

$$|q'| = l' \frac{d\bar{q}}{dy} \tag{16}$$

The earliest version of such theories is Prandtl's momentum transfer theory in which q is assumed to be the momentum. By further assuming a constant correlation between the fluctuation of the velocity components, it is shown that*

$$\overline{uv} = l^2 \left|\frac{dU}{dy}\right| \frac{dU}{dy}$$

* $l = kl'$ where $0 < k < 1$

Prandtl assumed l to be a constant for a jet in the absence of solid boundaries. Tollmien solved the problems for the plane mixing region and the two-dimensional jet, involving one arbitrary constant (as in the equation of motion) to be determined experimentally.

This constant can be determined by using either the decrease of axial velocity or the spreading of the jet. But the values obtained in the two ways differ by about 10 pc. [1]. This discrepancy should be interpreted as the invalidity of some assumptions. However, the more obvious defects of this theory are the zero radius of curvature of the 'theoretical' velocity profile at the jet axis and its prediction of an identical distribution profile for both velocity and other quantities such as temperature and admixture concentration.

The last defect was avoided in Taylor's vorticity transfer theory in which q of equation (16) is taken to be the vorticity. For two-dimensional jet flows, this theory predicts a velocity profile identical with Tollmien's, but the turbulent heat transfer is larger [1], which is in closer agreement with experiment. However, a similar analysis applied to the axi-symmetric case gives results in poorer agreement with experiment [24]. Besides, Liepman and Laufer observed that the effective mixing length is variable across the jet and that the calculated shear stress is quite in error.

To avoid the zero radius of curvature in the velocity profile, Prandtl suggested the hypothesis of constant exchange coefficient i.e.

$$\epsilon(x) = -\overline{uv} \Big/ \left(\frac{dU}{dy}\right) = k\, l_0\, (U_{max} - U_{min}) \qquad (17)$$

where k is a non-dimensional constant, U_{max}, U_{min} are respectively the maximum and minimum velocities in a constant section x of the jet. Gortler worked out the analysis for plane mixing region and the plane submerged jet. The calculated velocity profile falls off too slowly at the jet edge. But for a wake, it has been shown that if the exchange coefficient is assumed to be that given by (17) multiplied by the intermittency factor, the calculated velocity distribution agrees remarkably well with experiment. Thus though criticised as untenable on physical grounds [25] the combination of constant exchange coefficient with intermittency factor gives an undoubtedly important improvement on the conventional mixing length theory of free turbulence.

Karman's similarity theory can be regarded as an extension of the momentum transfer theory in which the mixing length is determined from the assumption that, referred to axes moving with the local mean velocity, the eddying motions are similar at all points. This leads to the formula [19]

$$\ell = k \left|\frac{\partial U}{\partial y}\right| \Big/ \left|\frac{\partial^2 U}{\partial y^2}\right|$$

where k = 0.4 is a universal constant. The theory appears to be much more logical than the others; nevertheless, it is difficult to be applied, especially at stationary points and inflexion points of the velocity profile [24].

The mixing length theories all suffer from two general defects. First, the eddy viscosity and the transverse perturbation are required to vanish in the plane of symmetry, but actually they attain their maxima there. Secondly, the mixing lengths determined from experimental data are all large fractions (greater than 0.1) of the width of jet or wake, which contradicts the basic argument of its smallness. It is believed [24] that the turbulence and eddy viscosity depend on the overall conditions rather than on the local conditions such as the velocity gradient.

Reichardt's theory is quite different from the various versions of the mixing length theory. He assumed a constant static pressure and that

$$UV + \overline{uv} = -\Lambda(x) \frac{\partial(U^2 + \overline{u^2})}{\partial y}$$

where Λ (x) is analogous to the mixing length but has no intuitive meaning. The equation of motion is then reduced to one in $(\overline{u}^2 + U^2)$ with Λ (x) as a coefficient. The function Λ (x) is then determined from the experimentally measured profiles of $(\overline{u}^2 + U^2)$. This inductive theory may also be generalized for the transfer of heat and mass.

2.6 Analysis of Turbulent Jets in a Coflowing Stream

The main problem for the macroscopic description of a turbulent jet in a coflowing stream is to determine the mean velocity field. Nearly all analyses assume the similarity of some experimentally determined transverse profiles. Then the momentum conservation equation provides one relation between the two scales (which are functions of the axial distance) for the universal profile. Another relation is either provided by multiplying the equation of

motion by $U^m y^n$ (m, n being integers) and then integrating across the plane x = constant, as done by Tetervin and Lin (33). Or it is left as an empirical relation (26) or obtained from further hypothesis (1). It should be noted that in the integral method it is required to evaluate the shear stress $\overline{uv}$. This can be done by using the mixing length theory as adopted by Squire and Trouncer, or it may be assumed to have the same dimensionless profile as for the free jet(11).

The initial region of the jet can be considered as a plane mixing region. This problem was examined by Kuethe using the mixing length theory and the constant exchange coefficient hypothesis (1, 18). Abramovich (1) presented a method in which the velocity profiles are assumed self-similar:

$$\frac{U_j - U}{U_j - U_1} = (1 - \eta^{1.5})^2 \quad , \quad \eta = \frac{y - y_2}{b_o}$$

where b_o is the distance from the axis to the edge of the jet.

U_j is the initial jet velocity, $y = \pm y_2(x)$ are the boundaries of the potential core, and mixing length theory was used to predict the spreading of the jet, giving

$$b_o = c \left| \frac{R - 1}{R + 1} \right| x \quad \text{where } R = \frac{U_j}{U_1} > 0$$

where C = 0.27 for a plane jet is an empirical constant. These, together with the equation of continuity and the conservation of momentum, determined the various geometric characteristic lines (e.g. $y_2(x)$) and the transverse velocity V as a function of R.

For the main region Abramovich assumed

$$\frac{U - U_1}{U_c - U_1} = (1 - \xi^{1.5})^2 \quad ; \quad \xi = \frac{y}{b_o}$$

and

$$\frac{db_o}{dx} = C_2 \frac{|U_c - U_1|}{U_c + U_1}$$

where U_c is the axial velocity and $C_2 \doteq 0.22$. Together with the conservation of momentum equation (11), b_o and U_c can thus be solved as functions of x. He further determined the transition region by assuming the outer boundary in this region to be approximately the straight line extended from the outer boundary of the initial part. The end of the transition region is determined from the condition that the velocity and the thickness of the jet at that section must be the same as at the beginning of the main region.

The effect of the non-uniformity of the initial velocity distributions due to the wall boundary layers was also investigated. It seems that this is but to lead to a faster diffusion along the jet axis.

Although this analysis is fairly complete, yet the two assumptions about b_o seem not very convincing. Besides, the assumption of self-preservation of velocity excess restricts its range of applicability.

$\frac{y}{l_o}$ In the analysis of Hill (11), the equation (10) is multiplied by and integrated across the entire jet. The universal distribution for the shear stress $\overline{uv}$ involved was assumed the same as for the free-jet. The results have been plotted and compared with experimental data. They agree fairly well for $1 < \frac{U_o}{U_i} < 2.5$. This lower limit is undoubtedly related to the self-preservation assumption while the upper limit seems a result of the assumed invariance of $\overline{uv}/U_o^2$ with R.

Much better agreement with experiment seems to be obtained in the correlation theory based on some assumptions suggested by the Engineering Experiment Station of the University of Illinois (26 and 34 a.b.c.). The basic assumptions are that the axial momentum flux, relative to that of the ambient stream, due to a point source is conserved, and that the momentum from individual point sources treated as infinitesimal area sources may be superimposed to give the momentum diffusion from a source of finite area. The momentum diffusion from a point source is obtained by generalizing Reichardt's assumption to include the case when there is a uniform coflowing stream. This generalized assumption is actually the self-preservation of excess dynamic pressure. The solutions to axi-symmetric (34a, b, c), and two-dimensional (26) jet-mixing problems have been worked out. The result for the two-dimensional case is

$$\frac{U^2 - U_i^2}{U_j^2 - U_i^2} = \frac{1}{2}\left\{\operatorname{erf}\left[\frac{D}{2b}\left(\frac{2y}{D} + 1\right)\right] - \operatorname{erf}\left[\frac{D}{2b}\left(\frac{2y}{D} - 1\right)\right]\right\} \qquad (18)$$

where D is the initial jet width, b is an empirical spreading coefficient.

From this the velocity distribution was computed:

$$\frac{U_c - U_i}{U_j - U_i} = \left\{\left(\frac{1}{2\epsilon}\right)^2 + \left(\frac{1+\epsilon}{\epsilon}\right)\operatorname{erf}\left(\frac{D}{2b}\right)\right\}^{\frac{1}{2}} - \frac{1}{2\epsilon} \qquad (19)$$

$$\frac{U-U_1}{U_c-U_1} = \frac{\{1+2\epsilon(1+\epsilon)\}\left[\mathrm{erf}\left(\frac{D}{2b}\left\{\frac{2y}{D}+1\right\}\right)-\mathrm{erf}\left(\frac{D}{2b}\left\{\frac{2y}{D}-1\right\}\right)\right]^{\frac{1}{2}}-1}{\left[1+4\epsilon(1+\epsilon)\,\mathrm{erf}\left(\frac{D}{2b}\right)\right]^{\frac{1}{2}}-1} \qquad (20)$$

where $\epsilon = \frac{U_j-U_1}{2U_1}$

When $\frac{D}{2b}$ is very small, (19), (20) reduce to

$$\frac{U_c-U_1}{U_j-U_1} = \left[\left(\frac{1}{2\epsilon}\right)^2+\left(\frac{1+\epsilon}{\epsilon}\right)\frac{2}{\sqrt{\pi}}\left(\frac{D}{2b}\right)\right]^{\frac{1}{2}}-\frac{1}{2\epsilon} \qquad (19a)$$

$$\frac{U-U_1}{U_c-U_1} = \frac{\left[1+\frac{8\epsilon(1+\epsilon)}{\sqrt{\pi}}\left(\frac{D}{2b}\right)\exp\left\{-\left(\frac{y}{b}\right)^2\right\}\right]^{\frac{1}{2}}-1}{\left[1+\frac{8\epsilon(1+\epsilon)}{\sqrt{\pi}}\left(\frac{D}{2b}\right)\right]^{\frac{1}{2}}-1} \qquad (20a)$$

Weinstein et al found that when $\frac{x}{D} > 30$, the two sets of equations (19, 20) and equations (19a, 20a) give practically identical results. It is important to note that this is also the region where close self-preservation is obtained.

From equation (18) we have

$$\frac{U^2-U_1^2}{U_c^2-U_1^2} = \frac{\mathrm{erf}\left[\frac{D}{2b}\left(\frac{2y}{D}+1\right)\right]-\mathrm{erf}\left[\frac{D}{2b}\left(\frac{2y}{D}-1\right)\right]}{2\,\mathrm{erf}\left[\frac{D}{2b}\right]} \qquad (21)$$

When $\frac{D}{2b}$ is very small (corresponding to about $\frac{x}{D} > 30$), this reduces to

$$\frac{U^2-U_1^2}{U_c^2-U_1^2} = e^{-\left(\frac{y}{b}\right)^2} \qquad (21a)$$

This has an important meaning, for it asserts the self-preservation of the excess dynamic pressure when $\frac{x}{D}$ is sufficiently large.

This theory is quite successful in correlating jet-mixing problems for both moving and stationary ambient by using one empirical parameter b. This is also indirectly upheld by the experimental confirmation of the self-preservation of excess dynamic pressure, and not of the velocity, for a round jet over a fairly long range of x values (16). Although it may seem that far downstream the two forms of self-preservation tend to be equivalent, yet their implications are different. At sufficiently far downstream of an axi-

symmetric jet (16),

$$(U_c^2 - U_1^2) \propto X^{-1} \tag{22}$$

Now when $(U_c - U_1) \ll U_1$,

$$U_c^2 - U_1^2 = (U_c + U_1)(U_c - U_1) \propto (U_c - U_1)$$

But for the wake-like self-preservation of velocity for an axi-symmetric jet to hold, we must have

$$(U_c - U_1) \propto X^{-\frac{2}{3}} \tag{23}$$

Equations (22) and (23) show the inconsistency between the two kinds of self-preservation within the range $X/H < 80$ where H is the momentum thickness.

2.7 Location of Axis for a Jet in a Uniform Deflecting Stream

It seems that all past works on jets emitted at an angle to an ambient stream have concerned mainly with the location of the jet axis. This is understandable since it is plausible that the jet will behave like an undeflected one along the axial direction.

Some analyses based on the superposition of flow patterns were worked out (1); but as can be expected, the results must be far from having satisfactory experimental agreement since the non-linearity of the equations of motion indicates at once that superposability can occur only if certain conditions are fulfilled (2). Empirical equations for the jet axis were also proposed (1). However, a more satisfactory approximate method is that proposed by Volinsky (1). The fluid jet is divided into slices and each slice is assumed to act as a "solid" wing in the external stream, thus producing a pressure difference at the forward and back surfaces of the jet. The curvature of the jet axis is then determined from the condition of balancing this force by the centrifugal force. Taking cartesian co-ordinates with x and y axes parallel and perpendicular respectively to the direction of the external stream in the plane containing the initial jet velocity vector, the resulting equation for the axis is

$$C_n \rho_w U_1^2 h \frac{(1+y'^2)^{1.5}}{y''} \sin^2\alpha = -2 \rho_r v^2 S_n \tag{24}$$

where ρ_w, U_1 are respectively the density and velocity of the external stream,

h is the jet width in z direction

S_n is the cross-sectional area of the jet normal to the axis,

C_n is a coefficient depending on the shape of S_n,

ρ_v, v are the density and the "mean" velocity of the jet in a cross-section

$\tan \alpha = y'$

One boundary condition is of course

$$x = 0 \quad , \quad y = 0 \quad , \quad \alpha = \alpha_0$$

i.e.
$$x = 0 \quad , \quad y = 0 \quad , \quad y' = \tan \alpha_0 \tag{24a}$$

Another condition is furnished by the conservation of y-momentum, which has been taken as (1).

$$\rho_v v^2 S_n \sin\alpha = \rho_{v0} v_0^2 S_{n0} \sin\alpha_0 = \text{constant} \tag{24b}$$

where suffix '0' refers to conditions at x = 0.

The axis equation for a plane jet with ρ_w = constant and U_1 = constant is found to be

$$y = \frac{2}{k}\left(\pm\sqrt{kx + \cot^2\alpha_0} - \cot\alpha_0\right) \tag{25}$$

where
$$k = \frac{C_n \rho_w U_1^2}{\rho_{v0} v_0^2 \sin^2\alpha_0} \cdot \frac{1}{D}$$

D being the initial jet thickness, as before; the two solutions of equation (25) correspond respectively to $\alpha_0 \lesseqgtr \frac{\pi}{2}$.

Though experimental verification of equation (25) has been claimed (1), this method has several defects. The assumption of "wing" action is doubtful, since ambient fluid is continuously entrained and there is strictly no finite boundary of the jet. Besides, the meaning of "mean" velocity is quite ambiguous. An evidence is that v in equation (24b) cannot be the same as the v used to derive equation (24) unless $\alpha = \alpha(x)$. In fact, even equation (24b) is not exact since the induced momentum in the ambient fluid has been neglected. A much more obvious source of error would be assumed constancy of C_n for the fitting of experimental data to

this "theoretical" curve depends on the choice of C_n which varies from 1 to 3(1). Indeed, Abramovich has shown that this last defect would require the analysis to produce an absurd result for the air curtain problem.

However, equation (25) gives some support to the experimentally-established proposition that for a jet emitted into a deflecting stream of the same fluid the location of jet axis is independent of the velocity ratio if all lengths are divided by $R^2 = U_j^2 / U_1^2$. For equation (25) may be written as

$$\frac{\lambda}{2}\left(\frac{y}{R^2}\right) = \pm\sqrt{\lambda\left(\frac{x}{R^2}\right) + \cot^2\alpha_0} \; - \cot\alpha_0 \qquad (25a)$$

where $\lambda = C_n/(D\sin^2\alpha_0)$. But this proposition must not be expected to hold for a large range of R values (at least from the consideration of equation (25) alone) for C_n actually depends on the ratio of local jet velocity to ambient stream velocity (see § 3), and hence on R. Nevertheless, it is of some practical value since the form of the axis equation is explicitly determined.

2.8 Conclusion

Most previous works have attempted to show the validity of the self-preservation of excess velocity for jet flows. However, this is not a good approximation for the whole flow field. Some of the criticism based on experimental facts have already been given in Section 2.2 (p. 10). We shall now give some theoretical discussion. The self-preservation of excess velocity

$$U = U_1 + U_0 f\left(\frac{y}{l_0}\right) \qquad (12)$$

permits us to write the momentum integral equation

$$\int_{-\infty}^{\infty} U(U-U_1)\,dy = F \qquad (11)$$

as

$$l_0 = \frac{F}{U_0(U_1 I_1 + U_0 I_2)}$$

where

$$I_n = \int_{-\infty}^{\infty} f^n(\eta)\,d\eta \quad , \eta = \frac{y}{l_0}$$

Now this self-preservation requires (see cases (b), (c), (d) of

Section 2. 4)

$$U_o = C\,(x - x_o)^{-\frac{1}{2}} \tag{26}$$

where c is a constant

$$\therefore \ell_o = \frac{F}{C}\,\frac{(x-x_o)}{U_1 I_1 (x-x_o)^{\frac{1}{2}} + C I_2} \tag{27}$$

Thus small and large values of $(x-x_o)$ correspond to type (c) and (d) respectively. This equation indicates clearly the necessary inexactness of the self-preservation of the excess velocity. However, it should be noted that although ℓ_o cannot be proportional to $(x-x_o)$, yet, by a proper choice of another virtual origin, it is possible to fit an approximate linear relation between l_o and x for a small range of x in the upstream region. Thus conditions for type (c) self-preservation can still be satisfied approximately even for not too large axial velocity excess. Hence, it is not surprising that this self-preservation was found (28) for values of U_o/U_1 down to 1.7 since the range of $\frac{x}{D}$ (D is the initial jet width) is only from 30 to 70.

The other form of self-preservation enunciated is that of excess dynamic pressure. We shall presently show that theoretically this is not any better approximation. Using equation (7), we can write the equation of motion, equation (10), for a turbulent jet as

$$\frac{\partial U^2}{\partial x} + \frac{\partial (UV + \overline{uv})}{\partial y} = 0 \tag{28}$$

The self-preservation of excess dynamic pressure is tantamount to

$$U^2 = U_1^2 + (U_c^2 - U_1^2)\, f\left(\frac{y}{b(x)}\right) \tag{29}$$

Further assuming*

$$UV + \overline{uv} = (U_c^2 - U_1^2)\, g\left(\frac{y}{b(x)}\right) \tag{29a}$$

we reduce equation (28) to

---

* This is analogous to, but more general than, the assumption used in Reichardt's inductive theory of turbulence.

$$\frac{d}{dx}(U_c^2 - U_1^2) f - (U_c^2 - U_1^2) \frac{y b'}{b^2} f' + (U_c^2 - U_1^2) \frac{1}{b} g' = 0$$

or
$$\frac{b}{U_c^2 - U_1^2} \frac{d(U_c^2 - U_1^2)}{dx} f - b' \left(\frac{y}{b}\right) f' + g' = 0 \qquad (30)$$

where dashes denote differentiation. Now the functions f, g are assumed universal functions of $(\frac{y}{b})$. The coefficients in equation (30) must therefore be constant since that of g' is unity

$$\therefore \quad b = k_1 = \text{constant or } b = k_1 (x - x_o) \qquad (31)$$

and
$$\frac{b}{(U_c^2 - U_1^2)} \frac{d(U_c^2 - U_1^2)}{dx} = \text{constant}$$

$$\therefore \quad U_c^2 - U_1^2 = k_2 (x - x_o)^n \qquad (31a)$$

where k_2 is also a constant and the indicial constant n is to be determined from the momentum integral equation (11). Thus

$$F = \int_{-\infty}^{\infty} U(U - U_1) dy$$

$$= b \int_{-\infty}^{\infty} (U^2 - U_1^2) \frac{dy}{b} - U_1 \int_{-\infty}^{\infty} (U - U_1) dy$$

$$\therefore F = (x - x_o)^{1+n} \left\{ k_1 k_2 \int_{-\infty}^{\infty} f(\eta) d\eta \right\} - U_1 \int_{-\infty}^{\infty} (U - U_1) dy \qquad (32)$$

Now the last integral is not a simple function of $(x - x_o)$ under the assumption of equations (29), (31a); in particular it cannot be proportional to $(x - x_o)^{1+n}$. Hence except when $U_1 = 0$, the self-preservation of excess dynamic pressure cannot hold theoretically. When $U_1 = 0$, the last term of equation (32) vanishes identically and $n = -1$, i.e. the axial dynamic pressure is inversely proportional to the axial distance from the virtual origin. However, the integral $\int_{-\infty}^{\infty} (U - U_1) dy$ actually represents the excess volume flow of fluid across a plane x = constant. It is a well-known experimental fact that this will tend to a constant as $x \to \infty$. Hence, sufficiently far downstream the last term of equation (32) can be treated as a constant and self-preservation of excess dynamic pressure will be approached with $n \to -1$. However, the rate of approach depends on the magnitude of U_1, or more correctly on $R = U_1 / U_1$. When R is not much greater than unity, the approach to self-preservation of excess dynamic pressure may be very slow.

It should be noted that the self-preservation of excess dynamic pressure implies a single linear law for the growth of jet width (equation 31) while that of excess velocity requires a single inverse square root law for the decay of axial velocity excess (equation 26). But actually neither of these are fulfilled by experimental data. Indeed, from the above critical discussions, it is evident that neither form of self-preservation can be exactly true. But the surprising fact revealed by experiments is that each of these seems to exist in an appropriate region. It appears, therefore, that this might be due to some characteristic nature of the mean velocity field, which is only loosely governed by the equation of motion. This is not novel, as is exemplified by the fairly successful prediction of the mean velocity profiles by the mixing length theories while the invalidity of these theories is now quite well-known.

In conclusion, we may, based on experimental evidence, tentatively suggest that when $\frac{U_o}{U_1} > 1$ (i.e. for those sections with the jet axial velocity excess greater than the ambient stream velocity) self-preservation of excess velocity is a good approximation while when $\frac{U_o}{U_1} < a$ where $a > 1$, say $\frac{U_o}{U_1} < 2$, (i.e. for those sections with the jet axial velocity excess less than a certain multiple of, say, twice, the ambient stream velocity) the self-preservation of excess dynamic pressure can be considered as valid. But it must be mentioned that very far downstream where $\frac{U_o}{U_1}$ is very small, no experimental data are yet available. Hence the above suggestion of validity for the two kinds of self-preservation must not be deemed to include the far-downstream region.

Turning to the location of the axis of a deflected jet, there does not seem to be any really theoretically sound method available. The proposition of the independence of the axial position on the jet-to-ambient velocity ratio, R, in reduced coordinates (i.e. when the co-ordinates of axial points are divided by R^2) may be at least of some practical use, if not of any general significance.

3. Analysis

The main purpose of the present investigation is to verify that a two-dimensional jet deflected by a small angle by the external stream behaves similarly to a straight jet. This will be so if the governing conditions referred to some appropriate coordinates are identical. It is the purpose of this analysis to ascertain whether this condition is fulfilled.

We shall define the jet axis as the streamline passing through the central plane of the jet nozzle exit. The suitable coordinate system is an orthogonal curvilinear one (S, n) where the S- and n-directions are respectively parallel and perpendicular to the jet axis (n = 0). The Navier-Stokes equations can be written as (see e.g. 31).

$$\frac{\partial V_s}{\partial t} + \frac{\rho}{\rho+n} V_s \frac{\partial V_s}{\partial S} + V_n \frac{\partial V_s}{\partial n} + \frac{V_s V_n}{\rho+n} = -\frac{\rho}{\rho+n}\frac{\partial p}{\partial S} + \nu\left[\frac{\rho^2}{(\rho+n)^2}\frac{\partial^2 V_s}{\partial S^2} + \frac{\partial^2 V_s}{\partial n^2} + \frac{1}{\rho+n}\frac{\partial V_s}{\partial n} - \frac{V_s}{(\rho+n)^2} + \frac{2\rho}{(\rho+n)^2}\frac{\partial V_n}{\partial S} - \frac{\rho}{(\rho+n)^3}\frac{d\rho}{dS} V_n + \frac{\rho n}{(\rho+n)^3}\frac{d\rho}{dS}\frac{\partial V_s}{\partial S}\right] \quad (33)$$

$$\frac{\partial V_n}{\partial t} + \frac{\rho}{\rho+n} V_s \frac{\partial V_n}{\partial S} + V_n \frac{\partial V_n}{\partial n} - \frac{V_s^2}{\rho+n} = -\frac{\partial p}{\partial n} + \nu\left[\frac{\partial^2 V_n}{\partial n^2} - \frac{2\rho}{(\rho+n)^2}\frac{\partial V_s}{\partial S} + \frac{1}{\rho+n}\frac{\partial V_n}{\partial n} + \frac{\rho^2}{(\rho+n)^2}\frac{\partial^2 V_n}{\partial S^2} - \frac{V_n}{(\rho+n)^2} + \frac{\rho}{(\rho+n)^3}\frac{d\rho}{dS} V_s + \frac{\rho n}{(\rho+n)^3}\frac{d\rho}{dS}\frac{\partial V_n}{\partial S}\right] \quad (34)$$

$$\frac{\rho}{\rho+n}\frac{\partial V_s}{\partial S} + \frac{\partial V_n}{\partial n} + \frac{V_n}{\rho+n} = 0 \quad (35)$$

where V_S, V_n are the components of the velocity vector, p is the static pressure, ρ is the radius of curvature of the S-axis. V_S, V_n and p are then separated into mean and fluctuating parts

$$V_S = U + u$$

$$V_n = V + v$$

$$p = P + p'$$

These are substituted into equations (33) - (35) and the mean values are taken, resulting in equations analogous to equations (5) - (7). The general assumptions of Section 2.3 are made.

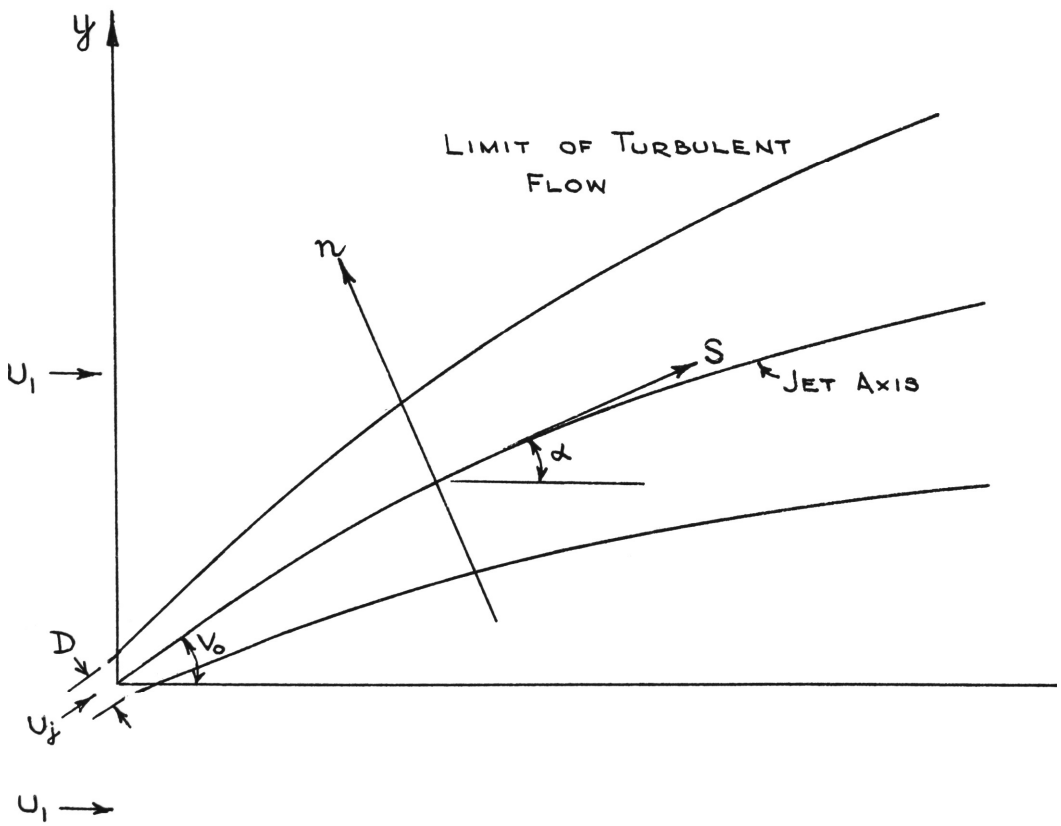

Fig. T2: Coordinate System.

(A1) $V \ll U$ and the length scale of variation of the velocity in the n-direction, l, is of an order less than that in the S-direction, L.

(A2) Reynolds number similarity is obtained.

(A3) $\bar{u}^2$, $\overline{uv}$, $\bar{v}^2$ are assumed of order $\left(\frac{l}{L}\right)^{\delta} U_s^2$, and U of order $U_s \left(\frac{l}{L}\right)^{\delta-1}$, where $U_s = U_{max} - U_{min}$ is the total variation of U in a section, and $\delta = 1$ for jets and $\delta = 0$ for wakes.

In addition, we shall assume

(A4)' ρ is of order not less than L.

Equation (35) approximates to

$$\frac{\partial U}{\partial S} + \frac{\partial V}{\partial n} = 0 \tag{36}$$

Hence V is of order $(\frac{1}{L})\, U_s$.

The terms of the mean value of equation (34)

$$\frac{\rho}{\rho+ny} U \frac{\partial V}{\partial S} + V \frac{\partial V}{\partial n} + \frac{\rho}{\rho+ny} \frac{\partial \overline{uv}}{\partial S} + \frac{\partial \overline{v^2}}{\partial n} - \frac{U^2-V^2}{\rho+ny} - \frac{\overline{u^2}-\overline{v^2}}{\rho+ny} = -\frac{\partial p}{\partial n} + \nu[\cdots]$$

$$U_s^2\left(\frac{l}{L}\right)^{\delta} L^{-1} \quad U_s^2\left(\frac{l}{L}\right)^{2} l^{-1} \quad U_s^2\left(\frac{l}{L}\right)^{\delta} L^{-1} \quad U_s^2\left(\frac{l}{L}\right)^{\delta} l^{-1} \quad U_s^2\left(\frac{l}{L}\right)^{-2+2\delta} \rho^{-1} \quad U_s^2\left(\frac{l}{L}\right)^{\delta} \rho^{-1}$$

have the orders of magnitude written below them. The largest terms are of order $U_s^2 (l L^{-1})^{\delta} l^{-1}$, and to this order, the equation is

$$\frac{\partial}{\partial n}\left(p + \overline{v^2}\right) = \frac{U^2}{\rho} \tag{37}$$

This equation (37) shows that to a first approximation the effect of jet axial curvature is to induce a transverse pressure gradient, thus justifying to some extent Volinsky's method (Section 2.7). But this is of course by no means produced by the "wing" action as assumed there. Integrating equation (37) across the jet, we have

$$\Delta\left(p+\overline{v^2}\right) = \frac{1}{\rho}\int_{-\infty}^{\infty} U^2\, dn + A(S) \tag{38}$$

where ∞ has the same meaning as in boundary layers. This shows that the pressure difference actually depends on the jet velocity as well as on that of the ambient stream. Thus the non-constancy of C_n of equation (24) is apparent.

The order of magnitude of $\frac{\rho}{L}$ can be estimated by using equation (25). If we now take (x, y) as the cartesian coordinates through (S=0, n=0), then from equation (25)

$$\rho = \frac{(1+y'^2)^{\frac{3}{2}}}{y''} = \frac{(1+4\cot^2\alpha_0 + 4kx)^{\frac{3}{2}}}{2k} \qquad (39)$$

where $k = C_n U_1^2/(DU_j^2 \sin^2\alpha_0)$.

Here we are considering a (plane) jet of initial thickness D with initial velocity U_j at an angle α_0 to the ambient stream of velocity U_1 in the x-direction. Equation (39) shows that ρ increases with x (and hence with S too) at a rate which increases with $R = U_j/U_1$. Thus for the region not too near the nozzle exit, we can replace (A4)' by (A4) $\rho \gg L$

Furthermore, for small x, equation (39) gives

$$\frac{\rho}{D} \doteq \frac{R^2 \sin\alpha_0 (1+4\cot^2\alpha_0)^{\frac{3}{2}}}{2C_n}$$

Now $C_n < 3$ (§2.7)

$$\therefore \quad \frac{\rho}{L} > \left(\frac{D}{L}\right)\frac{R^2}{6}\frac{(1+3\cos^2\alpha_0)^{\frac{3}{2}}}{\sin\alpha_0} \qquad (40)$$

Equation (40) shows that for a given $R \neq 0$, there always exists an ϵ such that $\frac{\rho}{L} \gg 1$ whenever $\alpha \ll \epsilon$. Hence assumption (A4) is also true in the region close to the nozzle exit if either R is sufficiently large or α_0 is sufficiently small.

The application of assumption (A4) shows that as far as the momentum diffusion is concerned, equation (37) may be simplified to

$$P + \overline{v^2} = P_0 \qquad (41)$$

where P_0 may be considered as the mean static pressure in the surrounding fluid in the region considered. With equations (41) and (36), equation (33) can be reduced to*

$$U\frac{\partial U}{\partial S} + V\frac{\partial U}{\partial n} + \frac{\partial \overline{uv}}{\partial n} = 0 \qquad (42)$$

by a comparison of order of magnitude for the different terms.

* Assuming $dP_0/dS = 0$. See last paragraph of Section 4.4

Now equations (36), (41) and (42) are the same as the set for a straight jet. But in addition, a momentum integral condition must still be satisfied, for it represents a boundary condition. Integrating equation (42), we have*

$$\int_{-\delta_i}^{\delta_0} U(U-U_A)\,dn \doteq \text{const.} \qquad (43)$$

where δ_2 , δ_0 are the jet thicknesses on the two sides of the axis, $U_A = U_1 \cos\alpha$ is the component of the ambient stream velocity in the S-direction, α (s) being the angle between the S- and x- axes. Equation (43) differs from equation (11) for a straight jet in the variability of α . They will be approximately equivalent ** if α is nearly constant in the range of S values considered, which is true either

(i) when α is small, for then $\cos\alpha = 1 - \frac{\alpha^2}{2}$ changes little, or

(ii) when $\frac{S_2-S_1}{\rho} \ll 1$ where (S_1, S_2) is the interval of S considered.

Another particular case is -

(iii) When $U \gg U_A$ in a large part of a jet cross-section in the S-interval considered. For then equation (43) simply approximates to that for a submerged jet.

When α_0, the initial angle between the jet and the ambient stream, is sufficiently small+, both conditions (i) and (ii) will be satisfied. Condition (i) is also true for all sufficiently far downstream regions+, , and condition (ii) holds too for a sufficiently large value++ of R. In any of these cases, therefore, equations (36), (41), (42), (43) for a two-dimensional deflected jet flow are the same as for straight jet flows. Hence we should expect the momentum diffusion to be similar. However, as these equations are not complete governing conditions, the similarity can only be regarded as possible and probable; full justification must still be completed by experiment. Subject to this, then assumptions (A1) to (A3), well verified for undeflected free turbulent flows, are justified for use in the present analysis.

---

* Using the assumption $\rho \gg L$

** The case $U_1 = 0$ needs no consideration, for the flow is simply a submerged jet.

\+ This means that for condition (i), $\cos\alpha$ may be considered as 1, commensurate with the accuracy of other measurements. A similar meaning applies to the case for condition (ii).

++ This value increases with (S_2-S_1). An estimate can be made using equation (40).

The important property of self-preservation should also be expected to hold for a deflected jet. In this present investigation we will be mainly interested in the intermediate region of the flow field, i.e. where $\frac{U_0}{U_1}$ is not very large. Hence we shall employ the approximation of self-preservation of excess dynamic pressure. Here we shall define it as

$$\frac{q - q_A}{q_c - q_A} = f\left(\frac{n}{b(S)}\right) \tag{44}$$

where $q = U^2$, suffices C and A refer respectively to the values at $n = 0$ and in the ambient fluid.

Now

$$\frac{q - q_A}{q_c - q_A} = \frac{U^2 - U_1^2 \cos^2\alpha}{U_c^2 - U_1^2 \cos^2\alpha}$$

$$= \frac{U^2 - U_1^2}{U_c^2 - U_1^2}\left[1 + \frac{U_1^2 \sin^2\alpha}{U_c^2 - U_1^2}\right]^{-1} + \frac{U^2 \sin^2\alpha}{U_c^2 - U_1^2 \cos^2\alpha}$$

But generally we should have

$$\frac{U_1^2 \sin^2\alpha}{U_c^2 - U_1^2} \ll 1,$$

for if $\left(\frac{U_c}{U_1}\right)^2$ is not much greater than 1, α must be small, and if α is not small, $\left(\frac{U_c}{U_1}\right)^2 \gg 1$. Hence

$$\frac{q - q_A}{q_c - q_A} \doteq \frac{U^2 - U_1^2}{U_c^2 - U_1^2} - \left[\frac{U_1^2(U^2 - U_1^2)\sin^2\alpha}{(U_c^2 - U_1^2)^2} - \frac{U^2 \sin^2\alpha}{U_c^2 - U_1^2 \cos^2\alpha}\right]$$

When α_0 is not too large, α will be sufficiently small in some interval of S for the expression in the square bracket to be negligible compared with the other term, for U not too close to U_1. To this approximation, then

$$\frac{q - q_A}{q_c - q_A} = \frac{U^2 - U_1^2}{U_c^2 - U_1^2} = f\left(\frac{n}{b(S)}\right) \tag{44a}$$

This equation is subsequently confirmed by experiment.

Although the analysis so far emphasises on the similarity of the deflected and undeflected jet flows, it must not be misconceived that they have no intrinsic difference. Because of the axial curvature,

the flow field is no longer symmetrical about the S-axis. Equation (36) shows this very clearly through the U^2/ρ term. This unsymmetrical pressure gradient implies that the diffusion must be different on the concave side (negative n) and on the convex side (positive n). Therefore different length scales b_i and b_o must be used for $n < 0$ and $n > 0$ respectively. The difference $(b_i - b_o)/b_i$ must of course be much less than 1 if assumption (A4) is satisfied. Indeed, when $S \to \infty$, (hence $\rho \to \infty$), $\frac{d}{dx}(b_i - b_o)$ must tend to zero as suggested by equation (42). Nevertheless, the universal function f of equation (44) should be approximately the same for $n < 0$ and $n > 0$ as for the undeflected jet, with a proper choice of b.

Anticipating* equation (44a) and taking f as a gaussian curve (equation 21a; Section 5.3)

$$\frac{q - q_a}{q_c - q_a} = f\left(\frac{n}{b}\right) = e^{-\frac{1}{8^2}\left(\frac{n}{b}\right)^2} \tag{45}$$

we can derive two important properties of the jet axis (S-axis). Consider an excess dynamic pressure contour, i.e. $q - q_a$ = constant. Equation (45) gives

$$(q_c - q_a) f\left(\frac{n}{b}\right) = C = \text{const.} \tag{45a}$$

The tangent to this curve is inclined to the local S-direction at an angle β given by

$$\tan\beta = \frac{dn}{dS} = -\frac{c b q_c'}{(q_c - q_a)^2 f'} + \frac{n b'}{b} \tag{46}$$

From equation (45) we find that when $n \to 0$

$$f' \sim n \quad , \quad f'' \to -\frac{2}{8^2} \tag{47}$$

By equation (47), then we have

$$\tan\beta \sim n^{-1} \tag{47a}$$

$$\therefore \quad \cos\beta \sim n \tag{47b}$$

$$\sin\beta \to 1 \tag{47c}$$

(P1) Hence the excess dynamic pressure contours intersect the S-axis orthogonally.

The curvature of the contour of equation (45a) is

*It should be noted that the following arguments are also valid with the assumption of self-preservation of excess velocity.

$$K = \frac{d}{d\bar{c}}(\alpha+\beta) = \cos\beta\,\frac{d\alpha}{dS} + \cos\beta\,\frac{\partial\beta}{\partial S} + \sin\beta\,\frac{\partial\beta}{\partial n}$$

$$= \frac{\cos\beta}{\rho} + \cos^3\beta\,\frac{\partial}{\partial S}\left(\frac{dn}{dS}\right) + \sin\beta\cos^2\beta\,\frac{\partial}{\partial n}\left(\frac{dn}{dS}\right) \qquad (48)$$

where $\bar{c}$ is the arc length of the contour. Differentiating equation (46), we have

$$\frac{\partial}{\partial S}\left(\frac{dn}{dS}\right) = \frac{C}{(q_c-q_\infty)^3 f'}\left[(bq_c' + bq_c'')(q_c-q_\infty) - 2bq_c'^2 + \right.$$
$$\left. + \frac{b'}{b}q_c'(q_c-q_\infty)\frac{f''n}{f'}\right] + \frac{(b''b-b'^2)}{b^2}n \qquad (46a)$$

$$\frac{\partial}{\partial n}\left(\frac{dn}{dS}\right) = \frac{Cq_c'}{(q_c-q_\infty)^2}\frac{f''}{f'^2} + \frac{b'}{b} \qquad (46b)$$

Hence equations (46)-(48) show that when $n \to 0$, $K \to K_0(S) = 0$. (49)
Further, differentiating equation (48) and making use of equations (46)-(48), we have

$$\frac{dK}{d\bar{c}} \to \frac{\partial K}{\partial n} \sim \frac{k_1(S)}{\rho} + k_2(S)n, \text{ as } n \to 0.$$

If ρ is sufficiently large, then

$$\frac{dK}{d\bar{c}} \to 0 \quad \text{as } n \to 0 \qquad (50)$$

(P2) Equations (49)-(50) together with physical intuition suggests that the excess dynamic pressure contours have maximum curvature at or very near the jet axis.

4. Test Facilities and Experiment

4.1 Test Objective

The principal objective of the experiments was to verify the similarity of momentum diffusion of a deflected jet with an undeflected one under the conditions stated in Section 3. This would be established if the excess dynamic pressure was found to be self-preserving and the transverse length scale b to vary with the axial distance in a way similar to a straight jet. Measurements of the dynamic pressure were therefore made at various positions of the jet for three different angles between the initial jet velocity and the ambient stream and for several different jet-to-ambient

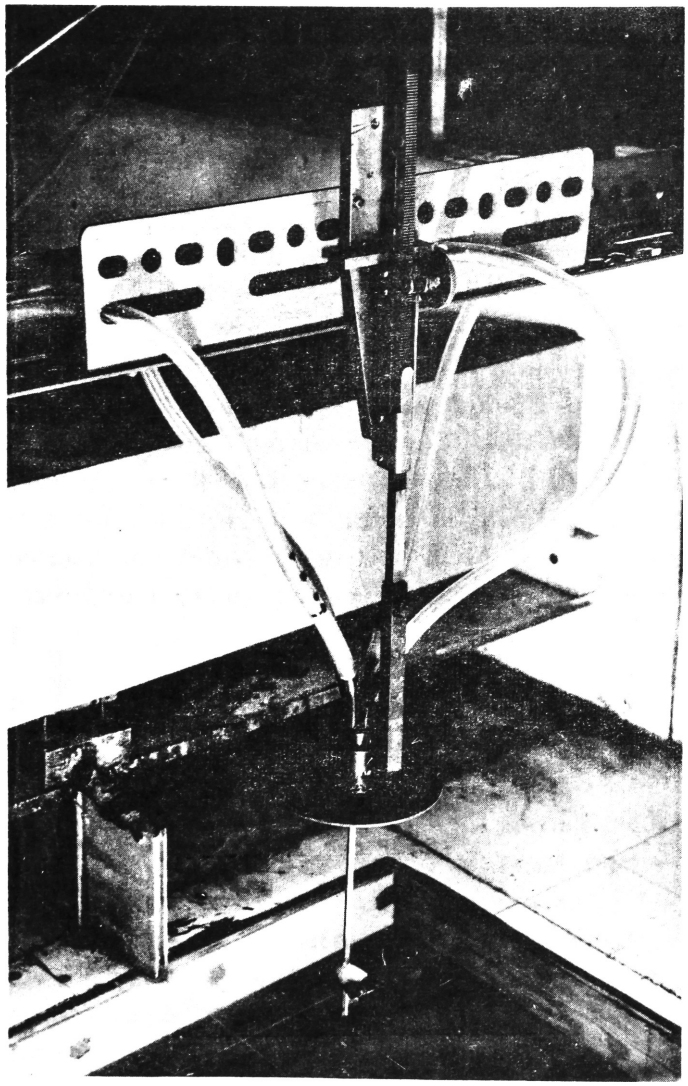

Fig. T3: General View of the Experiment Arrangement.

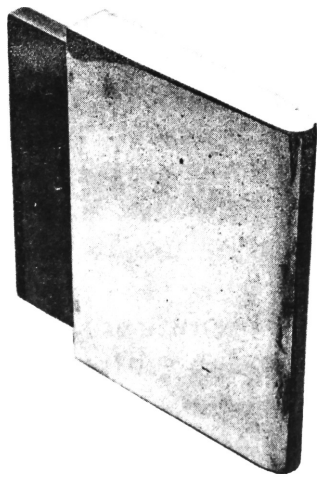

Fig. T4: Jet Deflector.

velocity ratios. The jet axis could then be located and the requisite analyses made.

4. 2 Experimental Arrangement

The experiments were carried out in a water flume, 3 ft. wide x 31 ft. long. The depth of flow was adjustable by means of a gate at the exit end of the flume and was kept at 4 in. throughout the experiments. The water jet was supplied through a $\frac{1}{2}$ in. wide rectangular pipe of 1/4 in. wide by 3-7/8 in. high internal cross-section. The pipe was 12 ft. long from the intake of the flume. The pipe was fixed in the central vertical plane of the flume. From the intake to the exit end of the jet pipe, the flume was covered with perspex plates at 3-7/8 in. above the flume bed in order to prevent the formation of surface waves.

At the exit end of the jet pipe a deflector was fitted which turned the jet by a desired angle. The design of the deflector was based on two principles. Firstly, the external shape must be symmetrical so that the effects of boundary and the wake were the same on both sides, and must be such that these effects were small and the same in all deflectors. The deflector was therefore tapered from 1/2 in. width (outside dimension) to about 1/4 in. width over approximately 3 in. Secondly, the centre-line of the jet should intersect the axis of symmetry of the external shape of the deflector at the exit plane so that the effects of boundary and the wake caused by the deflector in the external stream were the same on both sides of the jet at the initial cross-section. Three deflectors were constructed, for 25°, 17° and 9° turns of the jet.* The jets issuing from these deflectors were all reduced to 1/8 in. initial thickness, the height being very close to 4 in. The reason for reducing the thickness was twofold, viz., to increase the jet velocity and more importantly to obtain a higher height-to-thickness ratio so as to improve the two-dimensionality. The maximum angle α_o was chosen as 25° in order to cope with the conditions imposed by the analysis (Section 3). Besides, it would have been difficult to turn the jet smoothly by a larger angle without increasing the (outside) width of the deflector.

Flow rates of water supplied to the flume (to form the ambient stream) and to the jet pipe were separately gauged with carefully calibrated orifice plates. The orifice heads were frequently checked during all experiments so as to ensure constancy of flow rates in each set.

*Note: See Appendix 3 for details of experiments with deflection angle of 45°.

The maximum flow obtainable in the flume was about 2.5 cusecs, corresponding to an average velocity of 2.5 ft/sec. The maximum flow in the jet pipe was about 0.03 cusec, corresponding to an average initial jet velocity of about 9.5 ft/sec.

4.3 Instruments for Velocity-head Measurement

The instruments used were a velocity probe, a 3/16" (O.D.) Pitot tube, and a 1/8" (O.D.) Pitot tube. The 3/16" Pitot tube was purchased from C.F. Casella and Co. Ltd., London, and the 1/8" Pitot tube from Duff and Macintosh Pty. Ltd. Sydney. As they are standard Prandtl tubes, it is superfluous to describe them any further. The velocity probe was constructed in the laboratory. It consisted of four 1/16" O.D. hypodermic tubes (.011" wall thickness) soldered together to form a probing stem of rhombic cross-section, which was soldered to a brass cap resting on and rotatable about the axis of a brass seat soldered to a circular brass plate with a scale graduated in degrees. A pointer was soldered to the cap to indicate the angle of rotation on the scale. Four holes were drilled at 1/2 in. from the lower end of the probing stem, one into each of the hypodermic tubes. The two side holes, oriented symmetrically about the longitudinal axis of the cross-section, were used to orient the probe correctly for measurement of velocity head by the front and rear holes. A brass cover plate was provided at 1/2 in. above the holes to prevent air being sucked into the rear hole at higher velocities (> 4 ft/sec.). But contact between the plate and the metal stem was found to promote the vibration of the stem at high velocities which made the calibration vary with the depth of water above the plate. To prevent this, the brass cover plate was therefore glued to the lower side of a small piece of streamlined soft rubber which gripped firmly on the probing stem.

The velocity probe and the Pitot tubes were each fixed to a point gauge mounted on a dexion angle spanning horizontally across the flume. The point gauge permitted a vertical traverse of 6 in. measurable to .01 in. Longitudinal (x) and transverse (y) distances of the position of measurement were read from steel tapes (graduated to .01 ft.) fixed on the two walls of the flume and the dexions respectively.

The velocity probe was calibrated in another flume up to a velocity of 6.5 ft/sec. A linear relationship was found between the true velocity head (h) and the measured pressure difference (h_m) between

the front and the rear holes. That is

$$h = \lambda h_m + \mu \tag{51}$$

for h between .025 and .65 ft. or water,

where $\lambda \doteqdot 0.66$

$\mu \doteqdot 0.006$ ft. of water.

It is not improbable that the calibration of the probe might change due to e.g. the dislocation of the brass cover plate. Thus it is important to ensure that a small change in the calibration curve (51) will not affect the measurements. Consider first the ordinates of the dimensionless excess dynamic pressure profile. By equation (51)

$$\frac{q - q_A}{q_c - q_A} = \frac{h - h_A}{h_c - h_A} = \frac{h_m - h_{mA}}{h_{mc} - h_{mA}}$$

where suffixes C and A refer, as before to values at n = 0 and in the ambient fluid. Thus, only if a linear calibration (equation 51) holds, the dimensionless excess dynamic pressure profiles will be unaffected by any variation of λ and μ. However, a variation of λ or μ will change the actual value of the axial excess dynamic pressure, for

$$\frac{q_c - q_A}{q_A} = \frac{h_{mc} - h_{mA}}{h_{mA} + \frac{\mu}{\lambda}} \tag{52}$$

But $-\mu/\lambda$ is just the h_m - intercept of the calibration curve equation (51). Therefore $\frac{q_c - q_a}{q_a}$ will still be unaffected if the calibration curve changes in such a way that it always belongs to the family of straight lines through a common point on the h_m-axis. Furthermore, if $\mu \ll h_a$, then $\frac{q_c - q_a}{q_a}$ will not effectively differ from the true value even if $\frac{\mu}{\lambda}$ is varied. In view of the above discussion, the probe calibration was checked only once during the experiments and it was found that λ decreased slightly but $\frac{\mu}{\lambda}$ was practically unchanged.

4.4 Testing

The deflector was fitted into the jet pipe exit and well sealed against leakage. The depth of flow in the flume was adjusted after water supply to the flume and the jet had been turned on at the desired discharge rates. The measurements of velocity head were made at points at 2 in. from the flume bed in planes perpendicular to

the ambient stream (x = const.). The measuring points in each section were chosen at .01' or .02' or .03' apart as was necessary for obtaining a detailed profile of dynamic pressure. The velocity probe was used for measurements in the upstream sections where the flow direction was appreciably different from that of the ambient stream. The probe was oriented by turning the brass cap until there was a null reading on the U-tube differential manometer (magnification 10 to 20) connected to the direction tubes. As would be expected, this device will align the front and rear holes of the probe with the flow directions only if the transverse gradient of the velocity was not too large. However, it was fortunate to find out that within $\pm 7^{\circ}$ misorientation, the measured velocity head had no observable change. Nevertheless, the flow direction near the axis was fairly well indicated. When this differed from the ambient by less than 10°, the next section was then measured with a Pitot tube oriented at about 5° from the ambient stream and pointing towards the jet. This orientation will not affect the measurements of velocity head (32).

The initial jet velocity distribution along the height of the nozzle was determined from the total head measured with the 1/8" Pitot tube. At mid-height, i.e. in the horizontal plane of measurement, the velocity was found to be 1.08 times the average velocity determined from the orifice head readings. This was used to determine the initial jet velocities for all the experiments. The velocity of the ambient stream was determined with the Pitot tube.

The experiments were carried out for the following flow patterns:-

Experiment Number*	Angle between the initial directions of jet and ambient	Initial Jef Velocity U_j (ft/sec)	Ambient Stream Velocity U_1 (ft/sec)	$R = \frac{U_j}{U_1}$
I.1	25°	10.4	1.15	9.1
I.2	25°	10.4	1.55	6.7
I.3	25°	10.0	2.4	4.2
I.4	25°	6.8	2.6	2.6
II.1	17°	10.3	1.20	8.6
II.2	17°	10.3	1.54	6.7
II.3	17°	10.3	2.35	4.4
III.1	9°	10.0	1.11	9.0
III.2	9°	10.0	1.35	7.4

* The same numbers are used for the corresponding Figs. e.g. Fig. I. 2(c) refers to experiment I. 2 etc. These numbers will henceforth be referred to as N.n where N = I, II, III, n = 1 to 2 or 3 or 4.

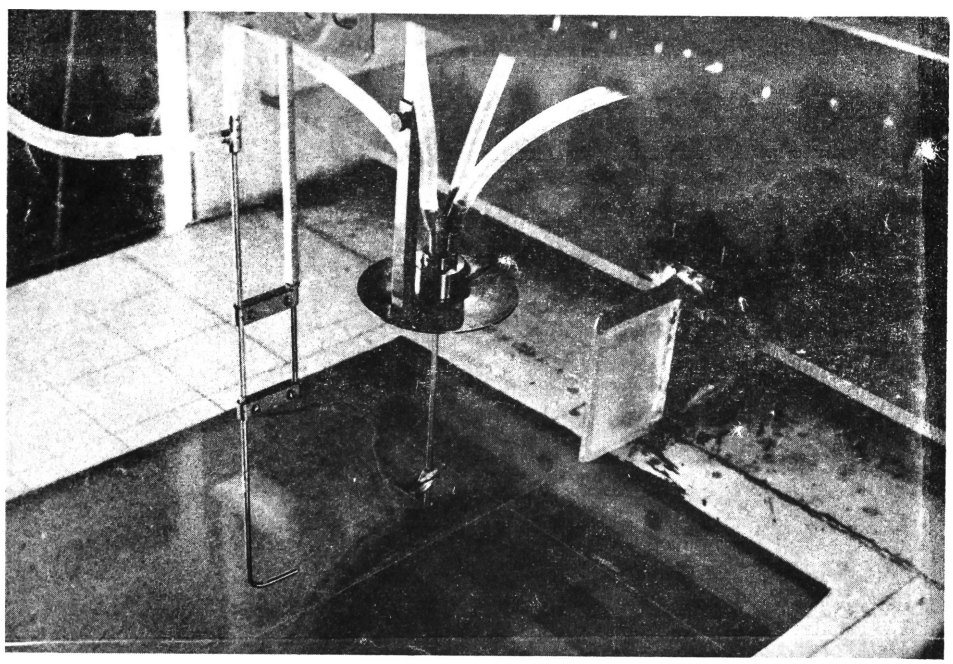

(a) General View

Fig. T5: Instruments for Velocity Head Measurement.

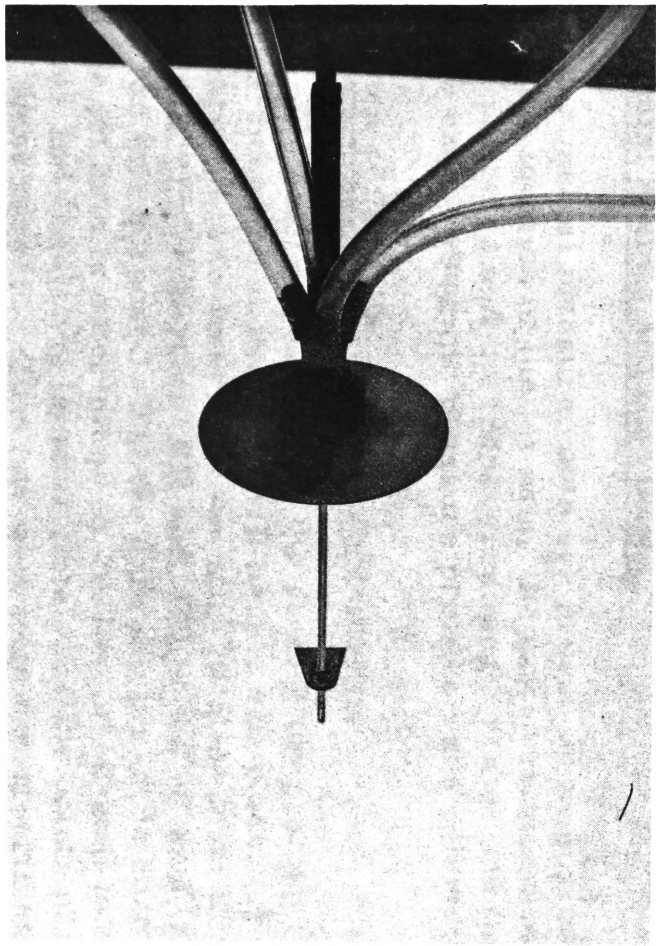

b. CLOSE-UP VIEW OF VELOCITY PROBE

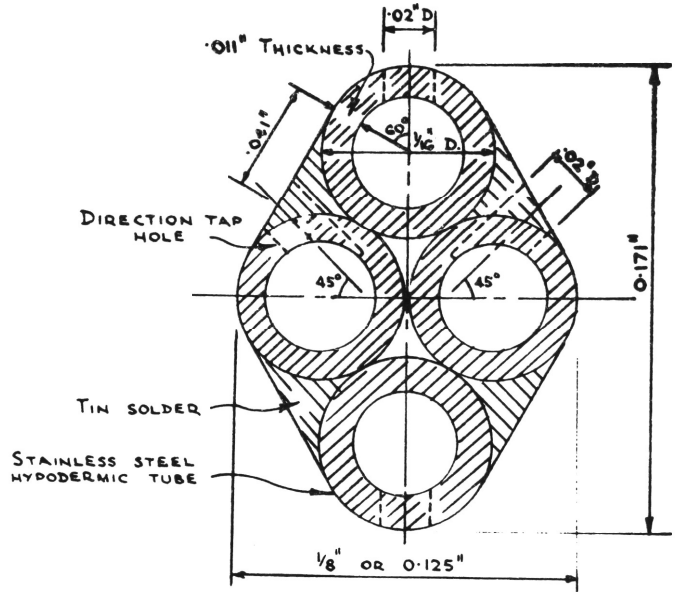

c. CROSS SECTION OF PROBING STEM
Scale: 1" = 1/16"

FIG. T5 INSTRUMENTS FOR VELOCITY HEAD MEASUREMENT

A number of repeatability checks were carried out during the experiments.

As shown in equation (38), the curvature of the jet axis is related to the variation of static pressure. This was well indicated by a depression in the free water surface for $n < 0$ and a rise for $n > 0$ near the nozzle exit. For experiments I. 3 and I. 4, the appreciably affected area was approximately $0 \leqslant x \leqslant .3$ ft., the maximum depression being nearly 3/8". It would therefore be most interesting and useful to measure the static pressure variation in the flow field. Two static pressure tubes had been constructed for this purpose with 1/16" hypodermic tubes according to a standard configuration (Fig. 5b, p. 187 of Ref. 32). But unfortunately it was found that in other flow regions and other experiments the variation was so small that it could not be measured with manometers available in the laboratory. It may be mentioned that it was also because of the static pressure variation that the measurements of velocity head in the upstream sections had to be made with the velocity probe, for in the Pitot tubes the static pressure openings are at least 3/8 in. from the opening for total head.

5. Experimental Results and Discussion

The experimental measurements are presented in Appendix I. From these, the location of the jet axis, the axial variations of excess dynamic pressure and the transverse length scale, and the dimensionless excess dynamic pressure profiles were determined.

5.1 Location of Jet Axis

The jet axis has been defined as the streamline passing through the central vertical line at the (vertical) nozzle exit plane. But it is practically impossible to determine the axial location from this definition. Instead, the properties (P1) and (P2) of the jet axis (p. 31-32) can be used for this purpose. Excess dynamic pressure contours are drawn and the jet axis is determined as the line orthogonal to these contour curves and consisting (approximately) of the points of maximum curvature of these curves. This has been done for experiment I. 2, as shown in Fig. I. 2(d). However, this method is cumbersome. In the present experiments, α is small (mostly less than 10° in the range of measurements).

Therefore by virtue of the two properties (P1) and (P2) of the jet axis (p. 31-32), geometrical intuition (see accompanying sketch)

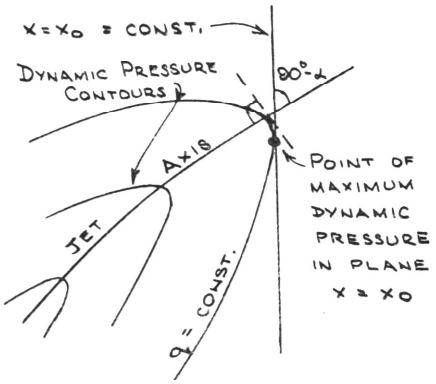

suggests that the point of maximum excess dynamic pressure in each section (x = const.) normal to the external stream will be very close to the jet axial point in that section. Fig. I. 2(d), where α is the second largest among all experiments, verifies this quite well. The jet axis for all other experiments were therefore determined in this way.

The locations of the jet axes are shown in Figs. I. 5(a), II. 4(a), III. 3(a). They have been replotted in Figs. I. 5(b), II. 4(b), III. 3(b), where the coordinates are divided by $R^2 = (U_j / U_1)^2$. It is seen that for $(x/R^2D) \leqslant 3$, a single curve for the jet axes can be drawn for each α_0, the angle between the initial directions of jet and ambient stream. Thus the proposition that jet axial location is independent of R in the reduced coordinates is approximately correct for $\frac{x}{R^2 D} \leqslant 3$. We cannot conclude, however, that when $\frac{x}{R^2 D} > 3$, this proposition is not even approximately true. For the velocity ratios R could not be determined accurately, and far downstream the peaks of the dynamic pressure profiles were too flat for a precise determination of their positions. Besides, the departure from two-dimensionality (Appendix 2) may have some effect.

5. 2 Axial Variations of the Excess Dynamic Pressure and the Transverse Length Scale

In view of the discussion in Section 5. 1, the maximum excess dynamic pressure of an experimentally determined profile for a plane x = const. can be taken as the value at the jet axial point in that plane. But the transverse length scale, b, is defined as the distance from the jet axis to the point where the excess dynamic pressure has fallen to half of the axial value in a plane S = const. It is therefore necessary to ascertain the nature of approximation involved if it is desired to determine b from the profiles for planes x = const. which is obviously an easier and more practicable way.

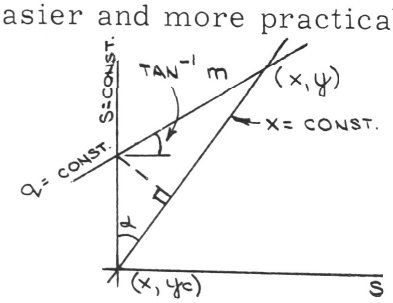

If α and n are small, the dynamic pressure contour can be approximated by a straight line* between the lines S = const. and X = const. through the same jet axial point (x, y_c). Let $m = \frac{dn}{ds}$ for the

*except when the contour is normal to the S-axis. But in the present case, this occurs only when n= 0 (Section 3) and we then do not have to prove anything.

contour. Then (see accompanying sketch),

$$y - y_c = n\cos\alpha + n\sin\alpha\,\frac{m+\tan\alpha}{1+m\tan\alpha}$$

$$\frac{y-y_c}{n} = \frac{\cos\alpha + 2m\sin\alpha + \sin\alpha\tan\alpha}{1+m\tan\alpha} \qquad (53)$$

$$= 1 + \frac{(\sec\alpha - 1) + m(2\sin\alpha - \tan\alpha)}{1+m\tan\alpha}$$

$$\therefore \frac{y-y_c}{n} = 1 + \frac{\frac{\alpha^2}{2} + m\alpha}{1+m\alpha} \qquad (54)$$

Hence, if m is not too large, the approximation of taking $\frac{y - y_c}{n} = 1$ is good to the first order of small quantities, and if m is also small, it is correct to the second order.

For the present experiments, both α and n are small; in addition m is also small for n not too close to zero (see Fig. I. 2(d)). Hence it is justified to take $(y-y_c)$ as n. Indeed, two profiles for n = const. have been plotted (see Fig. AI. 2 in Appendix 2) and found to be indistinguishable from those for x = const. This justification applies particularly to the determination of b from the excess dynamic pressure profiles for planes x = const. since at n = b, m is small.

The axial distances were determined by summing chord lengths of the S-axis divided into suitable intervals. They were used to plot the graphs of the decay of axial excess dynamic pressure, $(\frac{q_c - q_A}{q_A})^{-1}$ v. $(\frac{S}{D})$, (Figs. N. n(a))*, and the graphs of the lateral spread, $(\frac{b}{D})$ v. $(\frac{S}{D})$, (Figs. N. n(b))*. From the former graphs it is seen that $\frac{d}{d(\frac{S}{D})}(\frac{q_c - q_A}{q_A})^{-1}$ increases with $(\frac{S}{D})$ and appears to tend to a constant for large $(\frac{S}{D})$. This is in qualitative agreement with the results reported in [16] for a round jet in a coflowing stream. However, with a consideration of b, further discussion of $(q_c - q_A)$ is unnecessary, for the self-preservation of $(q-q_A)$ relates the two quantities through the momentum integral equation (43).

As suggested by the analysis (Sect. 3), two length scales were plotted against $(\frac{S}{D})$ in the graphs of lateral spread of jet, b_i for the concave side ($n < 0$) and b_o for the convex side ($n > 0$). It is seen that the rates of increase of both b_i and b_o decreases with S and appears

---

* See footnote on page 36

to tend to a constant, again similar to a two-dimensional jet in a co-flowing stream [26]*. There is, however, a difference between b_i and b_o. Except for experiments I. 1, I. 2 and II. 1, b_i is slightly greater than b_o and the difference tends to decrease with $(\frac{S}{D})$, as predicted by the analysis (Sect. 3). The three exceptions correspond to ($\alpha_o = 25^o$, R = 9.1, 6.7), and ($\alpha_o = 17^o$, R = 8.6) respectively. In these cases, $b_i \doteq b_o$ for $\frac{S}{D} < 100$, and for $\frac{S}{D} > 100$, $(b_o - b_i) > 0$ tends to increase with S. Here, the velocity ratio R is fairly high and α is no longer small. Nevertheless, the alternative condition (III) on p. 29 for similarity with an undeflected jet is still approximately satisfied in the upstream regions. But, since m_1 ($= \frac{dn}{ds}$) for the dynamic pressure contour used to determine the b's has the same sign as n, the present method of determining b overestimates b_o and underestimates b_i as clearly indicated by Equation (54). These account for the very smallness of and the predominant negative sign for $(b_i - b_o)$ in $(\frac{S}{D}) < 100$. For $(\frac{S}{D}) > 100$, the jet velocity has decreased to the same order as U_1, and α also changes appreciably. Hence the basic requirements for similarity are violated, but the reasons for the peculiar behaviour are not clear.

One important, but rather obvious, point to be noted from the graphs of $(\frac{b}{D})$ v. $(\frac{S}{D})$ is that the slopes of these graphs appear to be of the same order as those for the straight jets. Intuitively we may expect the effect of jet axial curvatures on the spreading to be large only when that curvature is large.** In the present experiments, the jet axial curvatures are obviously small. In fact, this is one of the conditions for similarity between curved and straight jet flows, and this similarity necessarily implies, among other things, that the rates of spreading of the two kinds of jets should be of the same order.

5.3 Self-preservation

For the same reasons as given in Sect. 5. 2, the dimensionless excess dynamic pressure profiles

$$\left(\frac{q - q_A}{q_c - q_A}\right) \text{ v. } \left(\frac{n}{b}\right)$$

will be determined directly from the experimentally obtained dynamic pressure profiles for planes x = const. The degree of approximation can be estimated from equation (53). Thus for a given ordinate, the

---

* b in [26] is 1. 2 times the length scale used here.

**It has been found [6] that the outer free-jet layer of a jet over a curved wall spreads more rapidly than that of a straight wall-jet.

correct value of the abscissa ($\frac{n}{b}$) and the value used ($\frac{y - y_c}{b'}$) are related by*

$$\frac{\left(\frac{y-y_c}{b'}\right)}{\left(\frac{n}{b}\right)} = \left(\frac{\cos\alpha + 2m\sin\alpha + \sin\alpha\tan\alpha}{\cos\alpha + 2m_1\sin\alpha + \sin\alpha\tan\alpha}\right)\left(\frac{1+m_1\tan\alpha}{1+m\tan\alpha}\right)$$

For small α , we have

$$\frac{\left(\frac{y-y_c}{b'}\right)}{\left(\frac{n}{b}\right)} \doteqdot 1 + \alpha(m - m_1) \qquad (55)$$

Now in the range of n values considered, m is an increasing function of n. Hence, compared with the correct profiles, the approximate ones are stretched laterally for $n < 0$ and compressed for $n > 0$ when $(\frac{n}{b}) < 1$; and are compressed laterally for $n < 0$ and stretched for $n > 0$ when $(\frac{n}{b}) > 1$. However, when α is small, the error is small.

These profiles are shown in Figs. N. n(c). It is seen that for each flow pattern the profiles are practically independent of the downstream distance from the nozzle, verifying the self-preservation of excess dynamic pressure. Furthermore, allowing for the approximate nature of the profiles as discussed above, these dimensionless self-preserving profiles are symmetrical about the S-axis, as suggested in Sect. 3. More scattering is present when $\frac{q - q_A}{q_c - q_A} < 0.2$; but this is due to the limited accuracy of measurements of the fairly low velocity near the jet edge. It also appears that there is a very slight but continuous change of the self-preserving profiles with α_o and R (Fig. IV). But the measurements were not accurate enough to be conclusive on this point. It can, therefore, only be ignored with a note of caution that this might indicate an intrinsic difference between the deflected and undeflected jet flows.

All the dimensionless excess dynamic pressure profiles are found to be very close to a gaussian probability curve, but falls off more rapidly near the jet edge on the concave side. It appears that this may be due to the low pressure in that region. Nevertheless, in the absence of more accurate measurements or a rigorous theory, a gaussian curve appears to be a sufficiently good approximate form of the "universal" dimensionless excess dynamic pressure profile.

In conclusion, the results of this and the last section (Sect. 5. 2) complete the verification of and the discussion on the similarity (macroscopic) of the momentum diffusion in the deflected and undeflected two-dimensional jet flows which was set out in the analysis (Sect. 3).

*b' is the value of b determined in Sect. 5. 2, and $m_1 = \frac{dn}{ds}$ at n = b.

6. Conclusions

The following conclusions may be drawn from the analytical and experimental studies on a two-dimensional jet emitted at an angle to a uniform ambient stream.

(1) The mean velocity field (momentum diffusion) of such a deflected jet in an interval of downstream distance (S_1, S_2) will be similar to that of an undeflected jet if either one of the following three conditions is satisfied (Sect. 3):

(I) α is sufficiently small

(II) $\frac{S_2 - S_1}{\rho} \ll 1$, where ρ is the radius of curvature of the jet axis.

(III) $U \gg U_1$ and α_o is not too large, where U is the velocity in the jet.

(2) The excess dynamic pressure is self-preserving in the (S, n) coordinates. The universal transverse profile can be closely approximated by a gaussian curve (equation 45, Sect. 5.3, Fig. IV).

(3) The jet spreads more rapidly on the concave side than on the convex side (Sect. 3, Fig. N.n(b), Sect. 5.2).

(4) The jet axis may be (approximately) determined as the locus of the point of maximum curvature of the excess dynamic pressure contours (Sect. 3, Sect. 5.1). Its location is approximately independent of the jet-to-ambient velocity ratio $R = U_j / U_1$ if the lengths are divided by R^2 (Sect. 2.7, Sect. 5.1, Figs. I.5(a), (b); II. 4(a), (b); III. 3(a), (b)).

Appendix 1.

Experimental Measurements.

The experimental measurements are shown in the following figures. The coordinates (X, Y) are related to (x, y) in the text by

$$X = x,$$

$$Y = y + 10$$

In order to non-dimensionalize the results and to reduce the calibration error (Sect. 4. 3), the measurements are plotted as

$$\left(\frac{q - q_A}{q_A} \right) \quad \text{Vs} \quad Y$$

where $\left(\frac{q}{q_A} \right)$ is of course equal to the ratio of the velocity head at the point of measurement to that of the ambient stream. A vertical line is drawn in each of these profiles to indicate the position of the peak for the determination of the jet axial location and of the transverse length scales b_i and b_o.

Appendix 2.

Departure from Two-dimensionality and Lateral Inflow*

From the self-preservation of excess dynamic pressure (equation 44a) and the conservation of momentum (equation 43), we have

$$M = \int_0^{\pm\infty} U(U - U_A)\,dn$$

$$= (q - q_A)\int_0^{\pm\infty} f\left(\frac{n}{b}\right) dn - U_A \int_0^{\pm\infty} (U - U_A)\,dn$$

$$\therefore \quad \frac{b}{\left(\frac{q - q_A}{q_A}\right)^{-1}} \int_0^{\pm\infty} f(\eta)\,d\eta = \frac{M}{q_A} + \int_0^{\pm\infty} \left(\frac{U}{U_A} - 1\right) dn$$

where $\eta = \frac{n}{b}$

M is the excess momentum of half of the jet (in the appropriate direction)

$b = b_i$ or b_o according as $n < 0$ or > 0.

Now the last integral simply represents the excess flow in the S-direction (or the accumulated lateral inflow). Hence $b/\left(\frac{q - q_A}{q_A}\right)^{-1}$ should increase with the downstream distance at a rate equal to the lateral inflow rate. But a rough examination of Figs. N.n(a)(b) shows that for the majority of the experiments that quantity increases with $\left(\frac{S}{D}\right)$ only up to about $\frac{S}{D} = 70$ and then decreases. One most obvious explanation is the departure from two-dimensionality.

Van der Hegge Zinjnen [10] made some preliminary investigations on this and concluded that for a height-to-width ratio $\left(\frac{H}{D}\right)$ of about 20 for the nozzle slot, the flow may be considered as approximately two-dimensional between $4 \leqslant \frac{S}{D} \leqslant 2\frac{H}{D}$. In the present experiments, $\frac{H}{D} = 4/\frac{1}{8} = 32$. Thus we should expect two-dimensionality up to somewhere beyond $\frac{S}{D} = 2\frac{H}{D} = 64$. However, the asymmetry of the initial velocity distributions about the mid-height (i.e. due to the difference between boundary layer on the flume bed and the free surface) and the fairly large thickness of the deflector (compared with D, the initial jet thickness) would be expected to reduce this region. In order to obtain some idea about the seriousness of the departure from two-dimensionality, some preliminary measurements were

* In this appendix the analysis will only be approximately right. In particular, α is assumed to vary little with S.

made on the variation of velocity with depth. The results are shown in Fig. A. IV.

The departure from two-dimensionality can also be seen from the nature of the lateral inflows into the jet computed from Figs. N. n(a), (b), and the self-preservation of $(q - q_A)$. The total excess flow in the S-direction is

$$\int_0^{\pm\infty} (U-U_A)\,dn = U_A \int_0^{\pm\infty} \left\{ \left[1+B_c f(\eta)\right]^{\frac{1}{2}} - 1 \right\} dn$$

where $B_c = \frac{q_c - q_A}{q_A}$ and $\pm\infty$ are to be used for the two sides $n \gtrless 0$ respectively. Using the continuity equation (36), we have the lateral inflow velocity V_1 at $(S, \pm\infty)$ given by

$$\frac{V_1}{U_A} = -\frac{1}{U_A}\frac{d}{dS}\int_0^{\pm\infty} (U-U_A)\,dn$$

$$= \frac{1}{2B_c^{-1}}\left[\left(\frac{b}{B_c^{-1}}\frac{dB_c^{-1}}{dS}\right) J_1 + \left(\frac{db}{dS}\right) K_1\right]$$

where $$J_1 = \int_0^{\infty} f(\eta)\left[1+B_c f(\eta)\right]^{-\frac{1}{2}} d\eta$$

$$K_1 = \int_0^{\infty} \eta f'(\eta)\left[1+B_c f(\eta)\right]^{-\frac{1}{2}} d\eta$$

The values V_{1i} for $n < 0$ and V_{10} for $n > 0$ are respectively given by $b = b_i$ and $b = b_0$. These have been calculated for all the experiments using a gaussian profile for $f(\eta)$, i.e.

$$f(\eta) = e^{-.693\eta^2}$$

and are plotted in Fig. AV. They show a very erratic behaviour. The most important fact revealed by these graphs is that in the majority of the experiments, V_1 changes sign at some value of $(\frac{S}{D})$ (about 70) and becomes having the same sign as n for greater $(\frac{S}{D})$ values. This means an outflow from the jet, instead of the familiar entrainment. It certainly brings out the serious effect of departure from two-dimensionality.

Notwithstanding these non-two-dimensional behaviours, the self-preservation of the excess dynamic pressure is little affected (Figs. N. n(c)). It might seem that this property may be of more far-reaching validity than in two-dimensional or axi-symmetric flows. Furthermore, it appears that the transverse length scales (b_i and b_0) and the existence of a single curve for the jet axes in the $(\frac{x}{R^2D}, \frac{y}{R^2D})$ plane for all velocity ratios with the same initial angle α_0 are not appreciably affected.

Appendix 3.

The work described in this report was carried out by the author in 1965. In 1966 further work was carried out at the Water Research Laboratory by P. R. Carter who repeated the work of the author using a deflection angle of 45^{o}. All other apparatus and techniques were the same for this later series of experiments.

In general, the experimental results agreed with the author's observations. The excess dynamic pressure was found to be approximately self preserving, the exception being low values of S on the concave side. However, this could be due to the breaking down of the conditions for similarity in this section, since

(i) α is large and is rapidly changing.

(ii) The radius of curvature is smaller than for the initial experiments.

(iii) Although the jet velocity is large compared with the ambient stream, α is no longer small and the jet does not approach the case of an undeflected jet due to the sharp curvature of the axis.

There were two important variations from the author's results. Firstly, the jet spread more quickly on the convex side, not on the concave side for the larger values of $\frac{S}{D}$. However, this tendency has been already noted for larger values of α_o and R. Secondly, the location of the jet axis was not independent of the jet to ambient velocity ratio R, when the length values were divided by R^2.

Bibliography.

1. Abramovich, G. N. The Theory of Turbulent Jets. M. I. T. Press

2. Ballabh, R., Hydrodynamic Superpsability. Uttar Pradesh Sci. Res. Comm. Monograph. Allahabad, India.

3. Batchelor, G. K. The Conditions for Dynamical Similarity of Motions of a Frictionless Perfect Gas Atmosphere. Quart. J. R. Meteor. Soc. 79 p. 224-235.

4. Birkhoff, G. Hydrodynamics. Dover.

5. Birkhoff, G and Zarantonello, E. H., Jets, Wakes and Cavities Academic Press.

6. Bradshaw, P. and Gee, M. T., Turbulent Wall Jets with and without an External Stream. Aero. Res. Council R. and M. No. 3252.

7(a) Chaplin, H. R., Theory of the Annular Nozzle in Proximity to the Ground. David Taylor Model Basin. Aerodyn. Lab. Rep. 1373.

7(b) Chaplin H. R., Effect of Jet Mixing on the Annular Jet. D. T. M. B. Aerodyn. Lab. Rep. 1375.

8. Craya, A. et Curtet, R., Sur L'evolution d'un Jet en Espace Confinee, 1955 C. R. Acad. Sci. Paris 241, 621.

9. Hansen, A. G., Similarity Analyses of Boundary Value Problems in Engineering. Prentice Hall, 1964.

10. Hegge Zijnen, B. G. van Der. Measurements of the Velocity Distribution in a plane Turbulent Jet of Air. App. Sci. Res. Vol. A. VII, p. 256.

11. Hill, P. G. Two-dimensional Jet in a Ducted Stream. J. Fl. Mech. Vol. 22, 1965, p. 161.

12. Hunt J. N. Incompressible Fluid Dynamics, Longmans, 1964.

13. Kobashi, Y. Experimental Studies on Compound Jets. Proc. 2nd Jap. Nat. Congress for App. Mech. 1952 p. 223.

14. Kobashi, Y. and Tani, I., Experimental Studies on Compound Jets. Proc. 1st Jan. N. C. T. A. M. 1951.

15. Kruka, V and Eskinazi, S., The Wall Jet in a Moving Stream. J. Fl. Mech. Vol. 20 1964, p. 554.

16. Maczynski, J. F. J., A Round Jet in an Ambient Coaxial Stream. J. Fl. Mech. 13, 1962, p. 597.

17. Morton, B.R., Taylor, G. and Turner, J.S. Turbulent Gravitational Convection from Maintained and Instantaneous Sources. Proc. Roy. Soc., A. Vol. CCXXXIV (1956) p. 1-23.

18. Pai, S.I. Fluid Dynamics of Jets. Van Nostrand.

19. Pai, S.I. Viscous Flow Theory, II. Van Nostrand.

20. Pai, S.I. Unsteady 3-dimensional Laminar Jet Mixing of a Compressible Fluid. AIAA Journal, Vol. 3, No. 4, April 1965.

21. Pozzi, A. and Sabatini, B., Plane Jet in a Moving Medium. AIAA Jnl. Vol. 1, No. 6, June 1963, p. 1426.

22. Reynolds, A.J. Similarity in Swirling Wales and Jets. J. Fl. Mech. 14, 1962, p. 241.

23. Reynolds, A.J. Observations of a Liquid-into-liquid Jet. J. Fl. Mech. 14, 1962, p. 552.

24. Squire, H.B. Reconsideration of the theory of Free Turbulence, Phil. Mag. 39, 1-20.

25. Townsend, A.A. The Structure of Turbulent Shear Flow, Cambridge University Press.

26. Weinstein, A. Osterle J.F. and Forstall, W., Momentum Diffusion into a Slot Jet Into a Moving Secondary. J. Appl. Mech. Sept. 1956 p. 437.

27. Keffer J.F. and Baines W.D., The Round Turbulent Jet in a Cross Wind. J. Fl. Mech. 15, 1963, p. 481.

28. Bradbury, L.J.S., The Structure of a Self-Preserving Turbulent Plane Jet. J. Fl. Mech., 23, 1965 p. 31.

29. Sridhar K., An Experimental Investigation of the Flow in and Behind 2-Dimensional Jet Sheets Bounding a Cavity. University of Toronto UTIA Rep. No. 94.

30. Stewartson, K. Theory of Laminar Boundary Layers in Compressible Fluids. Clarendon Press, Oxford.

31. Schlichting, Boundary Layer Theory, McGraw Hill Book Co.

32. Rouse H., Engineering Hydraulics. John Wiley.

33. Tetervin. N., and Lin C.C., A General Integral Form of the Boundary Layer Equation for Incompressible Flow with an application to the Calculation of the Separation Point of Turbulent Boundary Layers. N.A.C.A. Rep. No. 1046, 1952.

34. (a) Alexander L. G., Baron T., Comings E. W., Transport of Momentum, Mass and Heat in Turbulent Jets. Uni. of Illinois Eng. Expt. Station, Bulletin Series No. 413.

(b) Alexander L. G., An Ad Hoc Theory of Free Turbulent Jets, Uni. of Illinois Eng. Expt. Stn. Tech. Rep. No. 13, Aug. 1952. Quoted from (26).

(c) Kivnick, A. and Johnstone H. F., Application of the Reichardt Hypothesis to the Transport of Momentum and Mass in Coaxial Jets. Uni. of Illinois Eng. Expt. Stn. Tech. Rep. CML-2, June 1952. Quoted from (26).

Acknowledgements

The authors wish to thank the staff of the Water Research Laboratory for the interest shown and assistance given to this investigation.

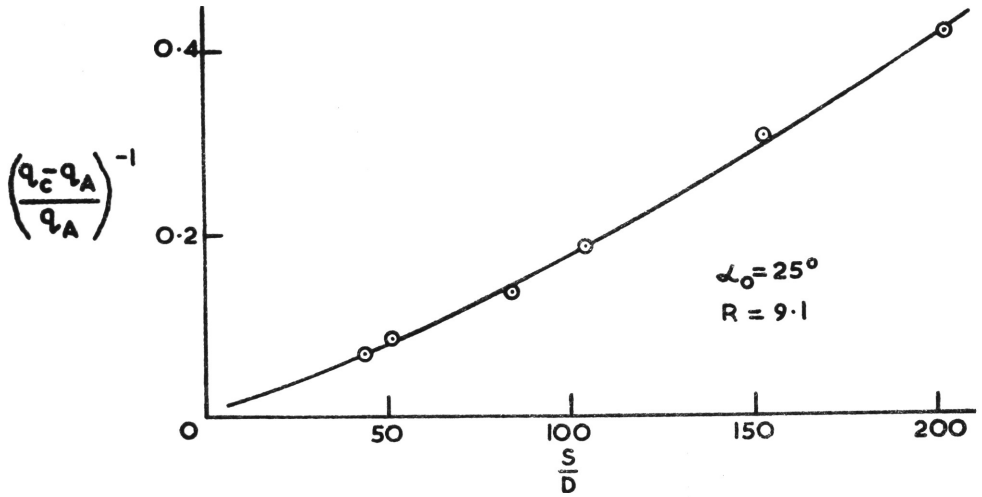

FIG. I·1(a) DECAY OF AXIAL EXCESS DYNAMIC PRESSURE

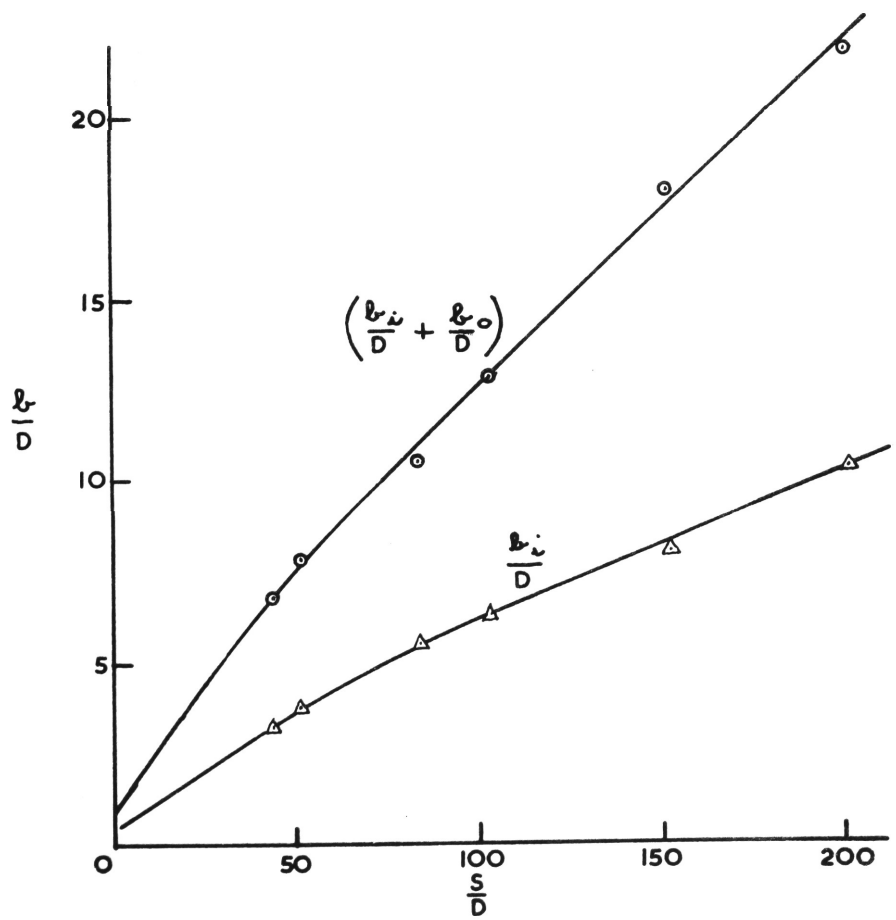

FIG. I·1(b) LATERAL SPREAD OF JET

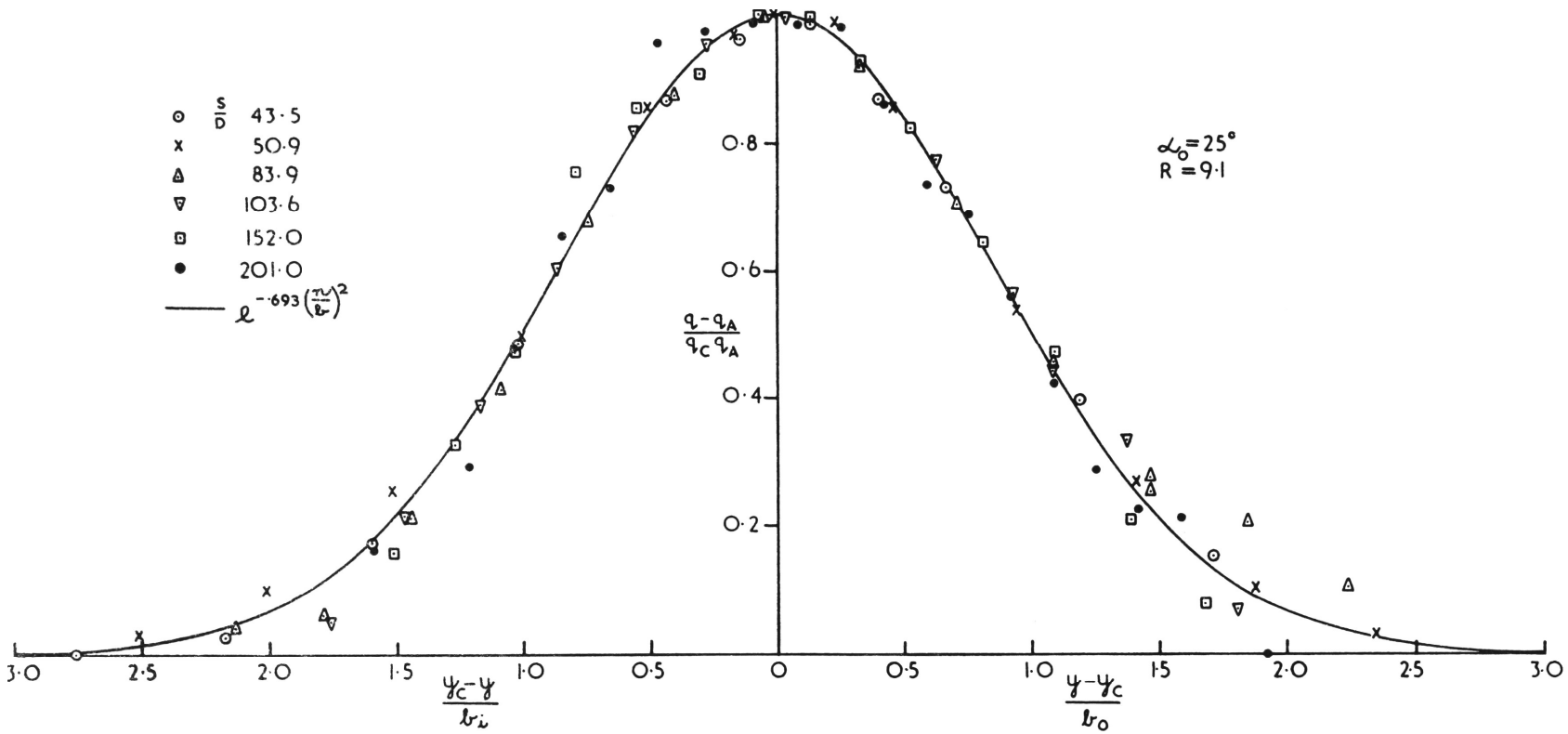

FIG. I·1 (c) DIMENSIONLESS EXCESS DYNAMIC PRESSURE PROFILES

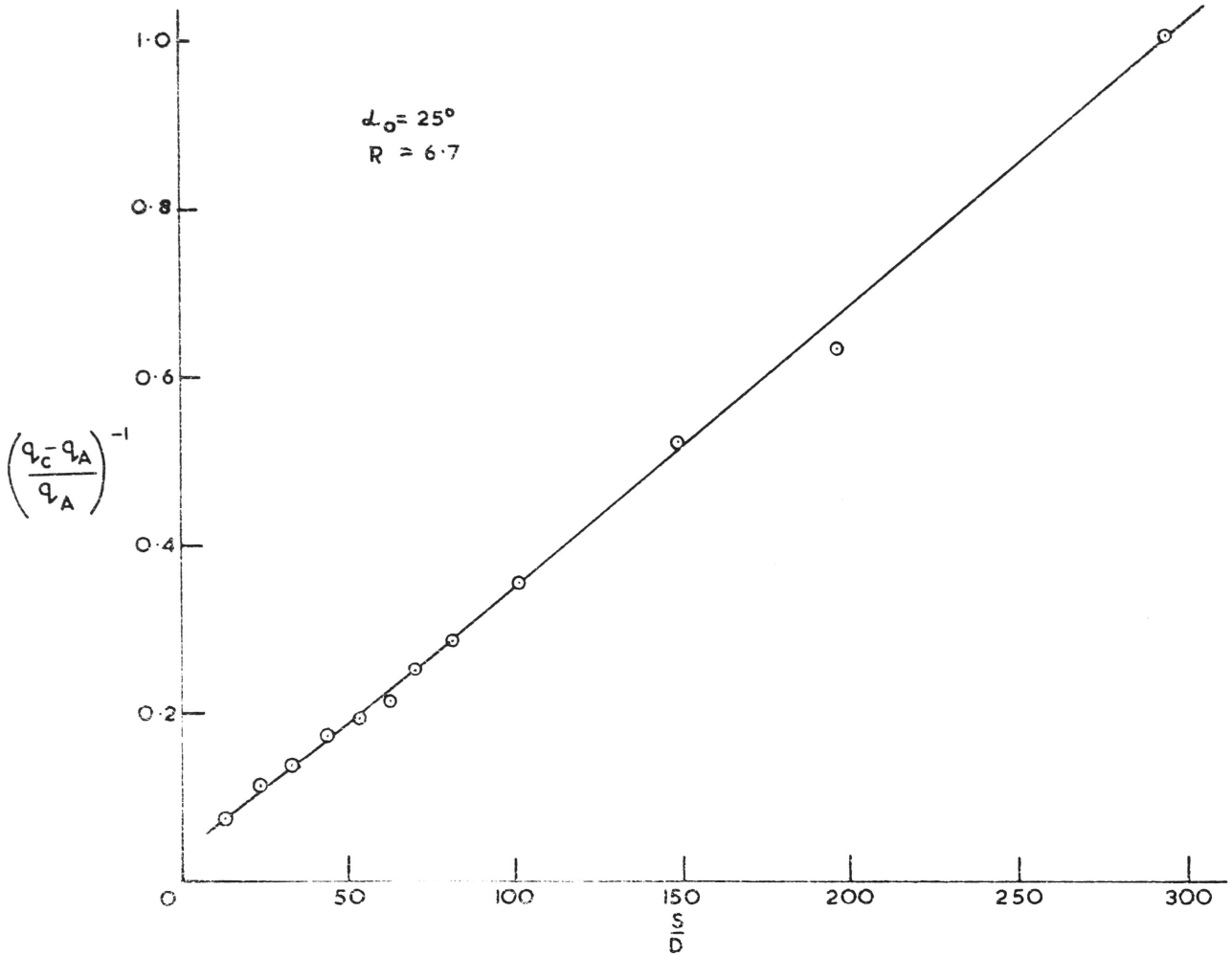

FIG. I·2(a) DECAY OF AXIAL EXCESS DYNAMIC PRESSURE

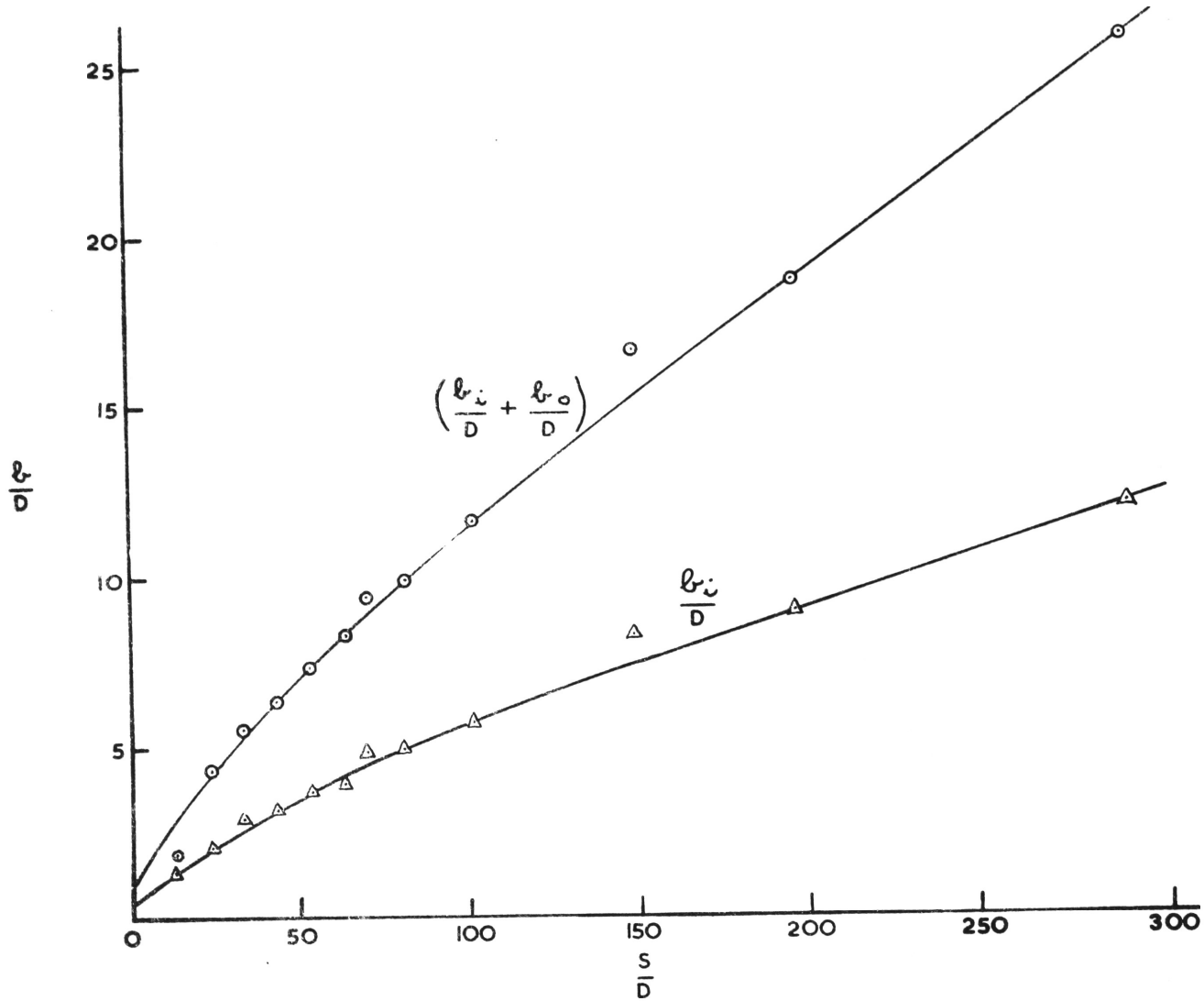

FIG. I·2(b) LATERAL SPREAD OF JET

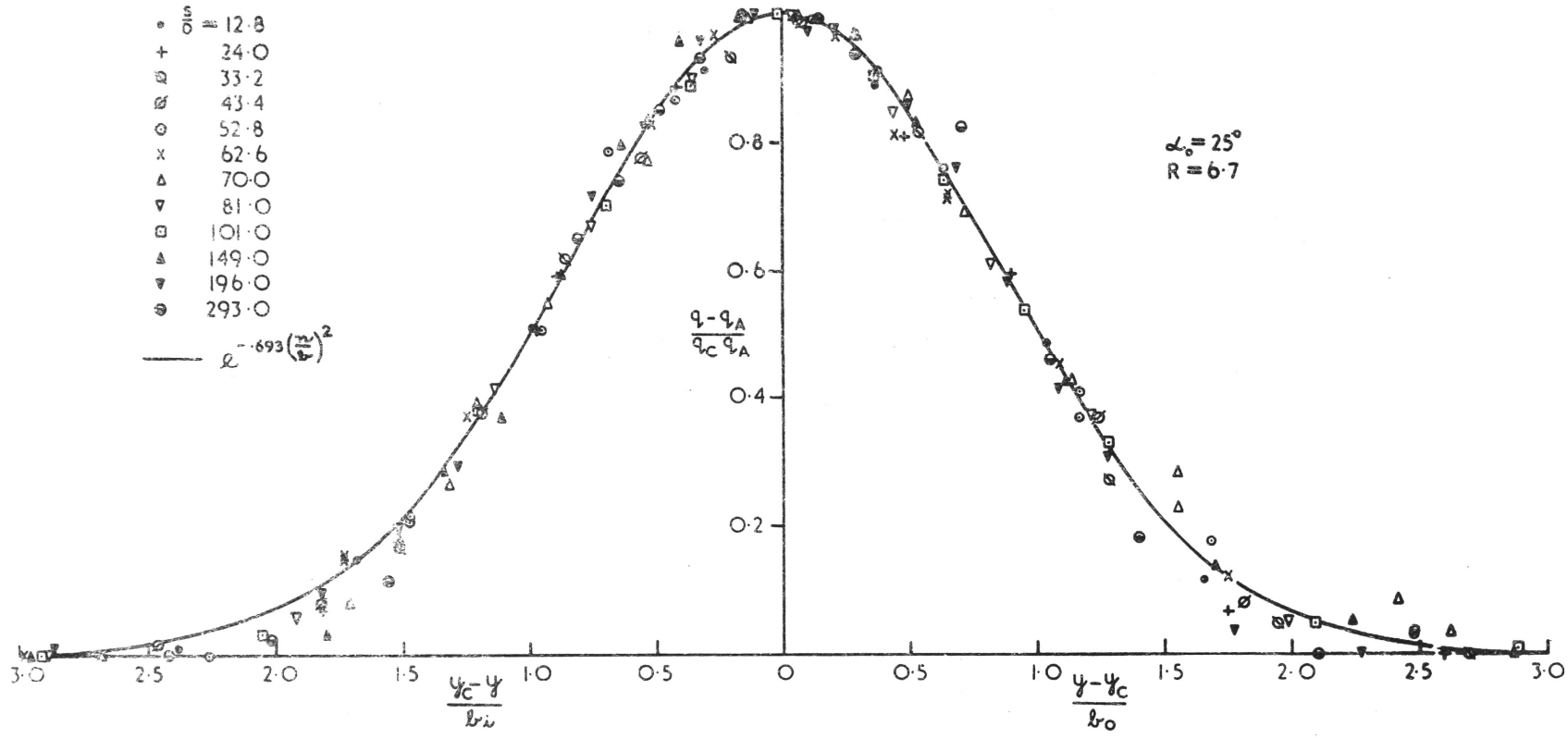

FIG. I·2(c) DIMENSIONLESS EXCESS DYNAMIC PRESSURE PROFILES

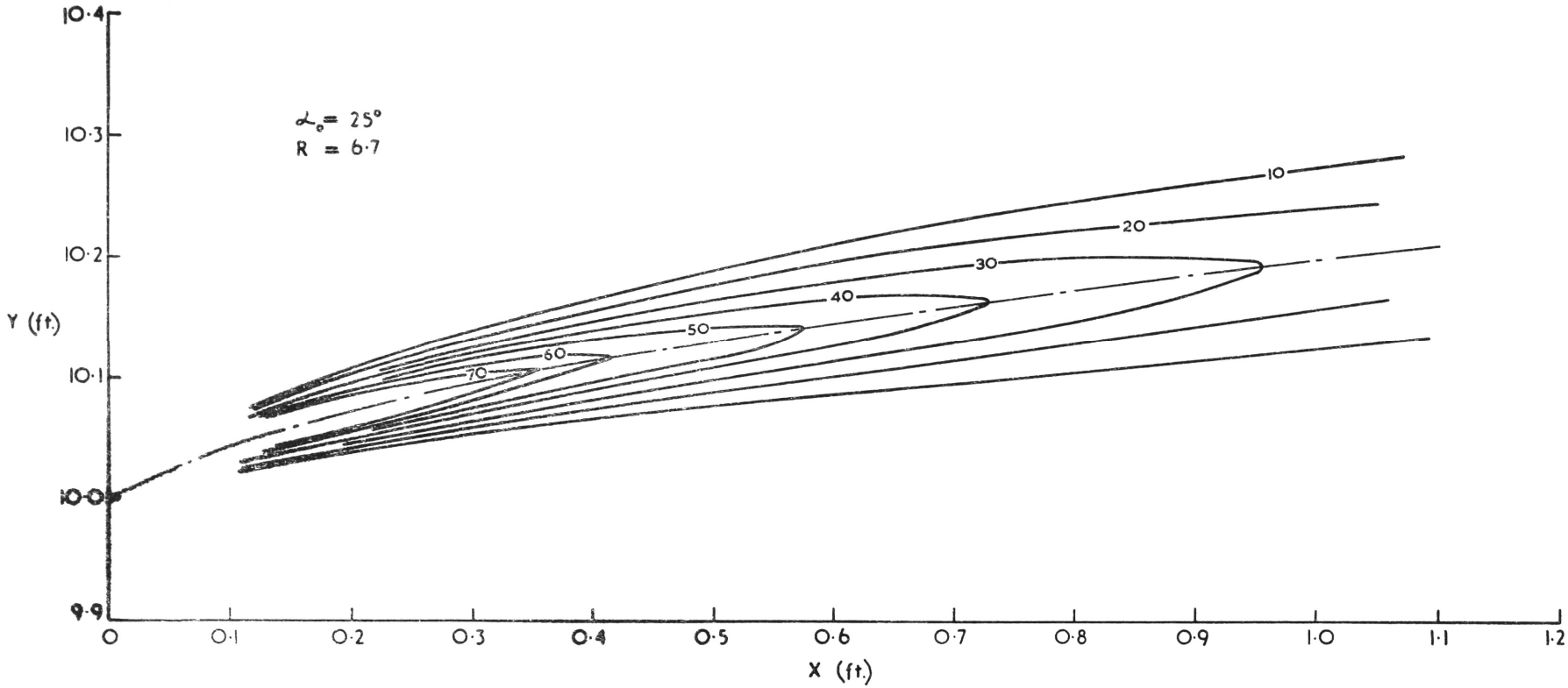

FIG. I·2(d) CONTOUR OF EXCESS DYNAMIC PRESSURE $\left(\frac{q-q_A}{q_A}\right)$

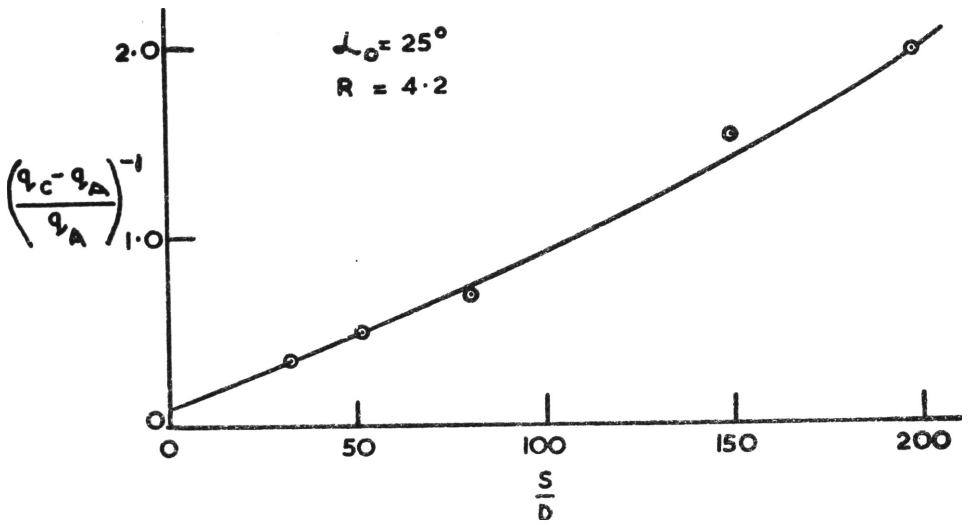

FIG. I·3(a) DECAY OF AXIAL EXCESS DYNAMIC PRESSURE

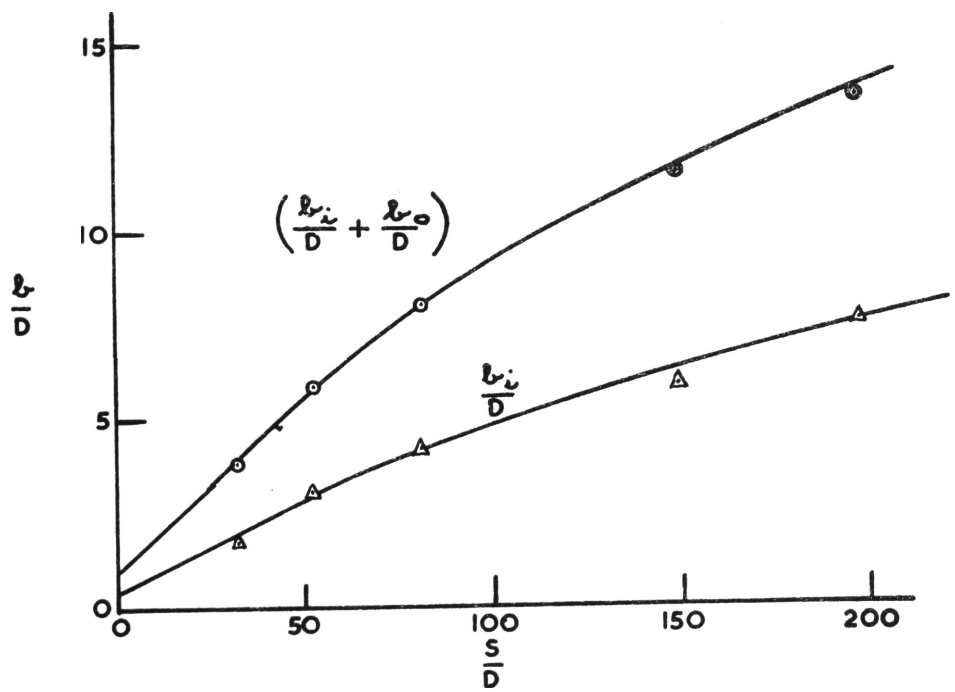

FIG. I·3(b) LATERAL SPREAD OF JET

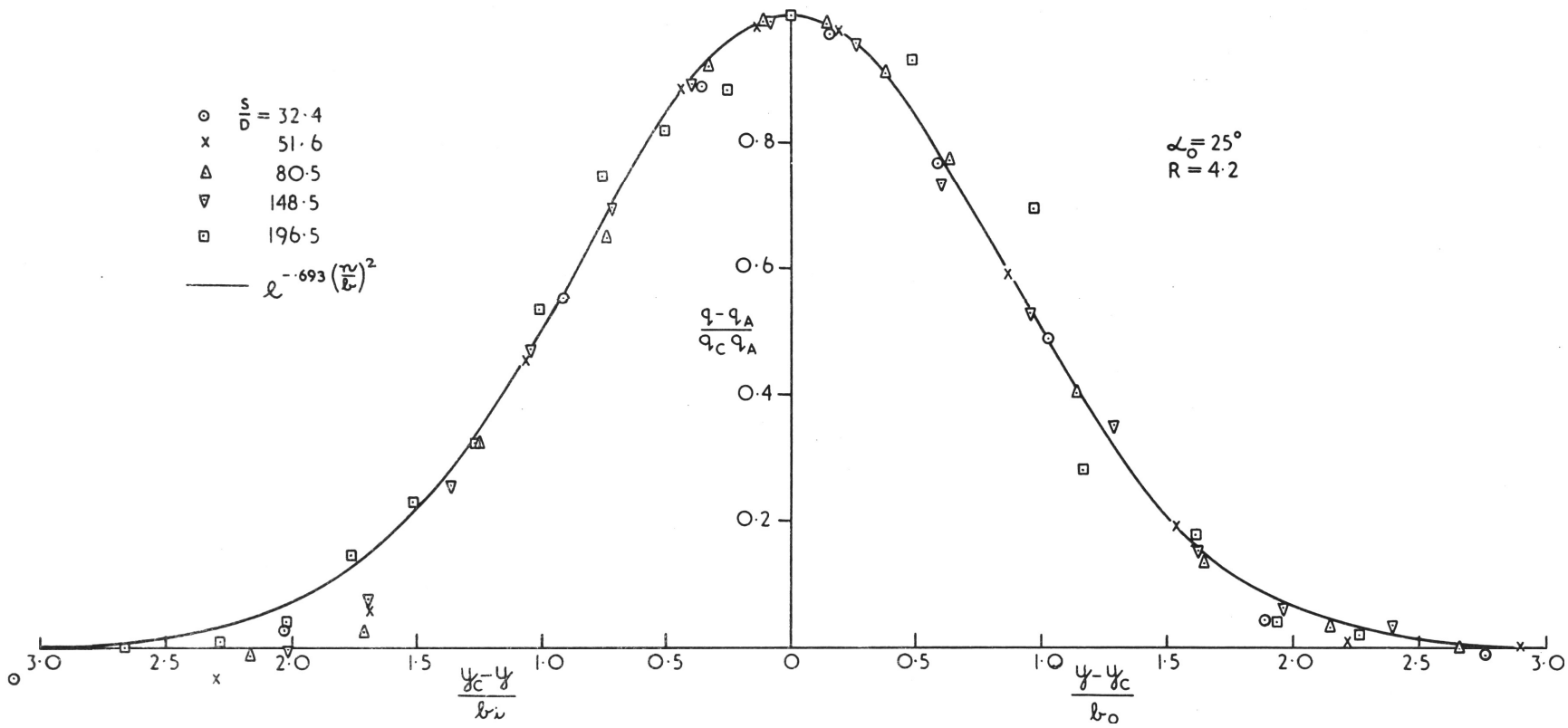

FIG. I·3 (c) DIMENSIONLESS EXCESS DYNAMIC PRESSURE PROFILES

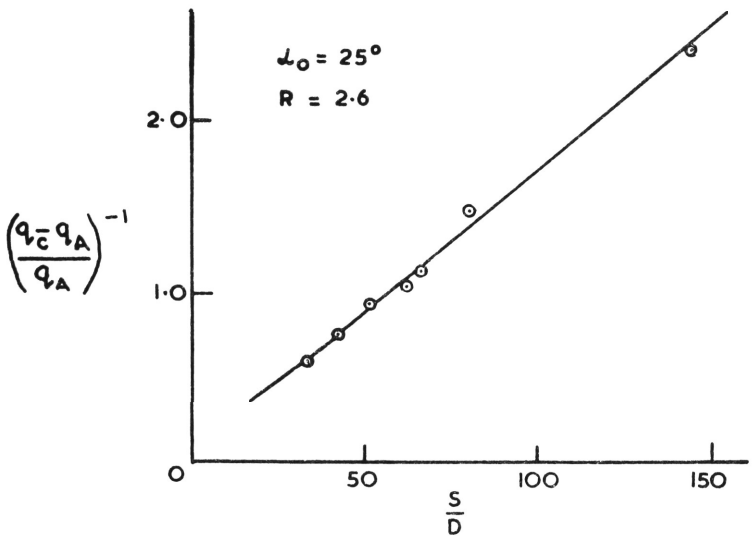

FIG I·4(a) DECAY OF AXIAL EXCESS DYNAMIC PRESSURE

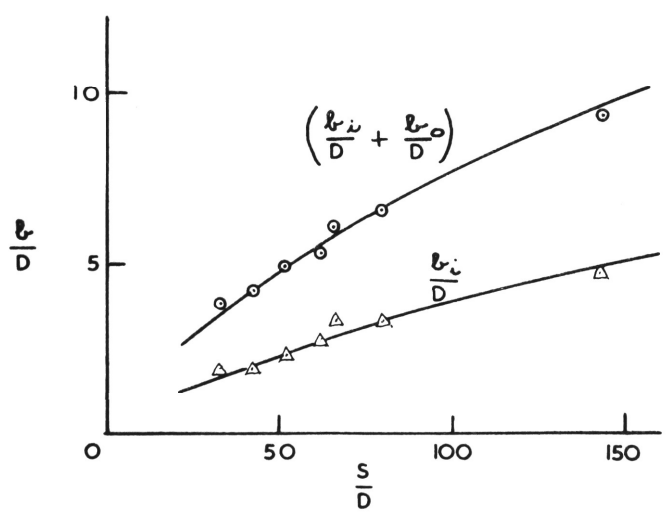

FIG. I·4(b) LATERAL SPREAD OF JET

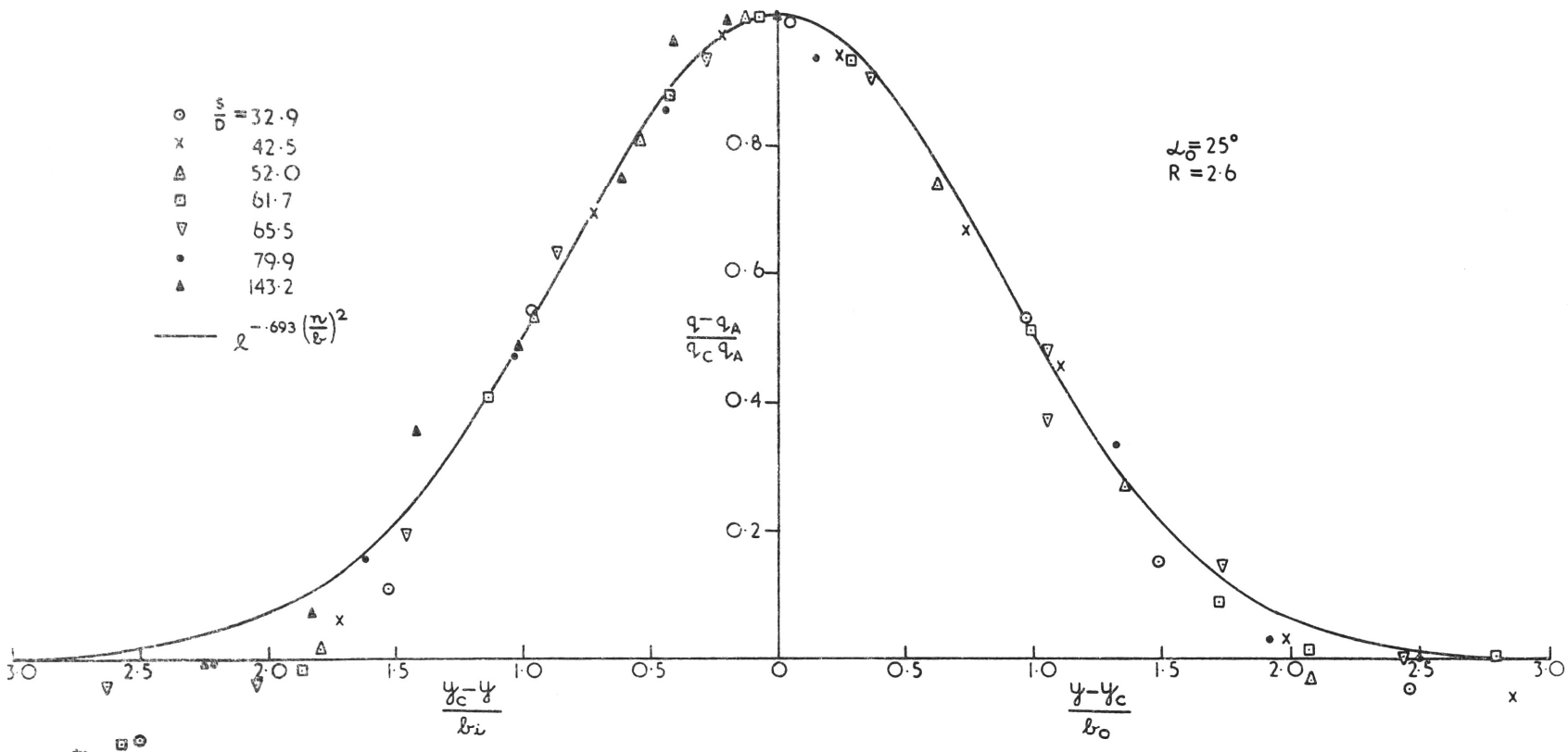

FIG. I-4(c) DIMENSIONLESS EXCESS DYNAMIC PRESSURE PROFILES

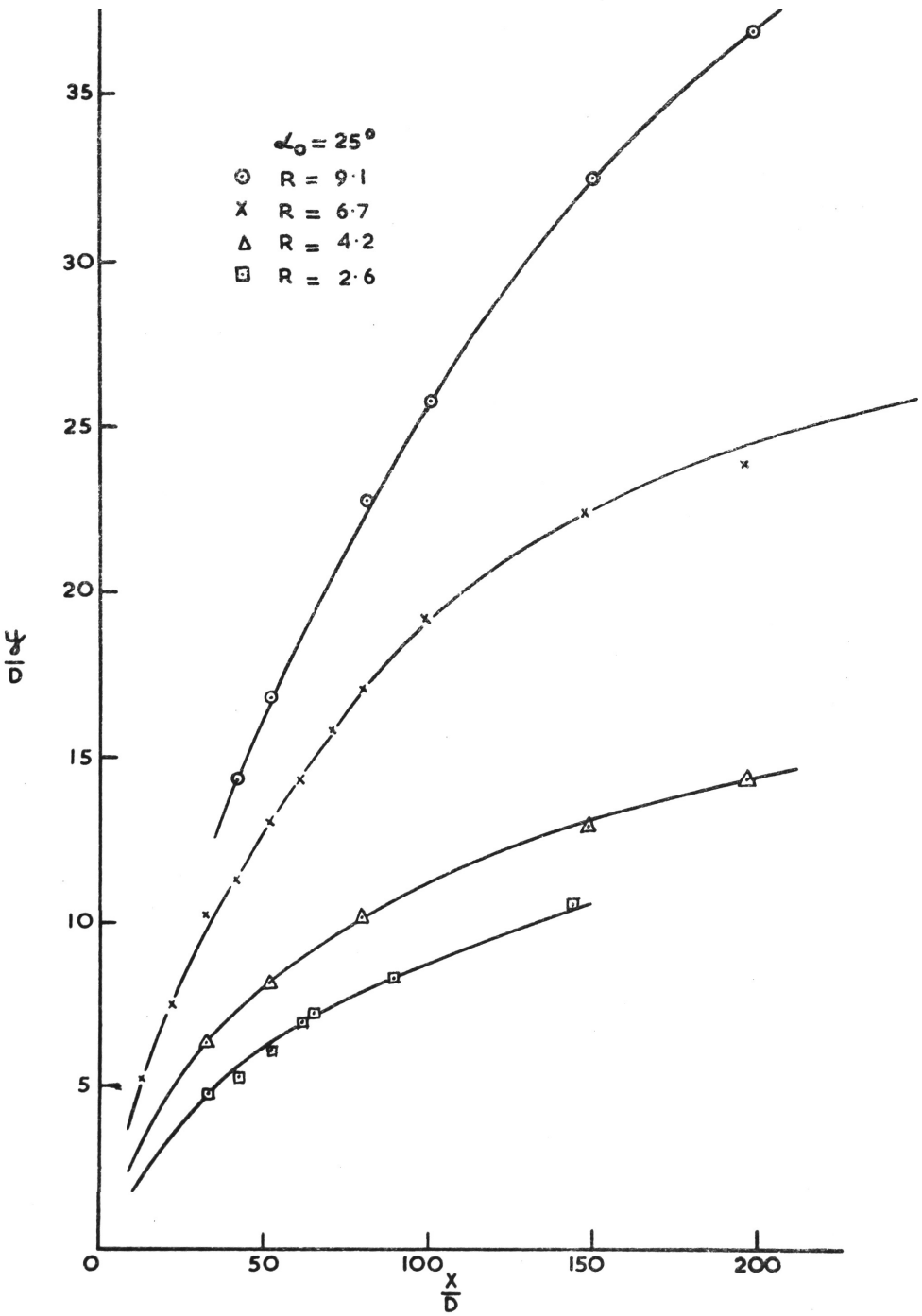

FIG. I·5(a) LOCATION OF JET AXIS

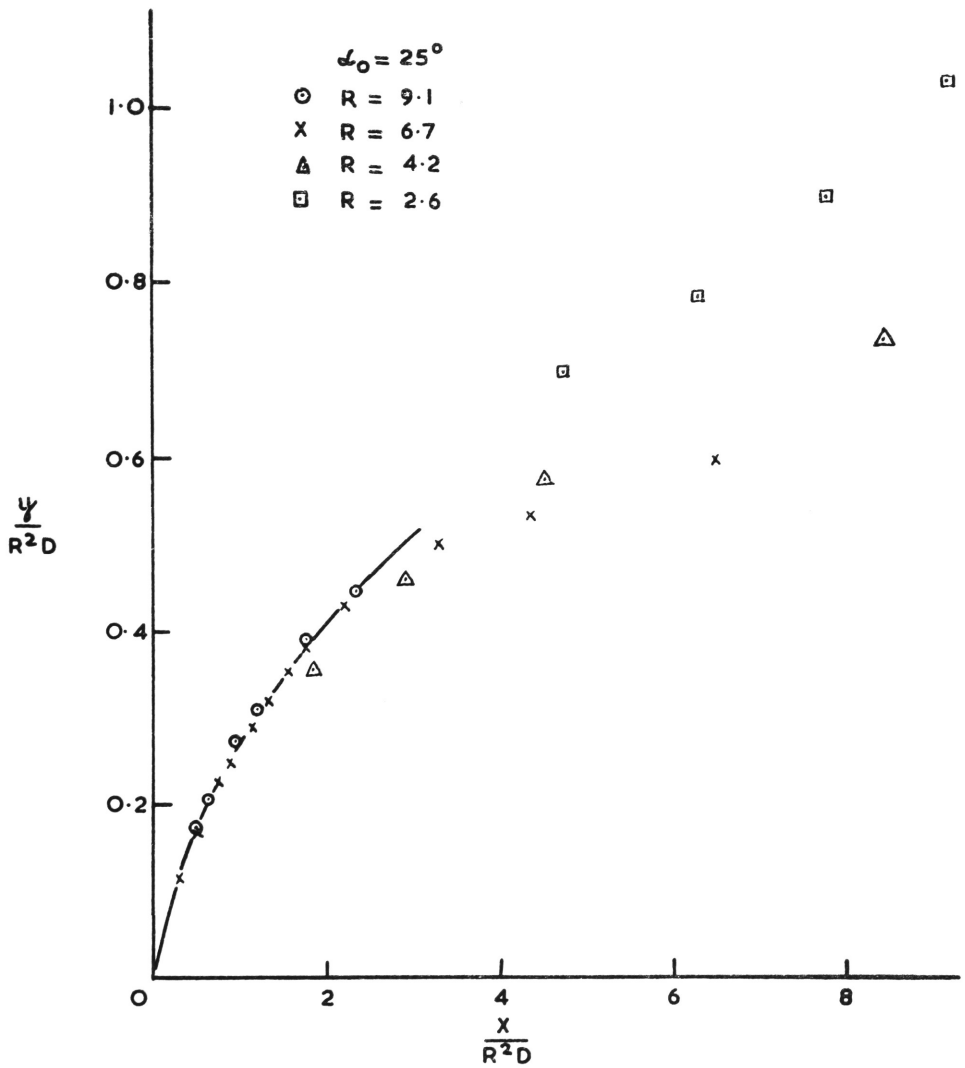

FIG. I·5 (b) LOCATION OF JET AXIS IN REDUCED CO-ORDINATES

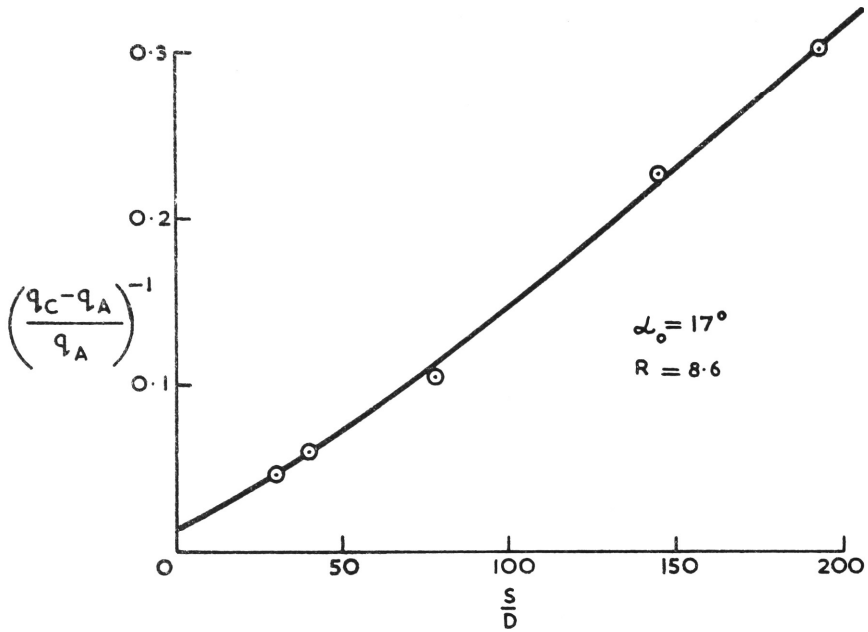

FIG. II·1 (a) DECAY OF AXIAL EXCESS DYNAMIC PRESSURE

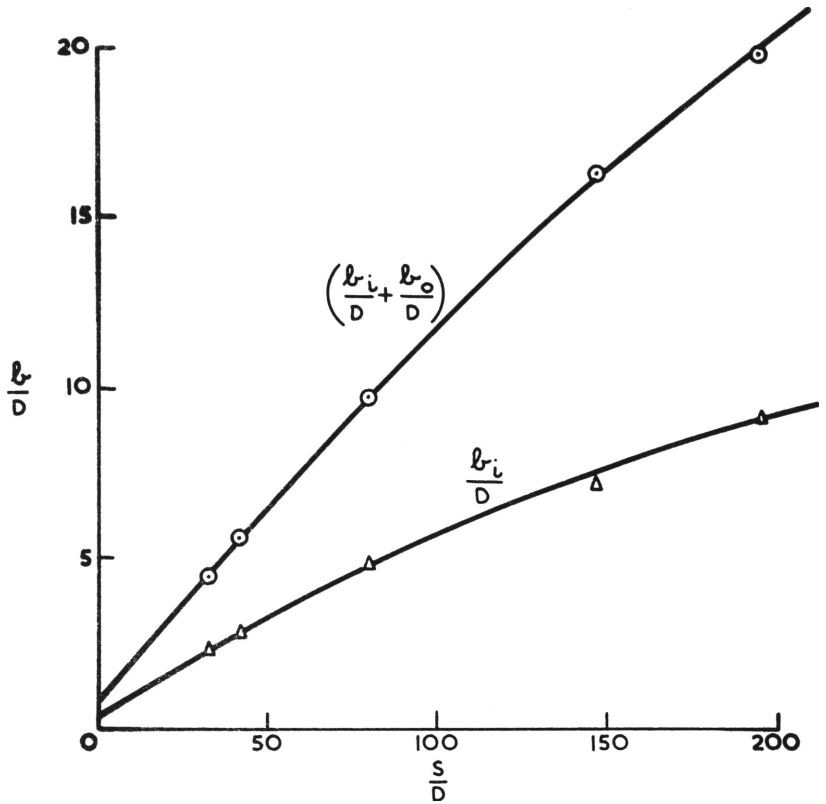

FIG. II·1 (b) LATERAL SPREAD OF JET

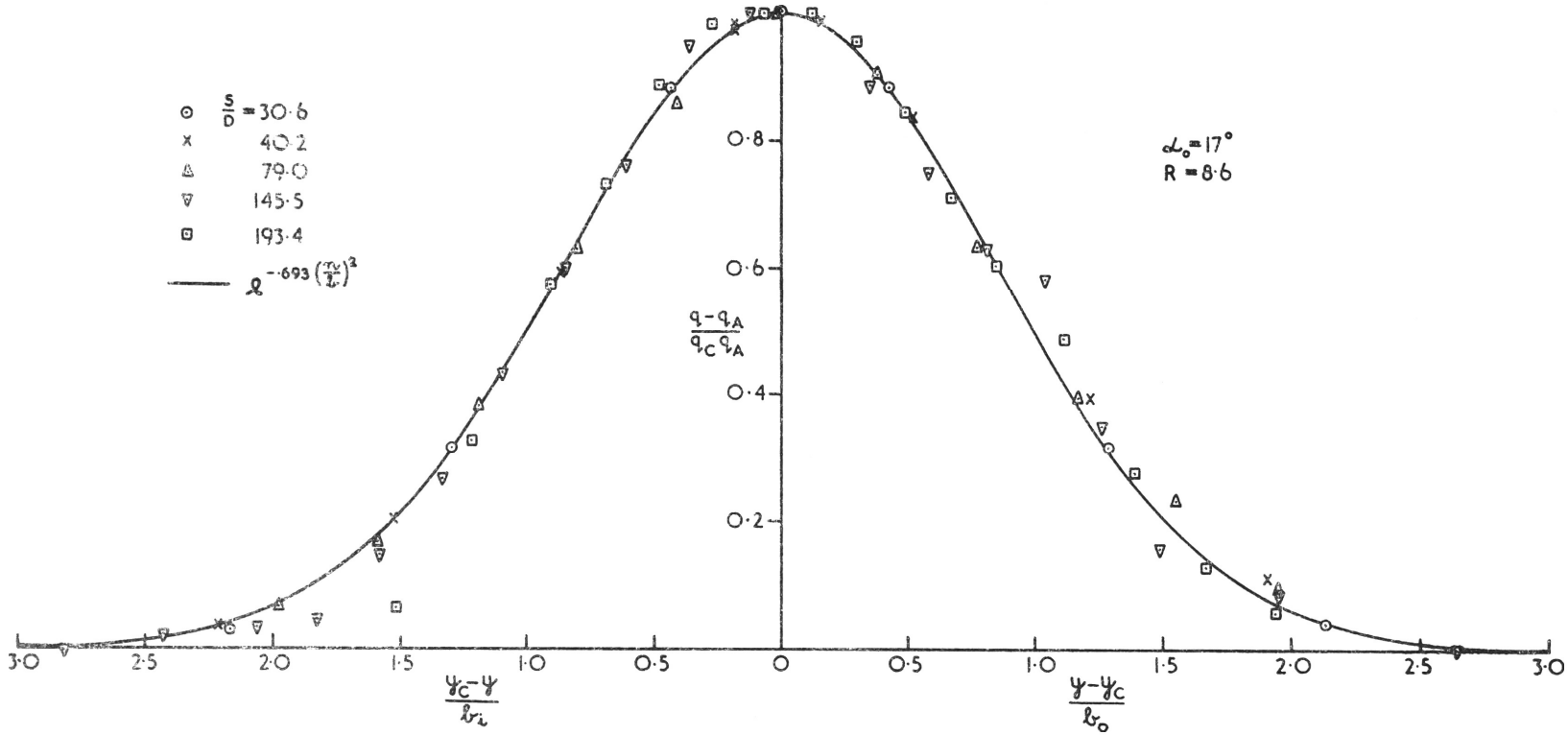

FIG. II·1 (c) DIMENSIONLESS EXCESS DYNAMIC PRESSURE PROFILES

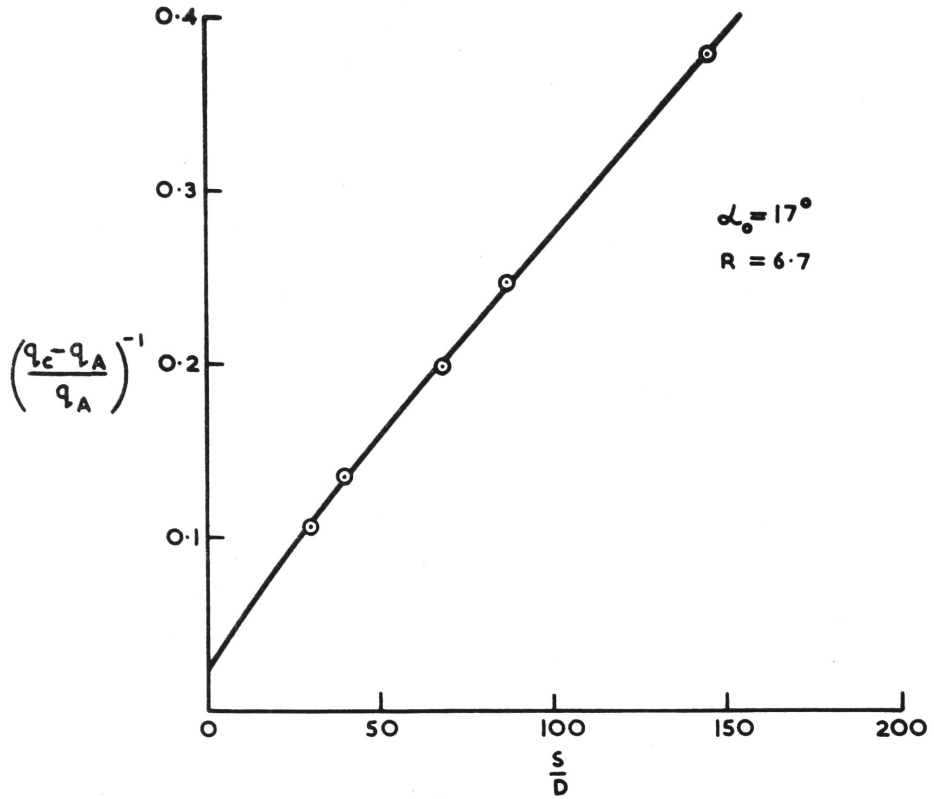

FIG II·2(a) DECAY OF AXIAL EXCESS DYNAMIC PRESSURE

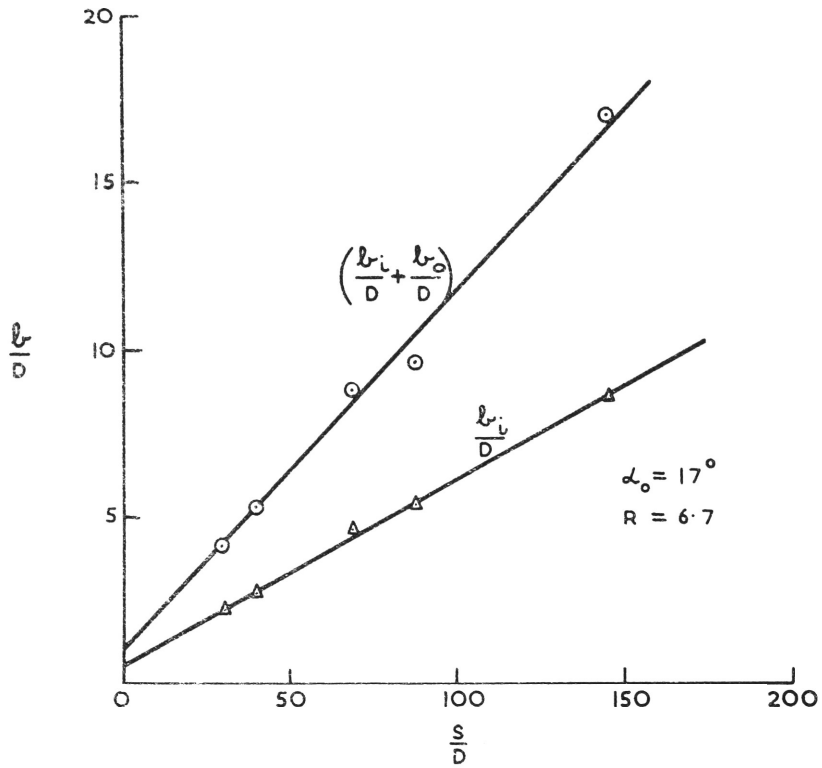

FIG. II·2 (b) LATERAL SPREAD OF JET

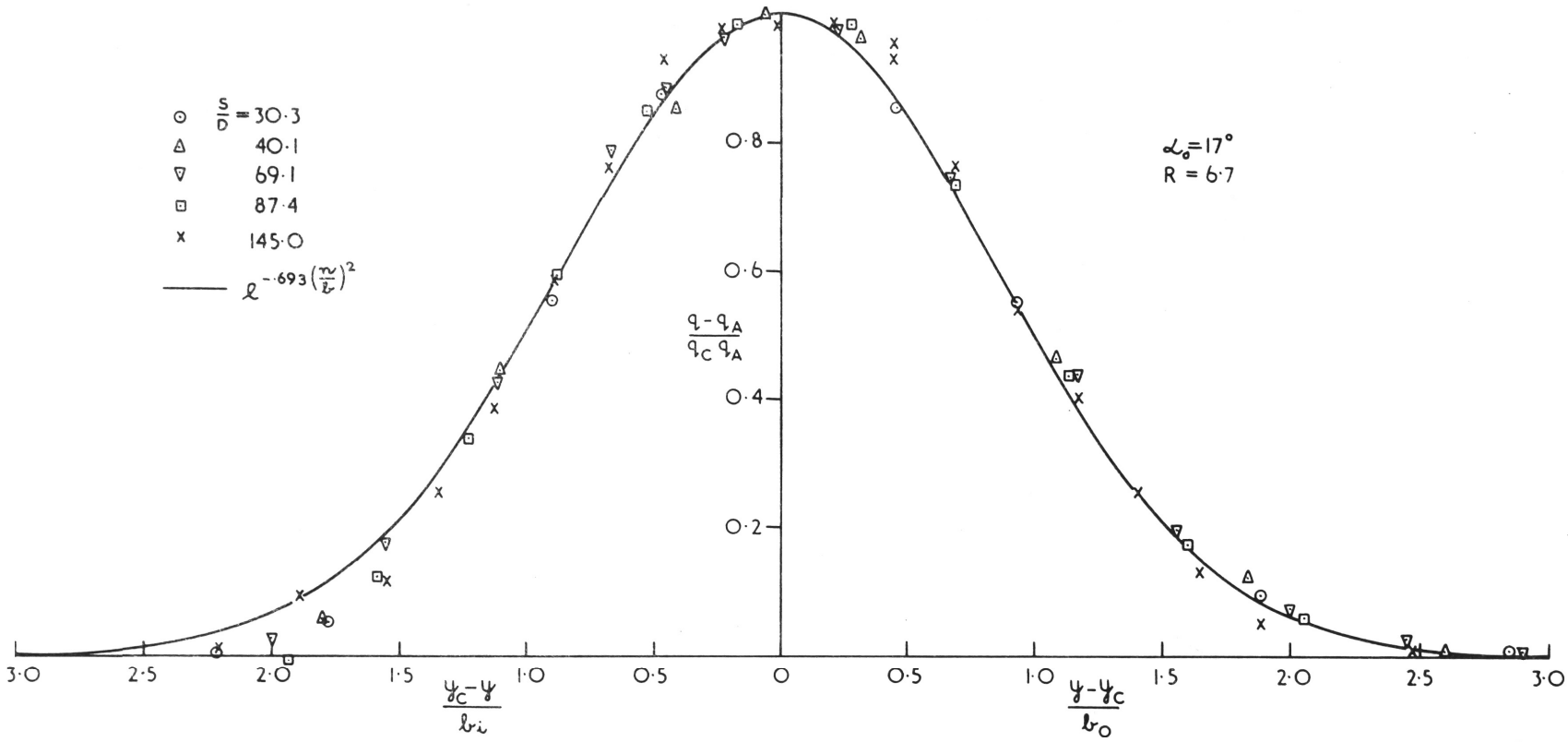

FIG. II·2 (c) DIMENSIONLESS EXCESS DYNAMIC PRESSURE PROFILES

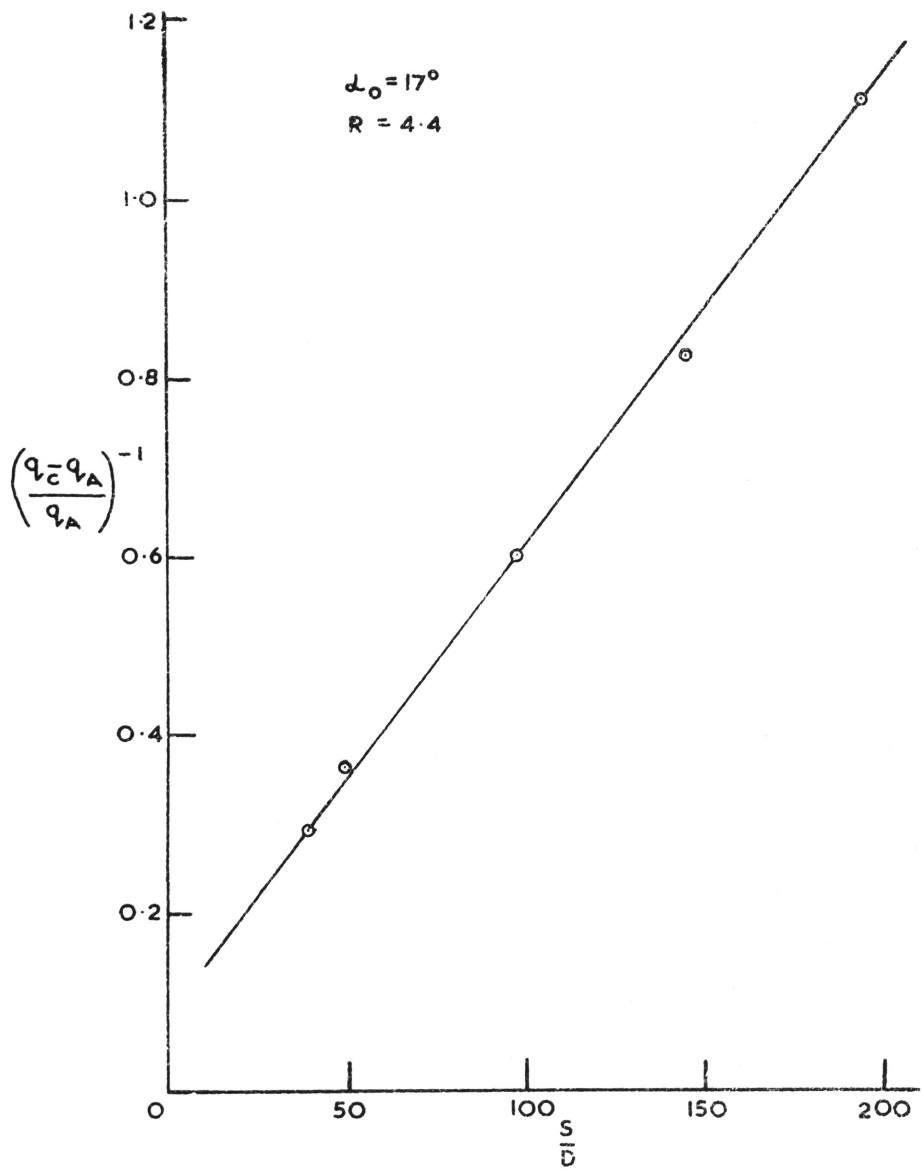

FIG. II·3(a) DECAY OF AXIAL EXCESS DYNAMIC PRESSURE

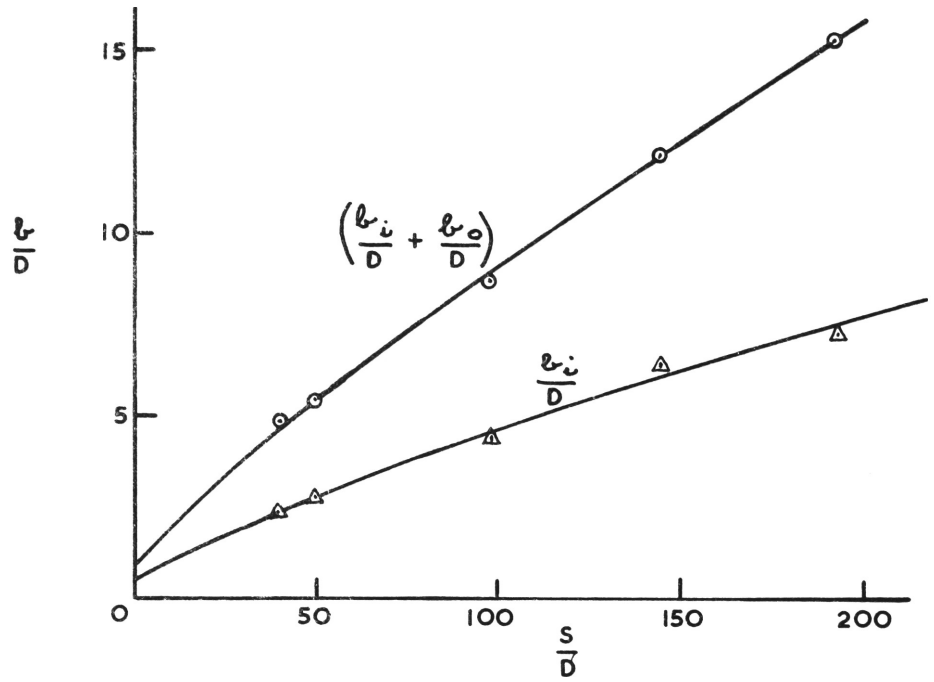

FIG. II·3(b) LATERAL SPREAD OF JET

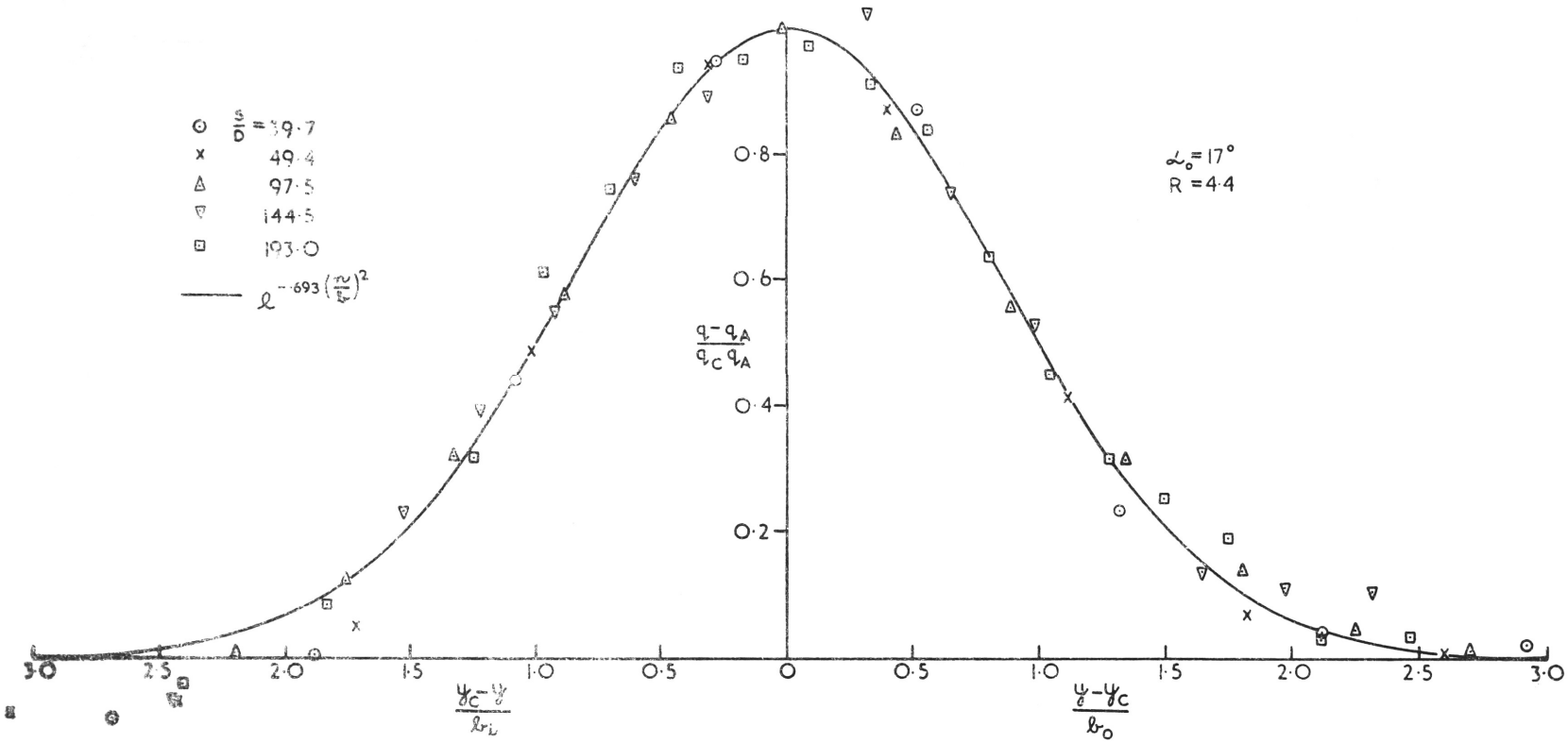

FIG. II·3(c) DIMENSIONLESS EXCESS DYNAMIC PRESSURE PROFILES

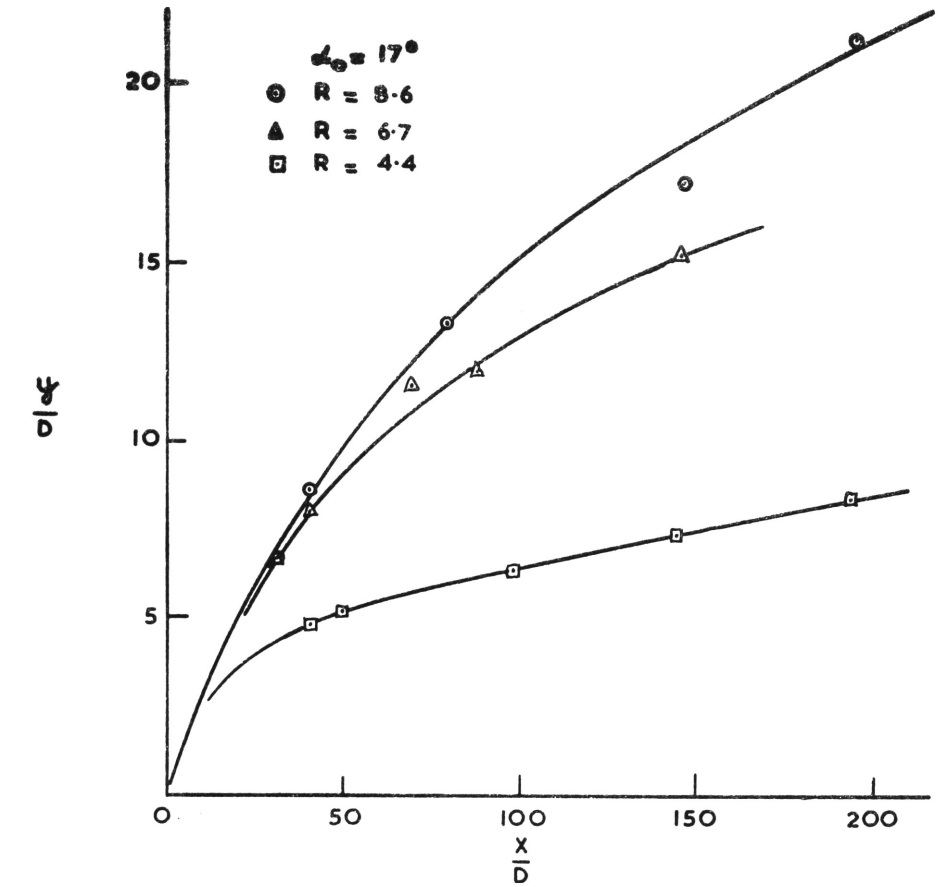

FIG. II·4(a) LOCATION OF JET AXIS

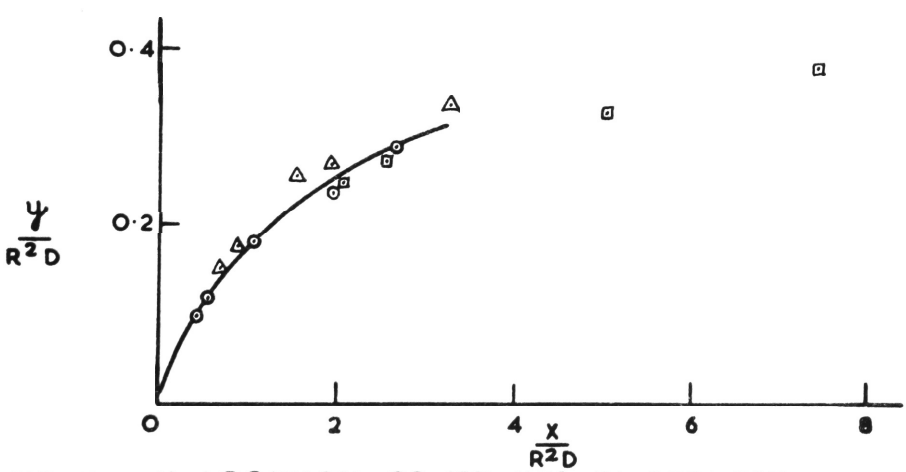

FIG. II·4(b) LOCATION OF JET AXIS IN REDUCED CO-ORDINATES

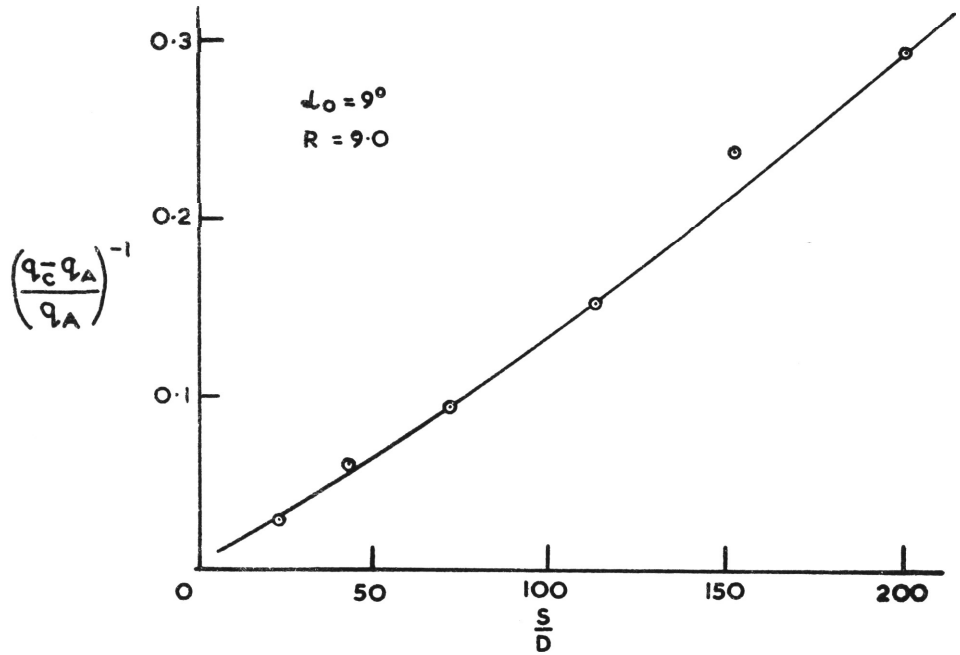

FIG. III: 1(a) DECAY OF AXIAL EXCESS DYNAMIC PRESSURE

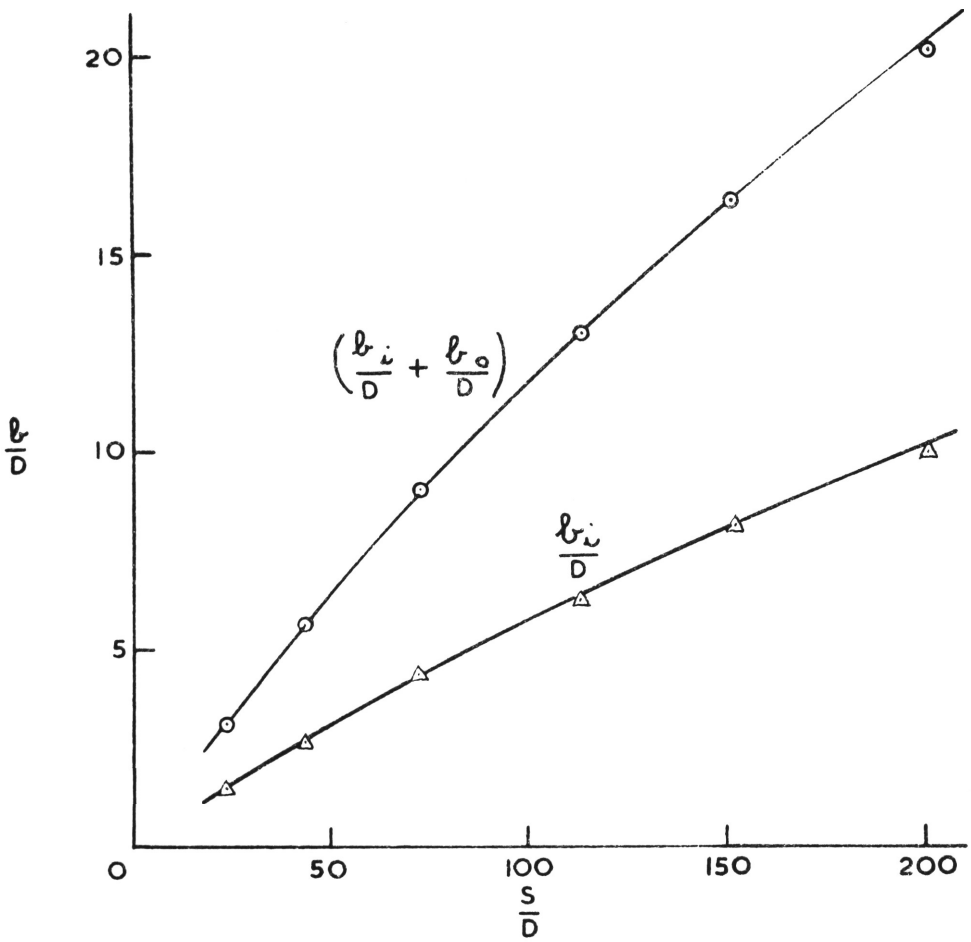

FIG. III-1(b) LATERAL SPREAD OF JET

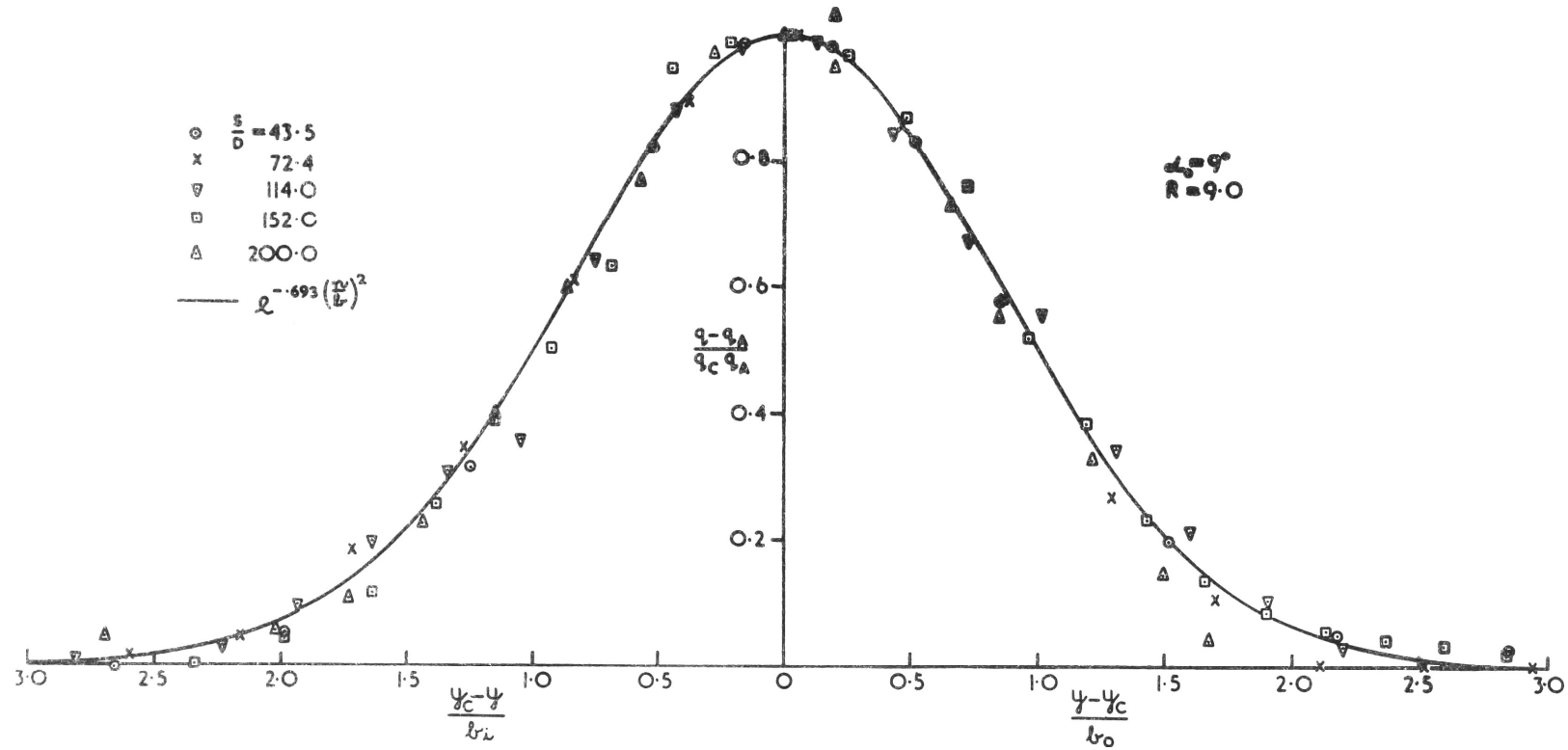

FIG. III·1 (c) DIMENSIONLESS EXCESS DYNAMIC PRESSURE PROFILES

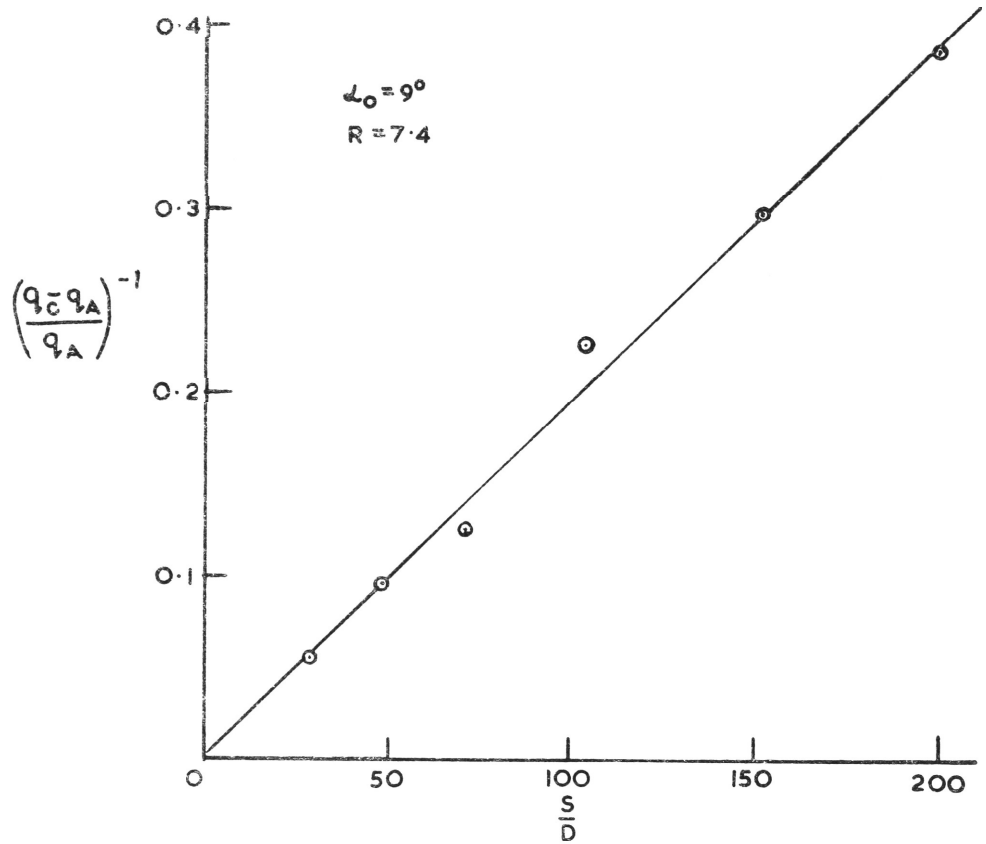

FIG. III·2(a) DECAY OF AXIAL EXCESS DYNAMIC PRESSURE

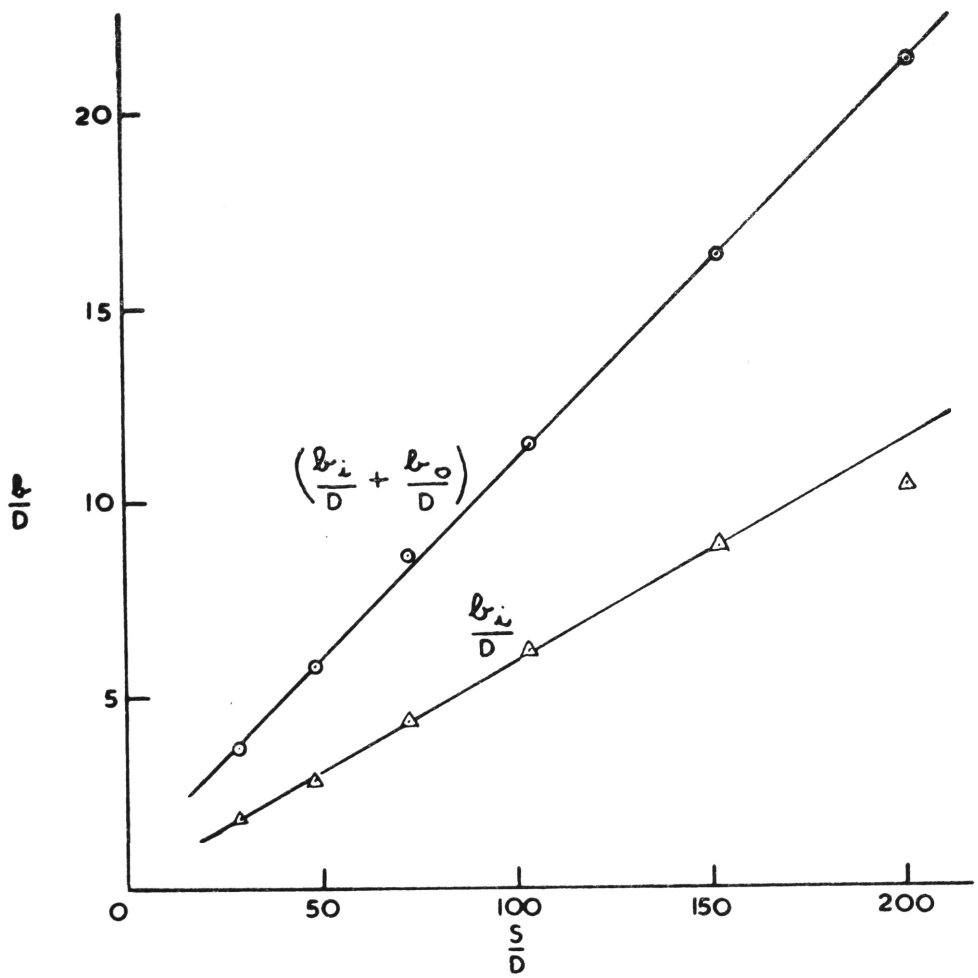

FIG. III·2(b) LATERAL SPREAD OF JET

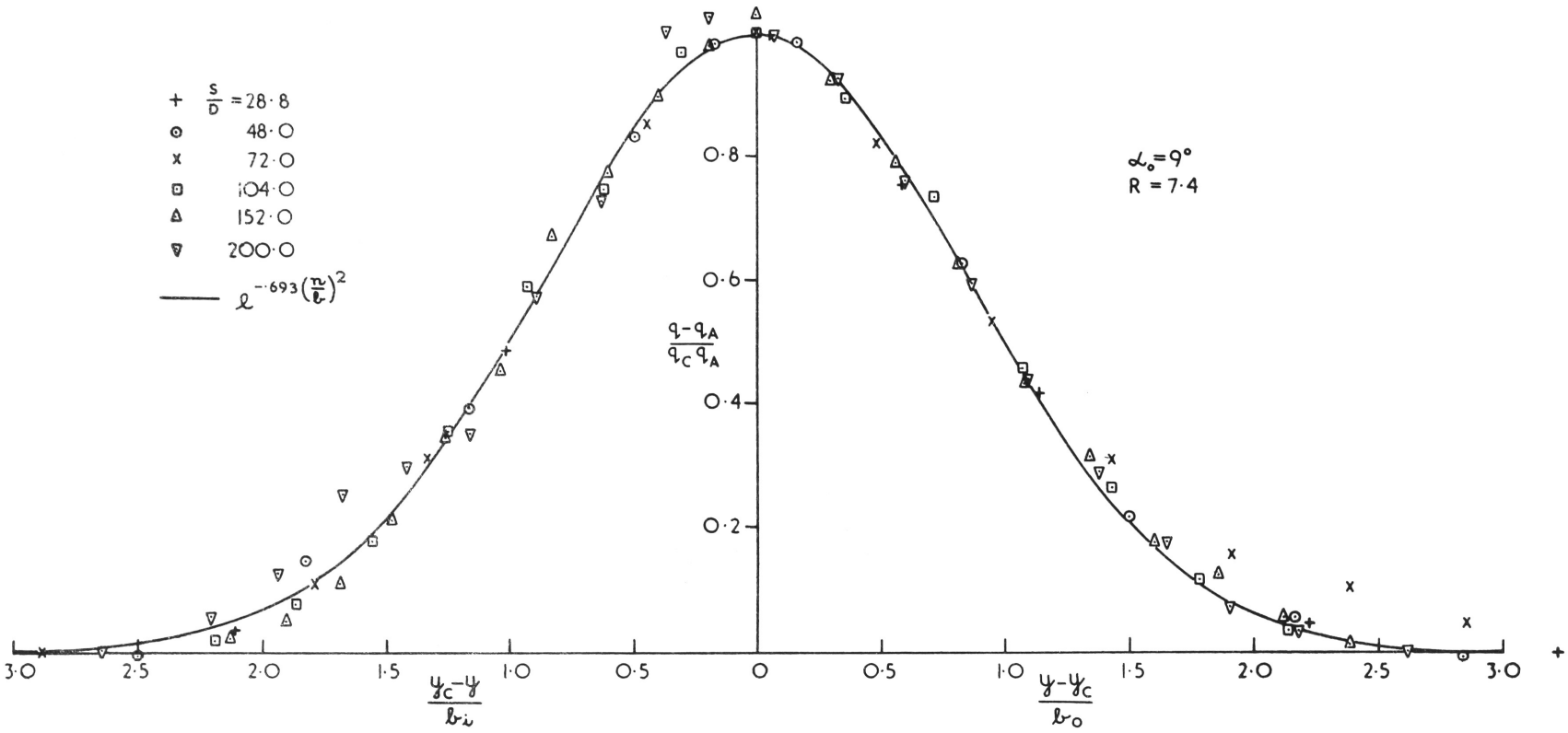

FIG. III·2(c) DIMENSIONLESS EXCESS DYNAMIC PRESSURE PROFILES

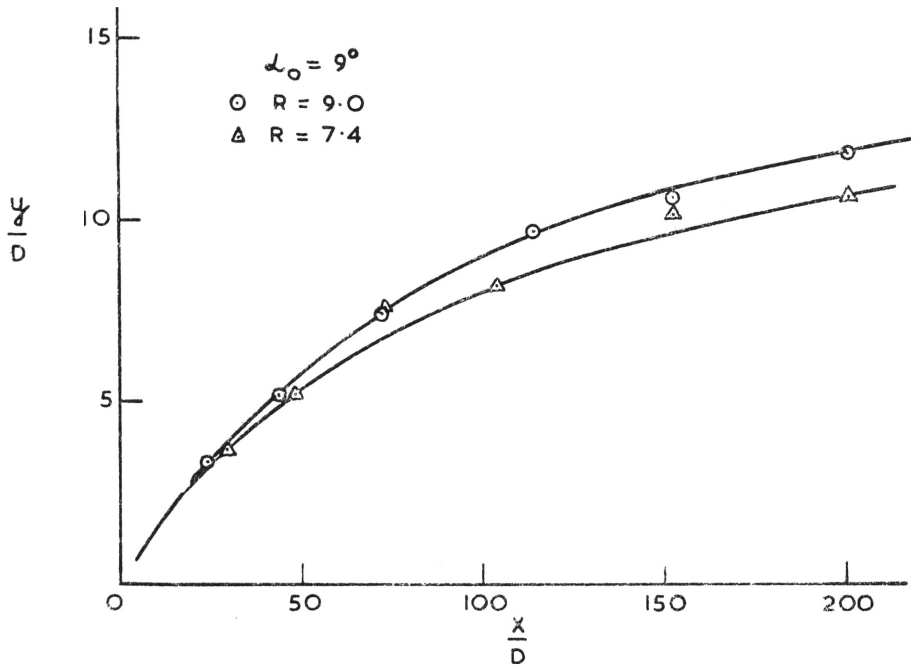

FIG. III·3 (a) LOCATION OF JET AXIS

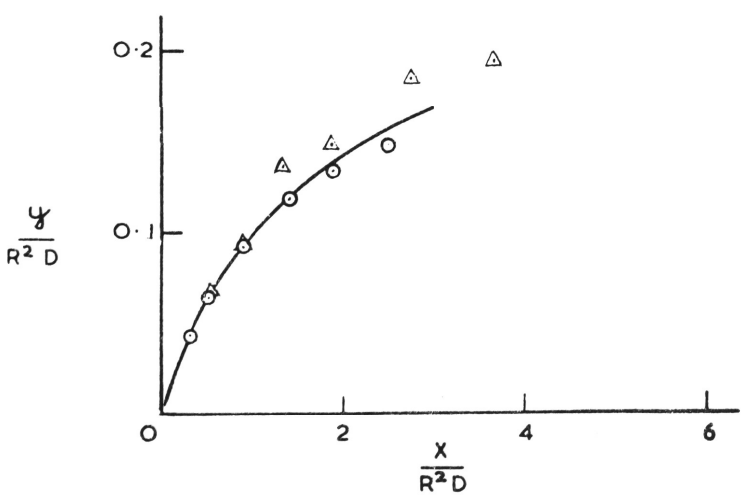

FIG. III·3 (b) LOCATION OF JET AXIS IN REDUCED CO-ORDINATES

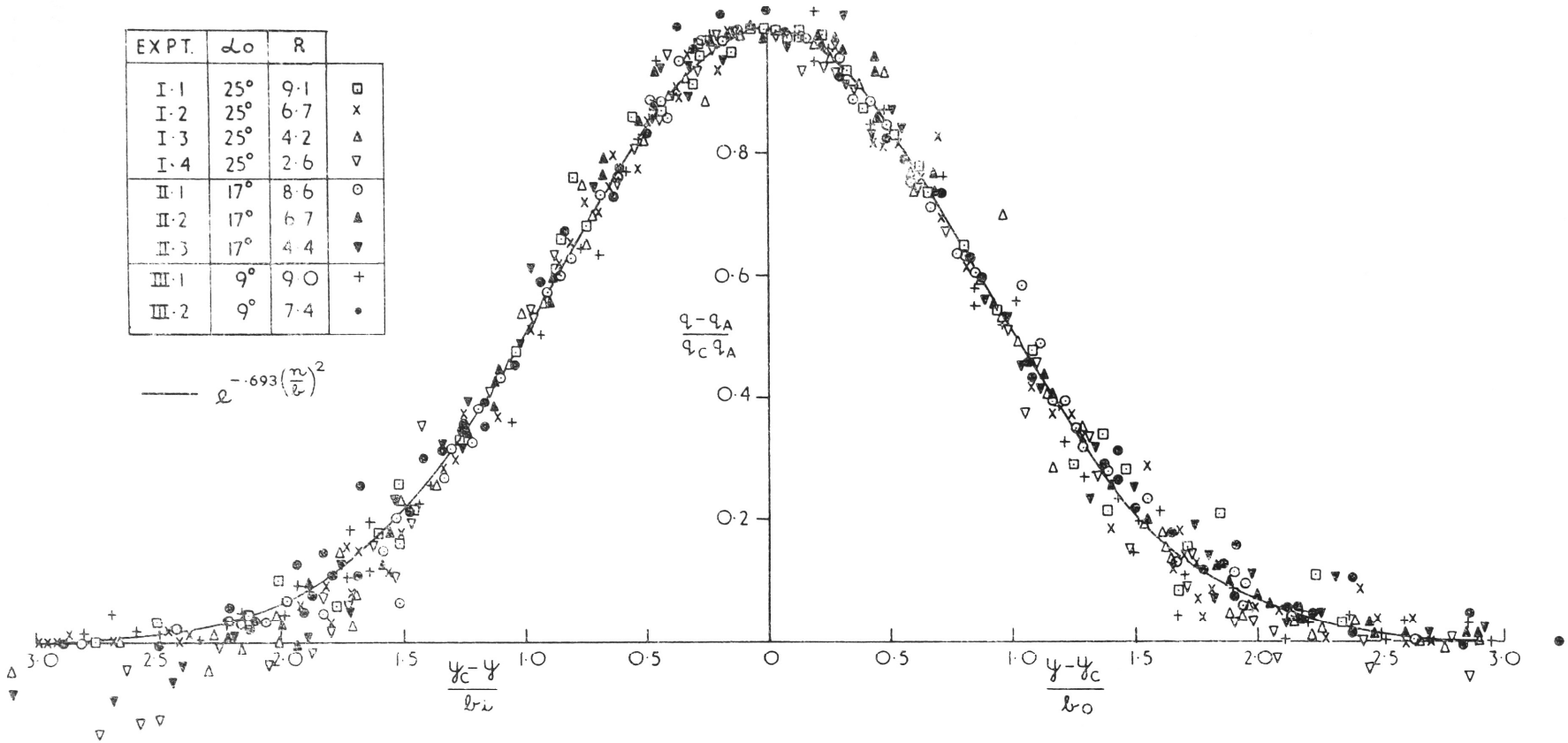

FIG. IV DIMENSIONLESS EXCESS DYNAMIC PRESSURE PROFILES

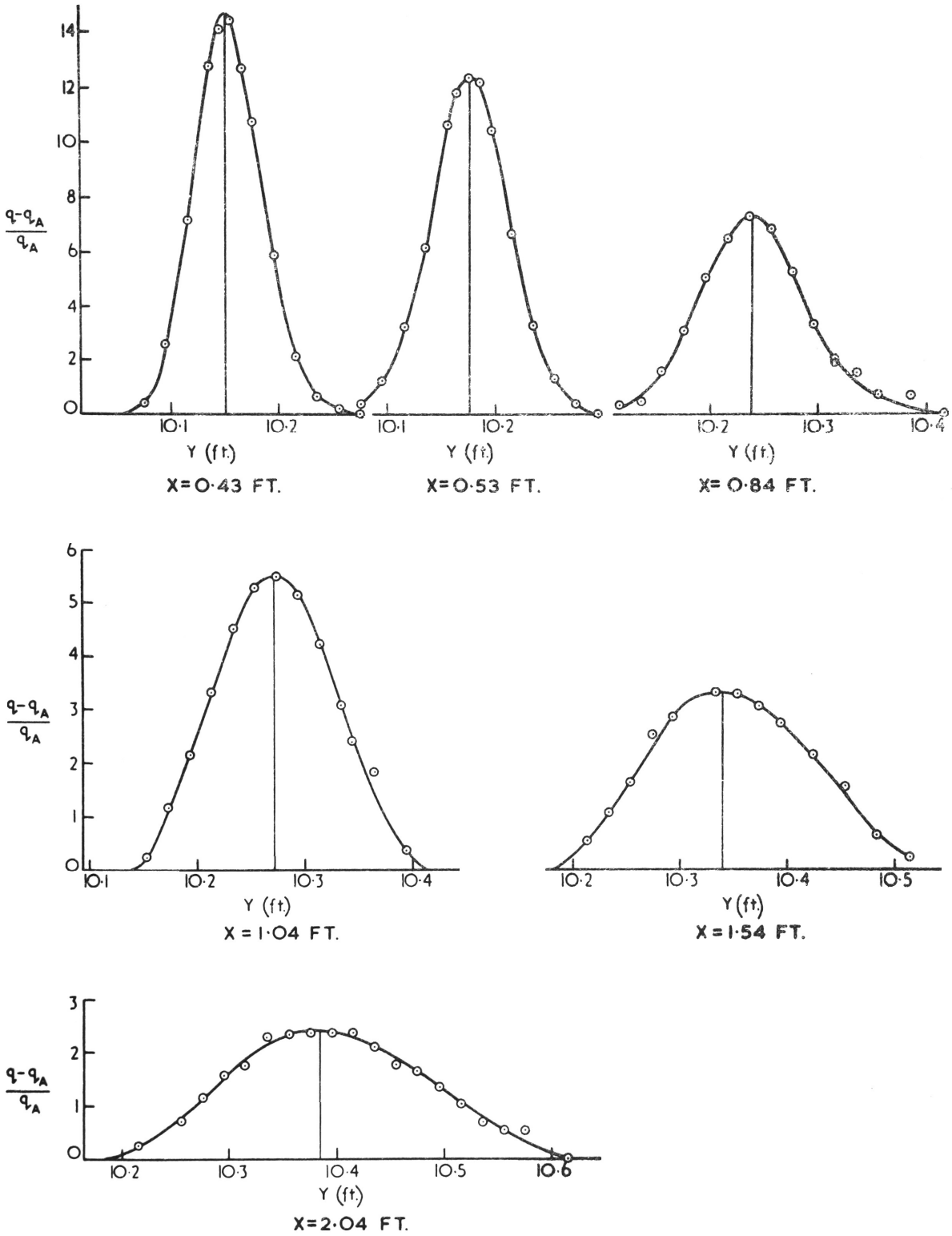

FIG. A I·1 PROFILES OF EXCESS DYNAMIC PRESSURE

Angle of Deflection $\alpha_0 = 25°$ Velocity Ratio (Jet/Ambient) R = 9·1

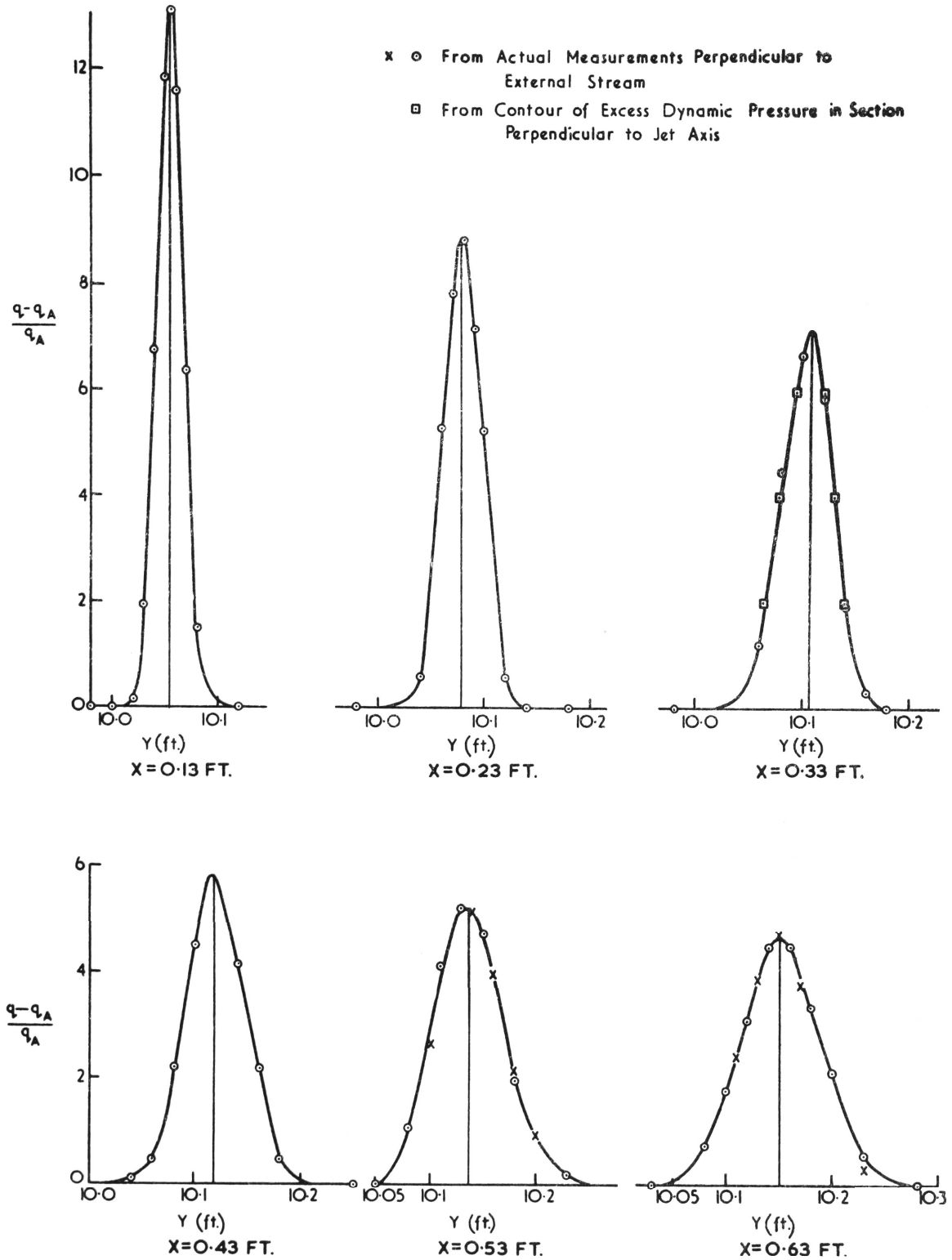

FIG. A I·2 PROFILES OF EXCESS DYNAMIC PRESSURE

Angle of Deflection $\alpha_0 = 25°$

Velocity Ratio (Jet/Ambient) R = 6·7

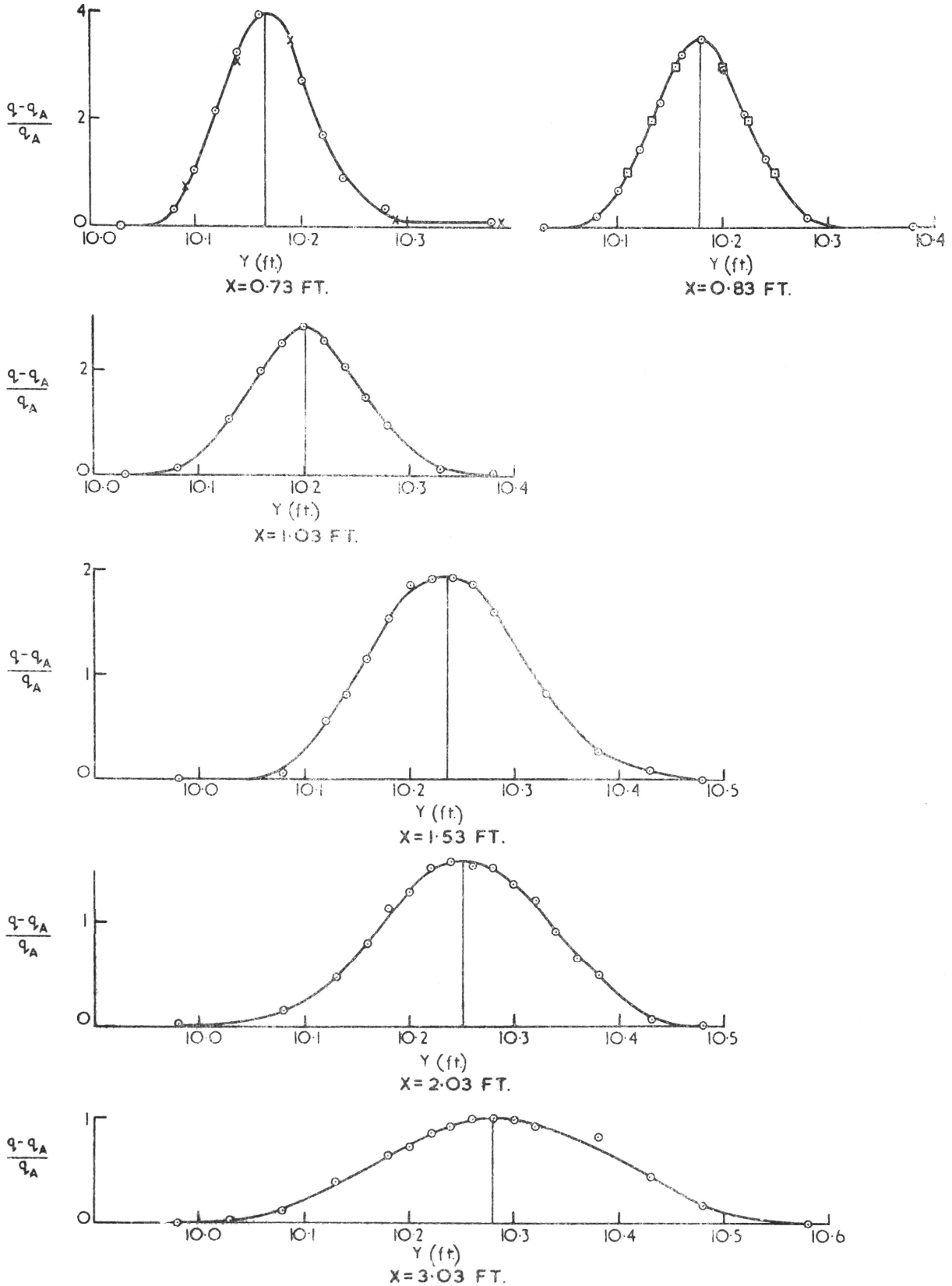

FIG. A I·2 (Cont'd) PROFILES OF EXCESS DYNAMIC PRESSURE

Angle of Deflection $\alpha_0 = 25°$ Velocity Ratio (Jet/Ambient) R = 6·7

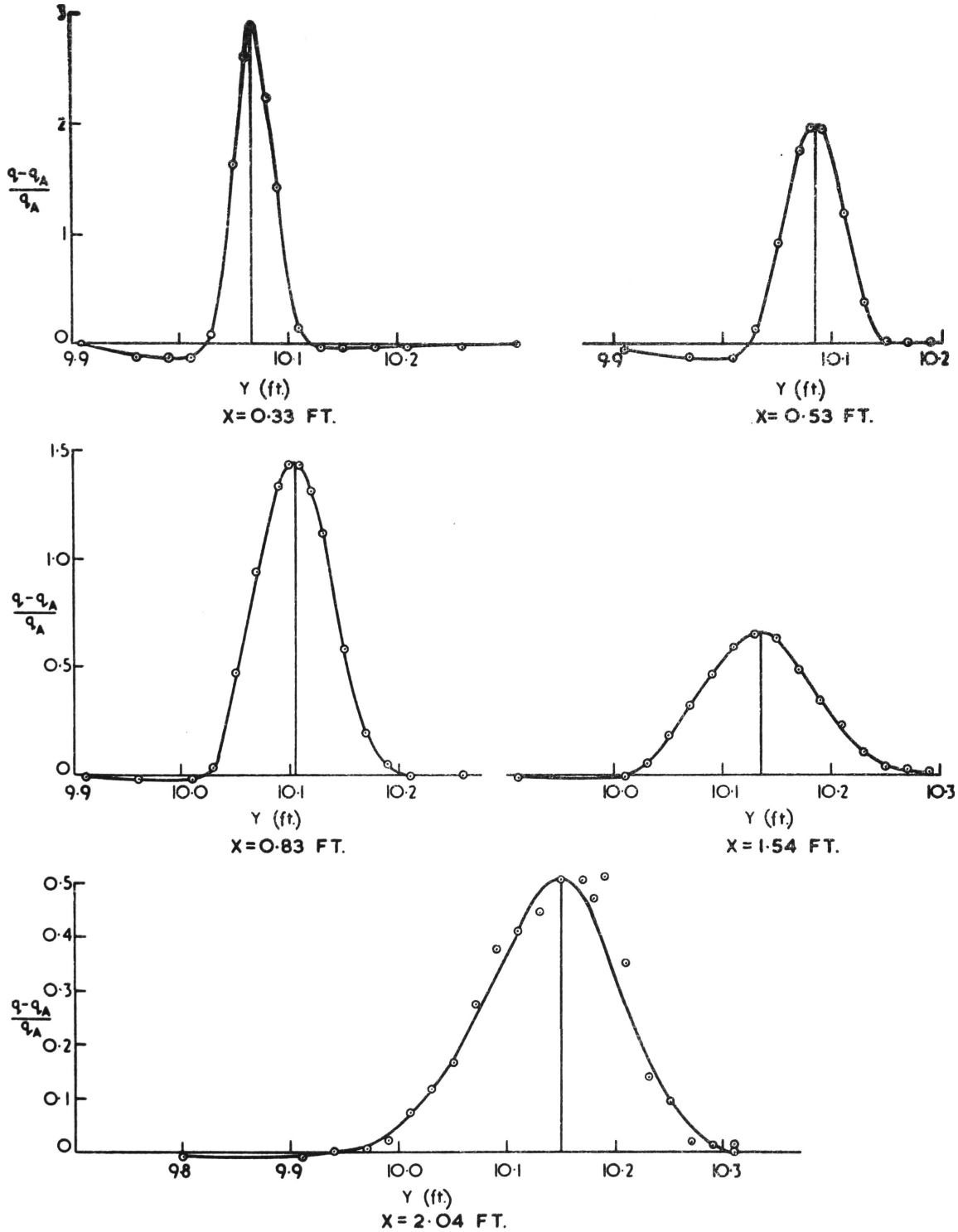

FIG. AI·3 PROFILES OF EXCESS DYNAMIC PRESSURE

Angle of Deflection $\alpha_o = 25°$

Velocity Ratio (Jet/Ambient) R = 4·2

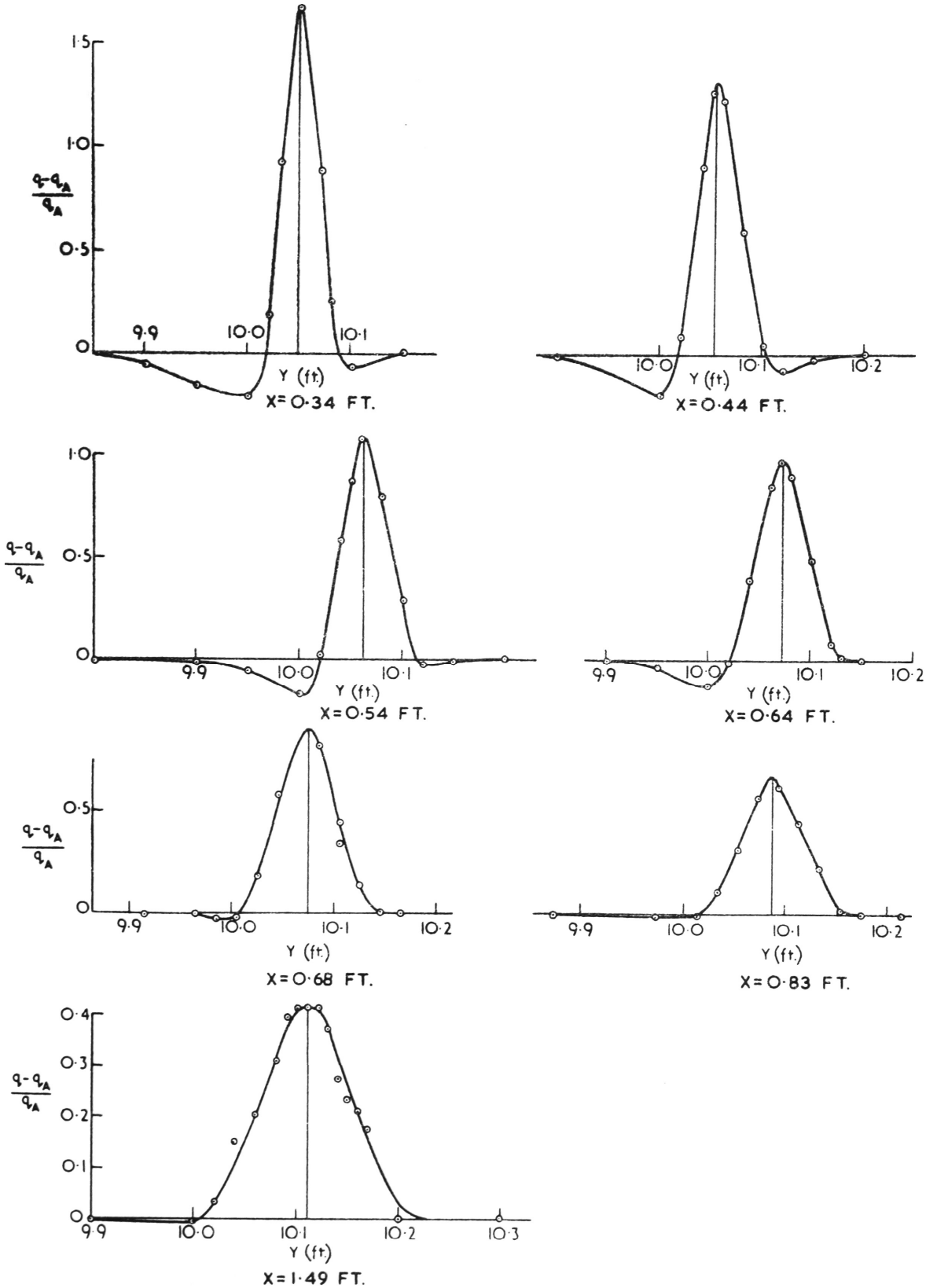

FIG. AI·4 PROFILES OF EXCESS DYNAMIC PRESSURE

Angle of Deflection $\alpha_0 = 25°$ Velocity Ratio (Jet/Ambient) R = 2·6

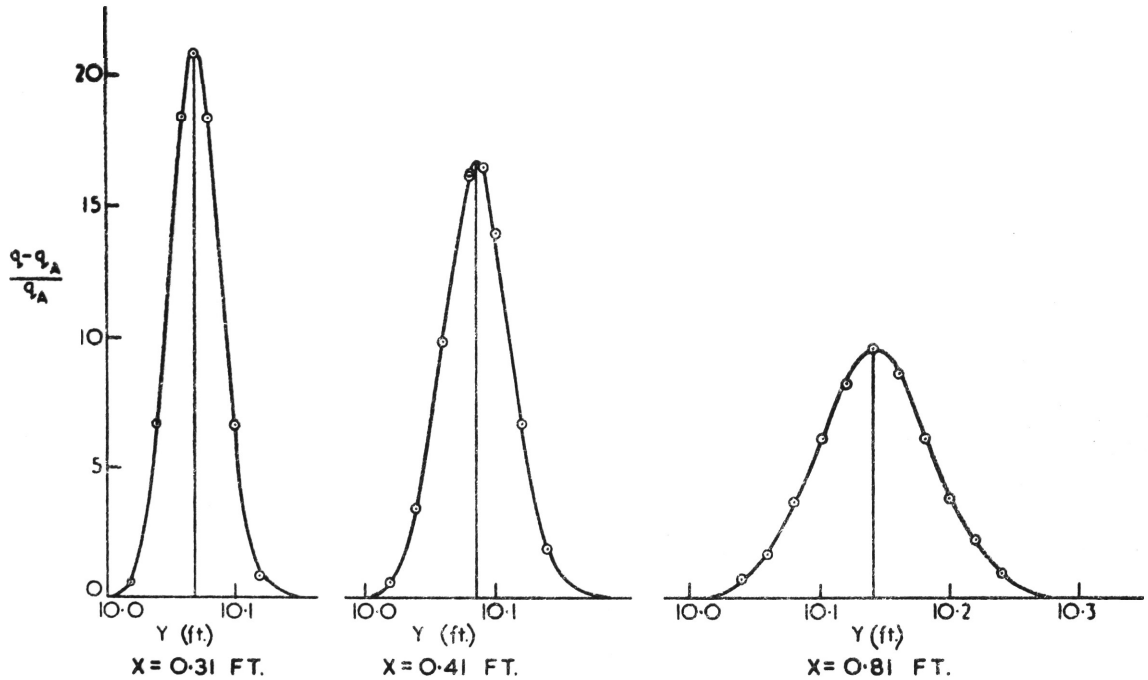

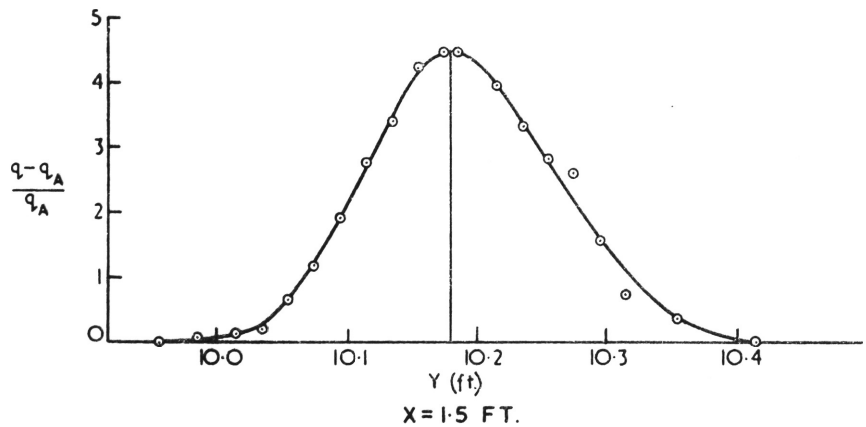

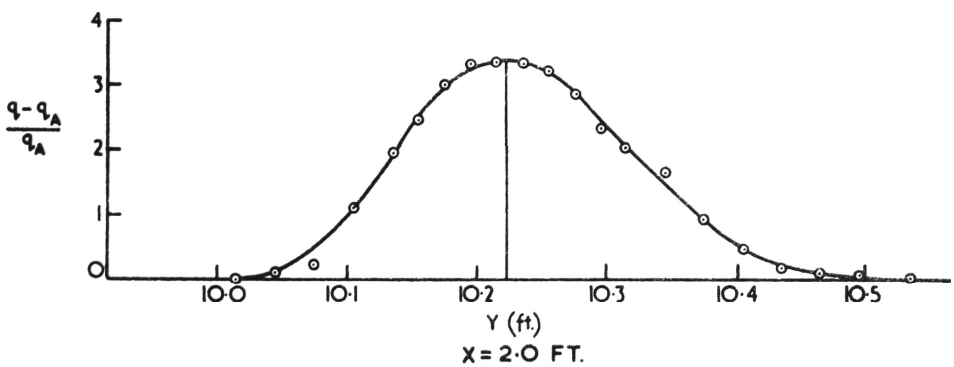

FIG. A II·1 PROFILES OF EXCESS DYNAMIC PRESSURE

Angle of Deflection $\alpha_0 = 17°$

Velocity Ratio (Jet/Ambient) R = 8·6

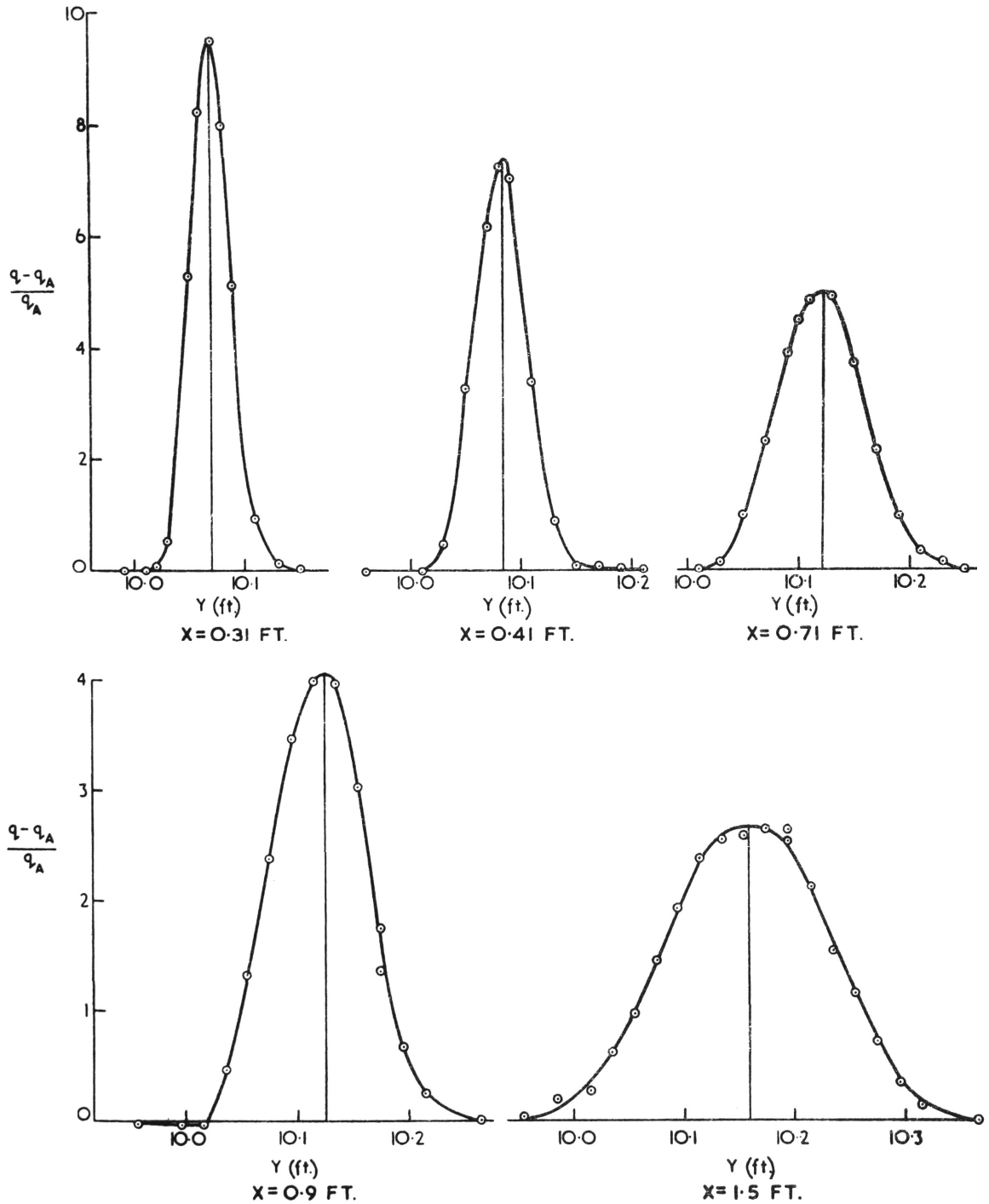

FIG. A II·2 PROFILES OF EXCESS DYNAMIC PRESSURE

Angle of Deflection $\alpha_o = 17^\circ$
Velocity Ratio (Jet/Ambient) R = 6·7

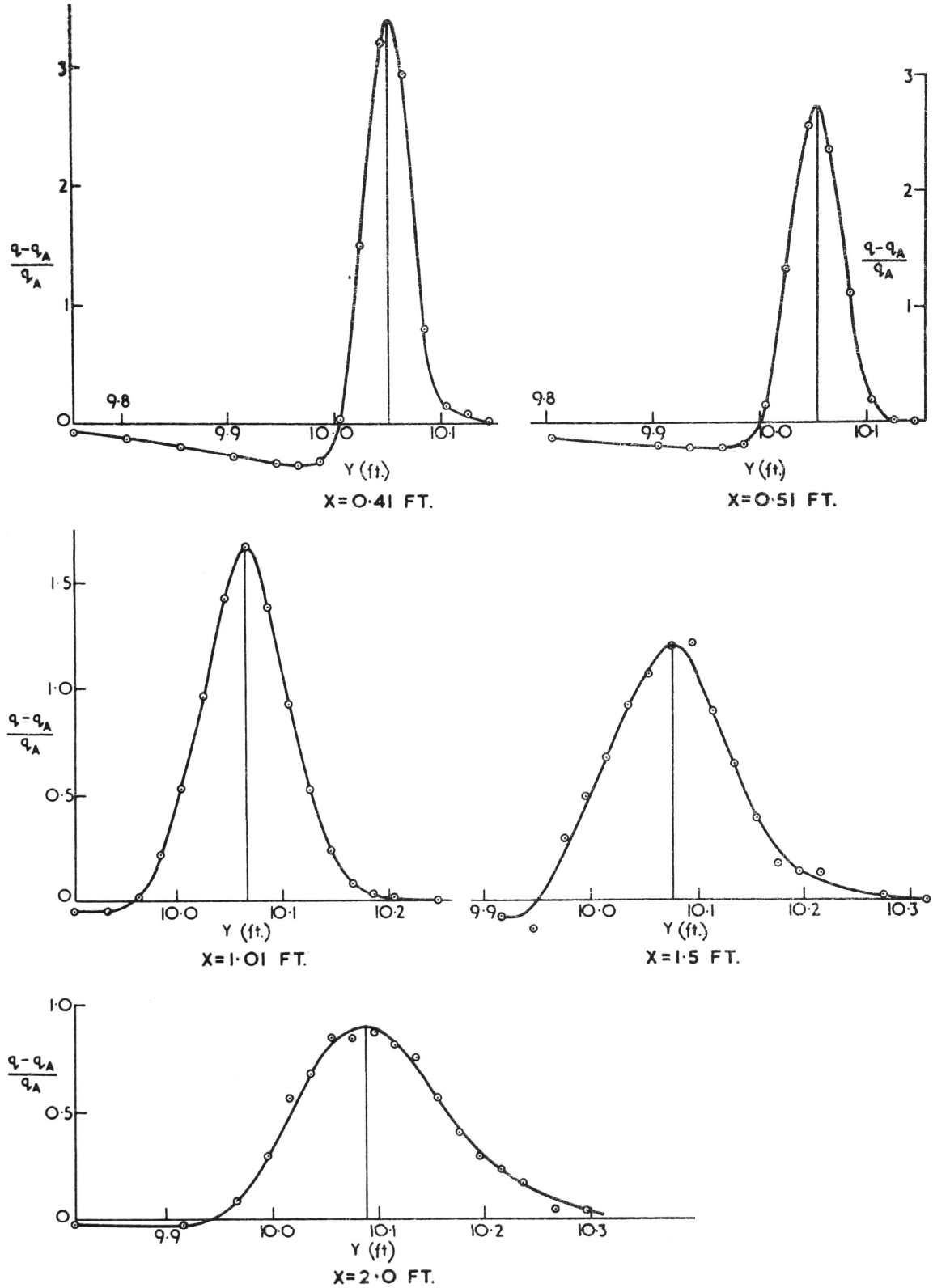

FIG. AII·3 PROFILES OF EXCESS DYNAMIC PRESSURE

Angle of Deflection $\alpha_0 = 17°$

Velocity Ratio (Jet/Ambient) R = 4·4

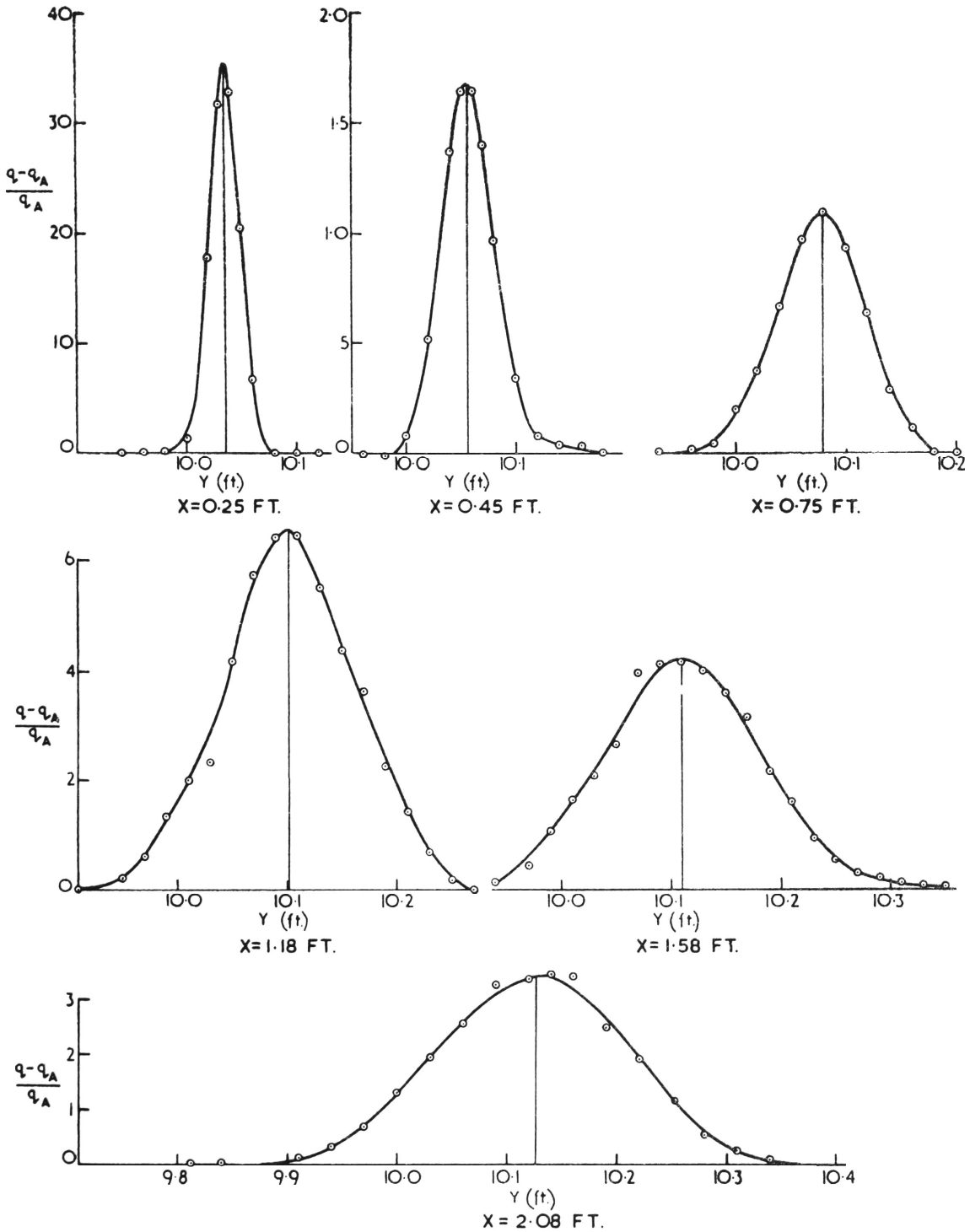

FIG. A III·1 PROFILES OF EXCESS DYNAMIC PRESSURE

Angle of Deflection $\alpha_o = 9°$

Velocity Ratio (Jet/Ambient) R = 9·0

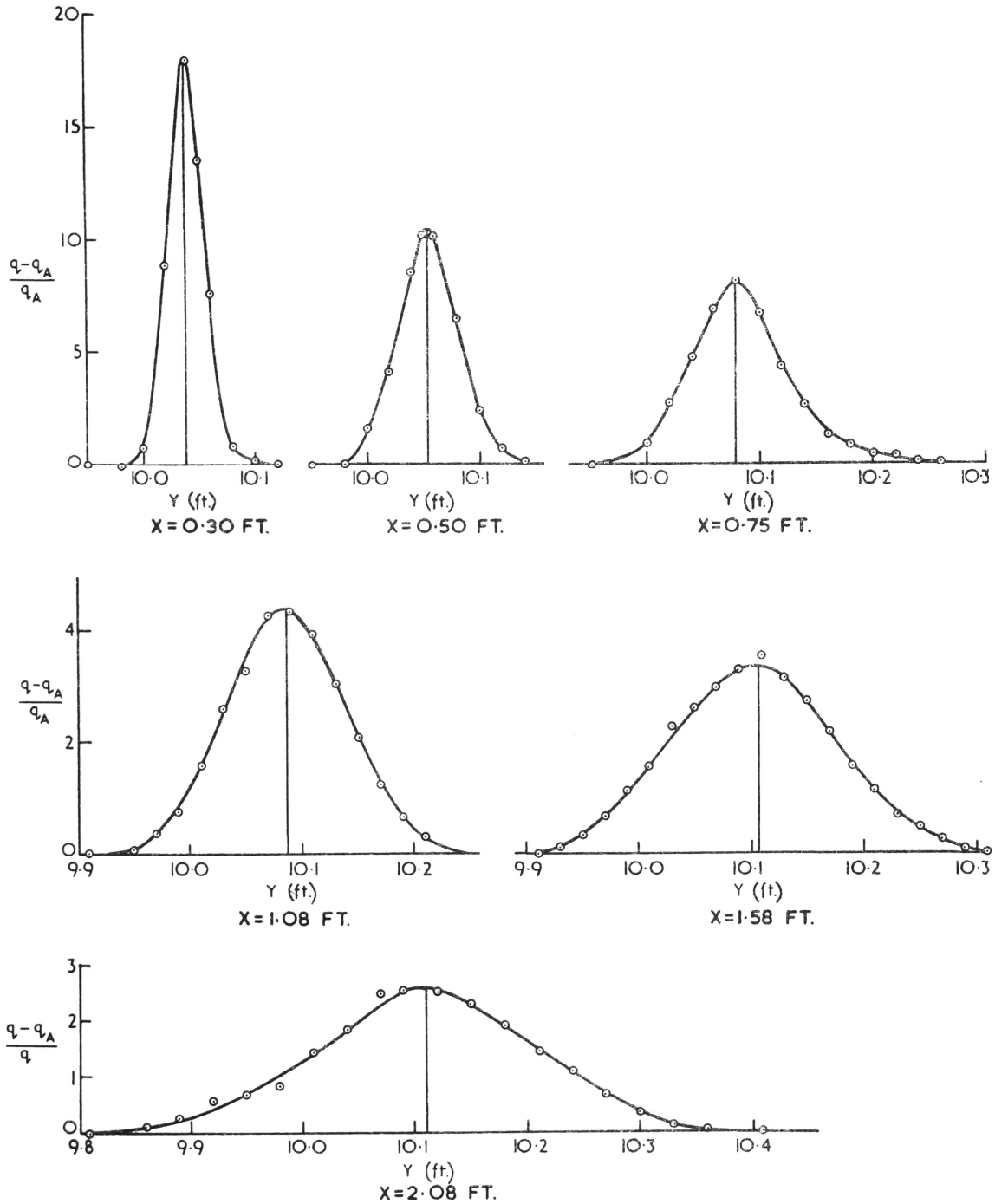

FIG. A III·2 PROFILES OF EXCESS DYNAMIC PRESSURE

Angle of Deflection $\alpha_0 = 9°$

Velocity Ratio (Jet/Ambient) $R = 7·4$

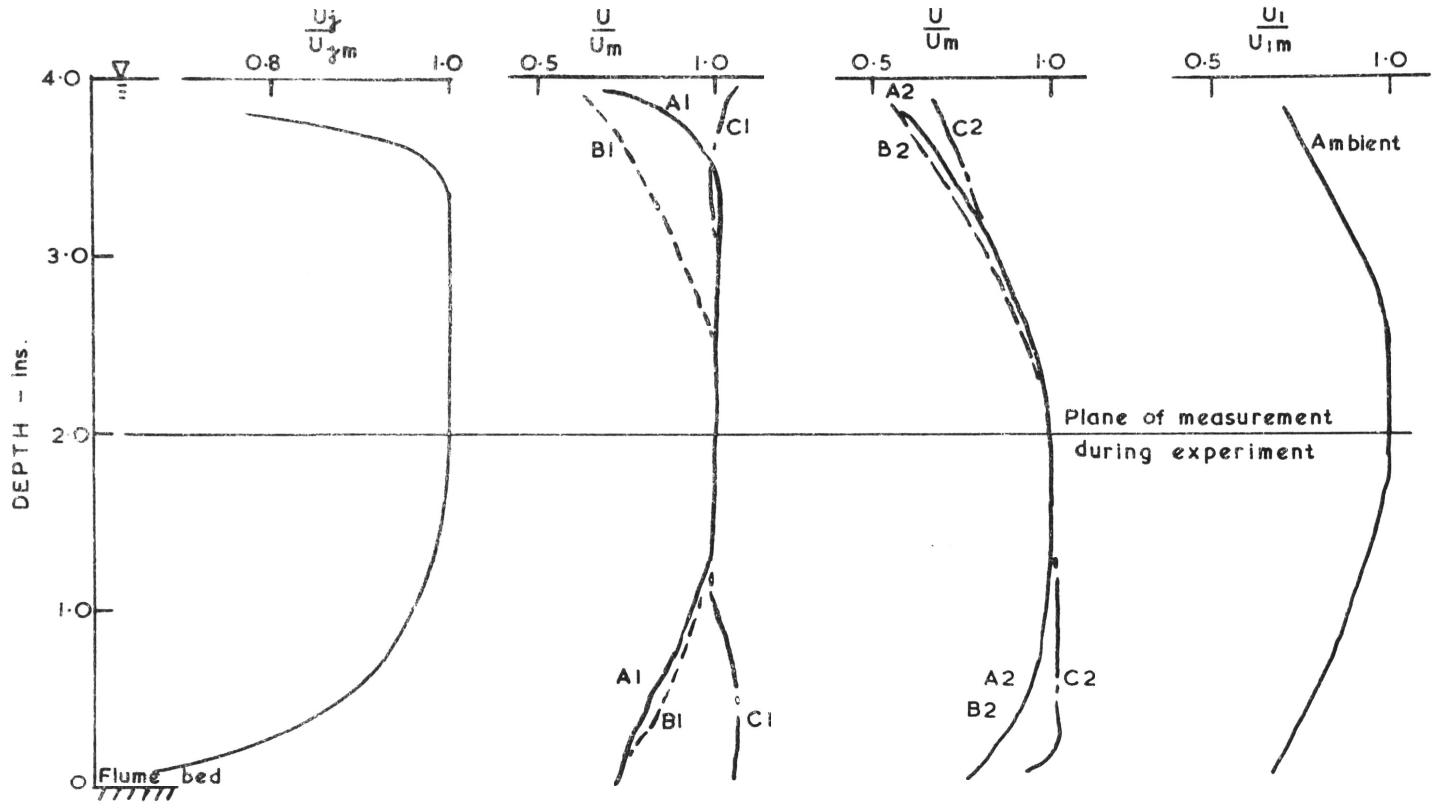

1.) INITIAL JET VEL. DISTRIBUTION

2.) AT JET AXIS $\eta = 0$

3.) AT $\eta = 2{\cdot}0$ FROM JET AXIS

4.) IN AMBIENT STREAM

A = X = 0·5 ft. (from nozzle)
B = X = 1·0
C = X = 2·0

Suffice m refers to the value at the plane of measurement during the experiments, i.e. at 2" from the flume bed

FIG. A IV DEPARTURE FROM TWO-DIMENSIONALITY

(MEASUREMENTS MADE IN FLOW FROM 9° DEFLECTOR. $V_j \doteq 10{\cdot}2$ FT/SEC. IN PLANE 'm' $V_A \doteq 1{\cdot}1$ FT/SEC IN PLANE 'm'

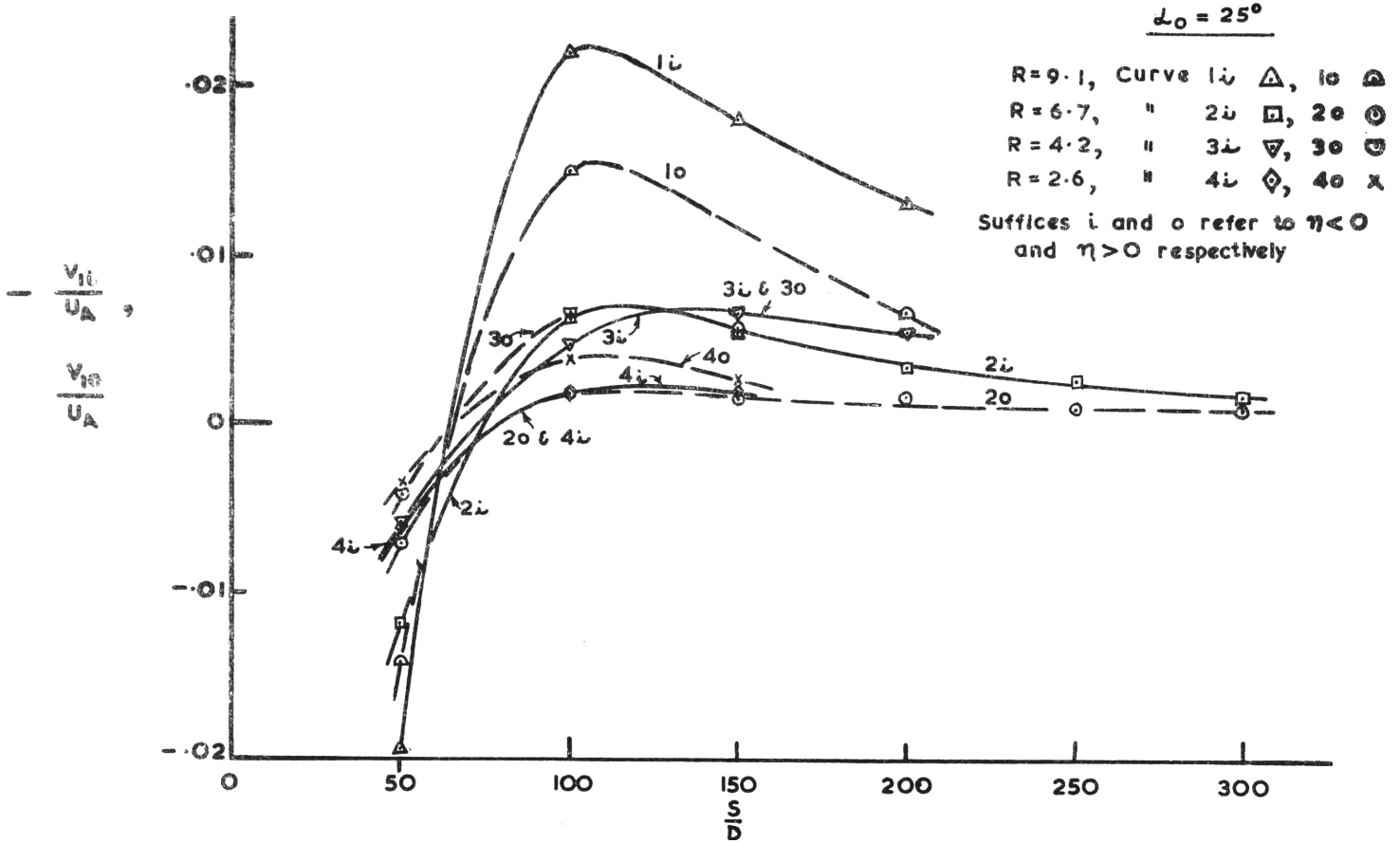

(a) FOR EXPERIMENTS I·1 – I·4

FIG. AV LATERAL INFLOW

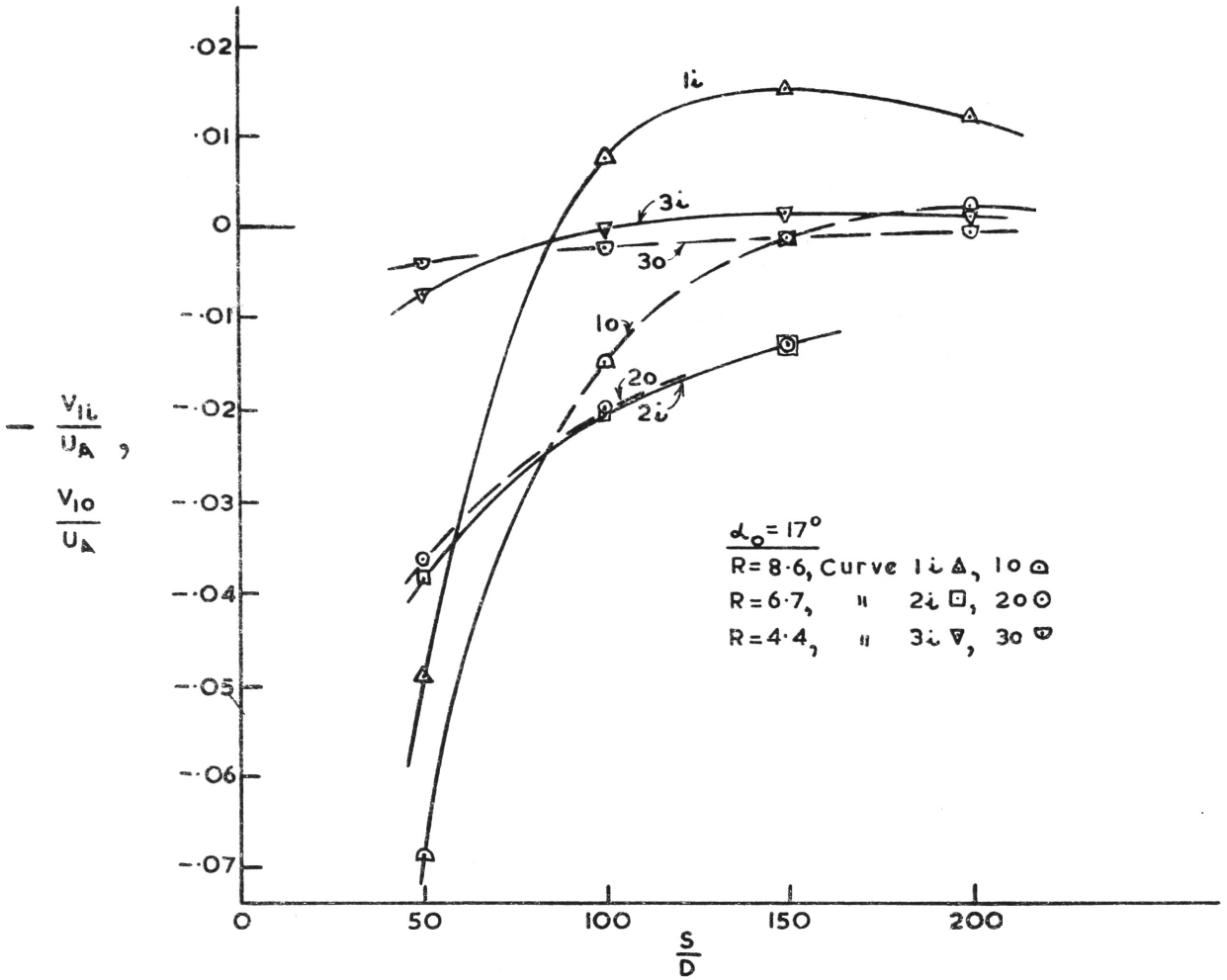

$-\frac{V_{1i}}{U_A}$, $\frac{V_{1o}}{U_A}$

(b) FOR EXPERIMENTS II·1 – II·3

FIG. AV LATERAL INFLOW

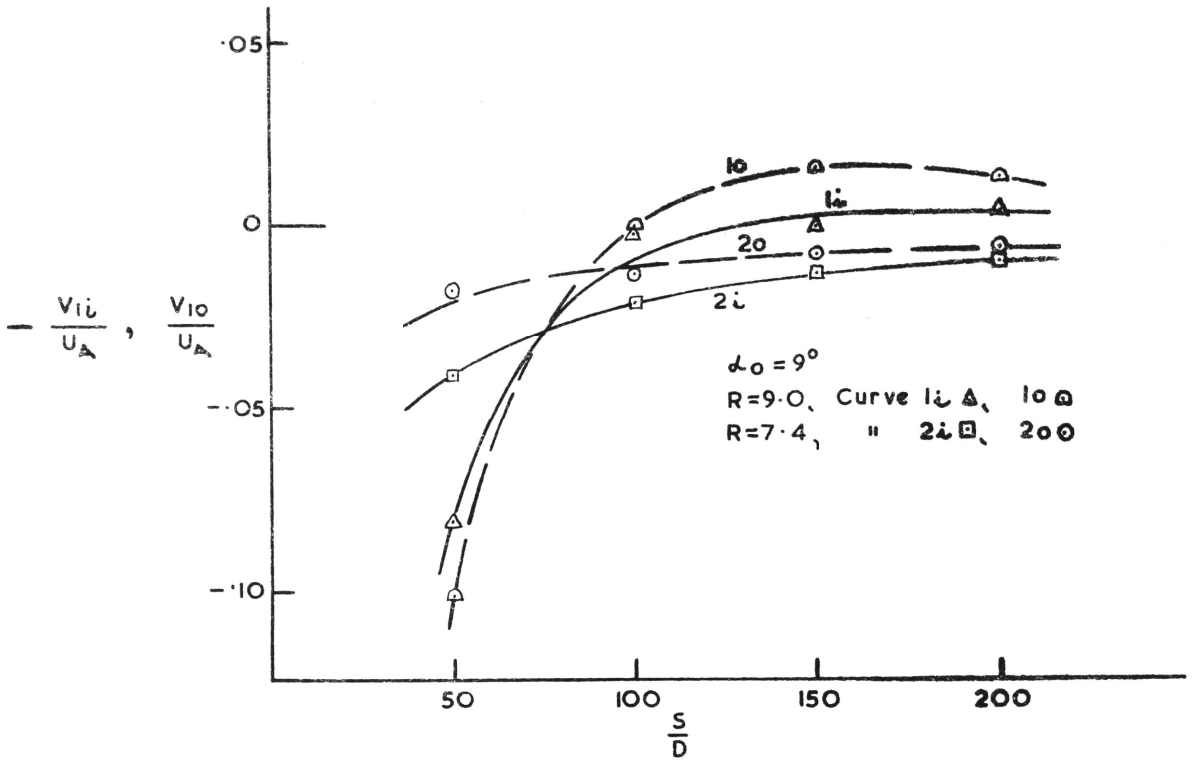

(c) FOR EXPERIMENTS III·1 – III·2

FIG. A V LATERAL INFLOW

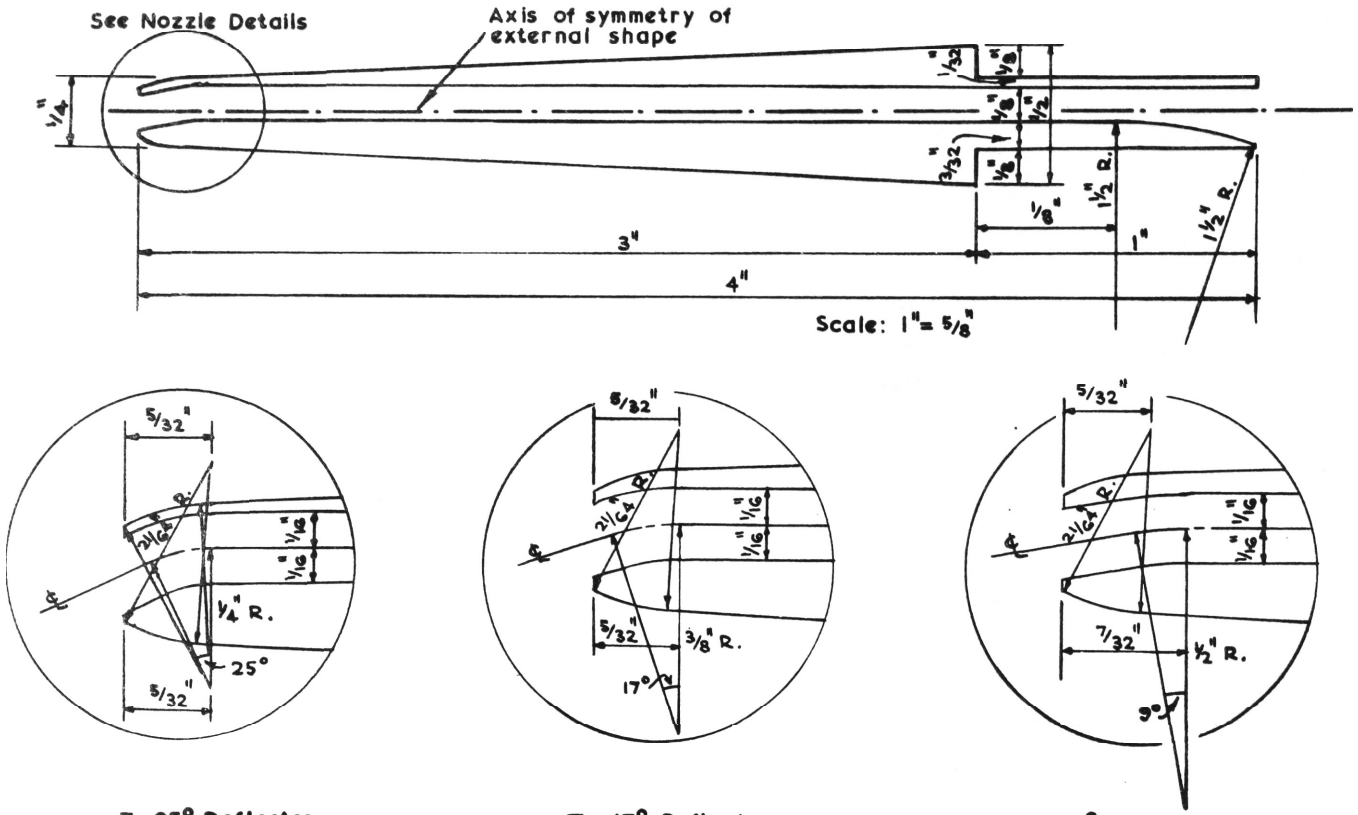

FIG. T4. JET DEFLECTOR